Assessment of soil moisture derived from radar satellite data in the Arctic for the purpose of permafrost studies

Dissertation for obtaining the Doctoral Degree
Dr. rer. nat. at the Faculty of Mathematics and Geoinformation
of the Technische Universität Wien

submitted by

Elin Högström

Supervisory Team: Priv.-Doz. Annett Bartsch, PhD
Birgit Heim, PhD

Department of Geodesy and Geoinformation

Vienna, March 7, 2023

This work is dedicated to my friend Mia Hedvigsdotter (1984.01.11 - 2015.08.31).

Eidesstattliche Erklärung

Hiermit erkläre ich, dass ich diese Arbeit selbständig verfasst habe, dass ich die verwendeten Quellen und Hilfsmittel vollständig angegeben habe und dass ich die Stellen der Arbeit – einschließlich Tabellen, Karten und Abbildungen -, die anderen Werken oder dem Internet im Wortlaut oder dem Sinn nach entnommen sind, auf jeden Fall unter Angaben der Quelle als Entlehnt kenntlich gemacht habe.

Wien, am .....

Parts of this cumulative thesis have been published in peer-reviewed journals:

Publication 1: Högström, E.; Trofaier, A.M.; Gouttevin, I.; Bartsch, A. Assessing Seasonal Backscatter Variations with Respect to Uncertainties in Soil Moisture Retrieval in Siberian Tundra Regions. *Remote Sensing* 2014, 6, 8718-8738. Citations (Scopus): 20.

Publication 2: Högström, E.; Bartsch, A.: Impact of Backscatter Variations Over Water Bodies on Coarse-Scale Radar Retrieved Soil Moisture and the Potential of Correcting With Meteorological Data. *IEEE Transactions on Geoscience and Remote Sensing*. 2017, 55(1), 3-13. Citations (Scopus): 14.

Publication 3: Högström, E.; Heim, B.; Bartsch, A.; Bergstedt, H.; Pointner, G.: Evaluation of a MetOp ASCAT-Derived Surface Soil Moisture Product in Tundra Environments. *Journal of Geophysical Research: Earth Surface*. 2018, 123. Citations (Scopus): 4.

Data Publication: Högström, Elin; Heim, Birgit; Bartsch, Annett (2018): Near surface volumetric soil moisture and temperature measurements in the Lena Delta for 2013/2014. PANGAEA, https://doi.org/10.1594/PANGAEA.894706, Supplement to: Högström, Elin; Heim, Birgit; Bartsch, Annett; Bergstedt, Helena; Pointner, Georg (2018): Evaluation of a MetOp ASCAT-derived surface soil moisture product in tundra environments. Journal of Geophysical Research-Earth Surface, 123, https://doi.org/10.1029/2018JF004658

Outreach: Högström, E., Heim, B., Bartsch, A. (2015): Validation of soil moisture data from the Lena Delta retrieved by satellite. In: Terry V. Callaghan, Hannele Savela (Ed.): INTERACT Stories of Arctic Science , 62-63. Aarhus University. http://doi.org/10.2312/GFZ.LIS.2015.002.

Further Publications:

- Fritz, M., Deshpande, B. N., Bouchard, F., Högström, E., Malenfant-Lepage, J., Morgenstern, A., Nieuwendam, A., Oliva, M., Paquette, M., Rudy, A. C. A., Siewert, M. B., Sjöberg, Y., and Weege, S. (2015): Brief Communication: Future avenues for permafrost science from the perspective of early career researchers, The Cryosphere, 9, 1715–1720, https://doi.org/10.5194/tc-9-1715-2015.

- Tanski G., Bergstedt H., Bevington A., Bonnaventure P., Bouchard F., Coch C., Dumais S., Evgrafova A., Frauenfeld O.W., Frederick J., Fritz M., Frolov D., Harder S., Hartmeyer I., Heslop J., Högström E., Johansson M., Kraev G., Kuznetsova E., J. Lenz, A. Lupachev, F. Magnin, J. Martens, A. Maslakov, A. Morgenstern, A. Nieuwendam, M. Oliva, B. Radosavljevic, J. Ramage, A. Schneider, J. Stanilovskaya, J. Strauss, E. Trochim, D. J. Vecellio, S. Weber, H. Lantuit (2019): The Permafrost Young Researchers Network (PYRN) is getting older: The past, present, and future of our evolving community. Polar Record , Volume 55 , Issue 4 , pp. 216 - 219. https://doi.org/10.1017/S0032247418000645

- Bartsch, A., G. Pointner, I. Nitze, A. Efimova, D. Jakober, S. Ley, E. Högström, G. Grosse, P. Schweitzer (2021): Expanding infrastructure and growing anthropogenic impacts along Arctic coasts. Environmental Research Letters, 16, 115013. https://doi.org/10.1088/1748-9326/ac3176.

- Widhalm, Barbara; Högström, Elin; Ressl, Camillo; Trofaier, Anna Maria; Heim, Birgit; Biasi, Christina; Bartsch, Annett (2014): Land surface hydrology from remotely sensed data at PAGE21 sites with links to geotiff images. PANGAEA, https://doi.org/10.1594/PANGAEA.834200

Abstract

The Arctic tundra lowlands are to a large extent underlain by permafrost, which counts as an essential climate variable. Observations show a nearly four-fold faster warming here than the rest of the world during the last decades. The remote nature of the Arctic means that collected ground data are scarce, which is why availability and applicability of satellite data are crucial here.

Soil moisture data from the active layer are of high demand for permafrost applications, such as modeling and flux up-scaling studies. Data from the C-band active microwave remote sensing instrument Advanced Scatterometer (ASCAT) provides an operational global coarse scale (25 km) surface soil moisture (SSM) product in near real time since 2008. However, there are challenges to the radar retrieval, related to the specific character of the Arctic, such as frozen ground conditions, landscape heterogeneity and seasonal variations.

Here, such typically expected influences were examined for C-band backscatter derived SSM. Comparisons with Permafrost Land Surface Model output and analysis of finer resolution C-band SAR data showed backscatter deviations originating from water body surface roughness rather than actual SSM variations. The influence of water surfaces together with investigations of in-situ soil moisture data and meteorological data formed the base for suggesting precautions to the use of the satellite product as well as improvements to it. A potential bias could be explained by the lake fraction and to a great extent be attributed to wind. Hence, a correction was suggested with meteorological data in lake rich areas.

The usage of higher spatial resolution data than currently available for operational global SSM is required in lowland permafrost environments. Temporal variations of soil moisture across tundra are high, theoretically pointing to applica-

bility of the temporal evolution of C-band backscatter soil moisture products. Soil temperature measurements indicate an influence of temperature variations during the first half of the summer.

Zusammenfassung

Das Tiefland der Arktischen Tundra ist zu einem großen Teil von Permafrost unterlagert, der als wesentliche Klimavariable gilt. Beobachtungen zeigen, dass sich dieses Gebiet in den letzten Jahrzehnten fast viermal schneller erwärmt hat als der Rest der Welt. Durch die Abgeschiedenheit großer Teile der Arktis, können vor Ort kaum Bodendaten erhoben werden, weshalb Satellitendaten hier von entscheidender Bedeutung sind.

Daten über die Bodenfeuchte sind essenziell für Anwendungen im Zusammenhang mit Permafrost, insbesondere für Modellierungs- und Flux-Up-Scaling-Studien. Daten des aktiven C-Band-Mikrowellen-Fernerkundungsinstruments Advanced Scatterometer (ASCAT) werden seit 2008 verwendet, um ein grob aufgelöstes (25 km) Bodenfeuchteprodukt (Surface Soil Moisture, SSM) in nahezu Echtzeit zu erzeugen. Die Herausforderungen für die Ableitung von SSM aus Radardaten, die mit dem spezifischen Charakter der Arktis zusammenhängen, sind z.B. gefrorener Boden, Landschaftsheterogenität oder saisonale Schwankungen.

In der vorliegende Arbeit wurden solche typischerweise erwarteten Einflüsse für durch C-Band-Rückstreuung abgeleitete SSM in der Arktis untersucht. Auf der Grundlage eines Vergleichs mit den Ergebnissen eines Landoberflächenmodells und Untersuchungen von C-Band-SAR-Daten mit feinerer Auflösung konnten Rückstreuungsabweichungen festgestellt werden, die eher auf die Oberflächenrauhigkeit als auf tatsächliche SSM-Variationen zurückzuführen sind. Der Einfluss von Wasseroberflächen bildete, zusammen mit Untersuchungen von in-situ-Bodenfeuchtedaten und meteorologischen Daten, die Grundlage, um Vorsichtsmaßnahmen für die Verwendung des Satellitenprodukts sowie dessen Verbesserungen vorzuschlagen. Der potenzielle systematische Fehler lässt sich durch den Seeanteil erklären und zu

einem großen Teil auf den Wind zurückführen. Daher wird eine Korrektur mittels meteorologischer Daten für seenreiche Gebiete vorgeschlagen.

Die Verwendung von Daten mit höherer räumlicher Auflösung als sie derzeit für operative globale SSM verfügbar ist, ist in Permafrostumgebungen im Tiefland erforderlich. Es gibt in der Tundra starke Schwankungen der Bodenfeuchte im Satellitenprodukt über den Sommer, was auf die Anwendbarkeit der zeitlichen Entwicklung von C-Band-Rückstreuprodukten der Bodenfeuchte hindeutet. Messungen der Bodentemperatur deuten jedoch auf eine weitere fehlerquelle, einen Einfluss der Temperaturschwankungen in der ersten Sommerhälfte hin.

Acknowledgements

The work has altogether been conducted as part of the research project PAGE21 (Changing Permafrost in the Arctic and its Global Effects in the 21st Century), grant agreement number [282700], funded by the EC Seventh Framework Programme theme FP7-ENV-2011. Parts of the work was made possible through data sharing through the ALANIS project, which was funded by the European Space Agency (ESA) Support to Science Element (STSE) program (ESRIN Contr. No. 4000100647/10/I-LG). Furthermore, the International Network for Terrestrial Research and Monitoring in the Arctic (INTERACT) provided financial support for Fieldwork in Siberia as well as data sharing.

Above all, I would like to thank my supervisor Annett Bartsch, for her continuous support and never ending motivation, her scientific expertise and feedback. In particular, I appreciate her enormous patience and her readiness, for being there whenever guidance was needed. I am also very grateful to my second supervisor, Birgit Heim, who provided me with a great amount of inspiration, valuable advice when it comes to fieldwork, and last but not least, a good time in field.

There are a number of co-workers, collaborators and field assistants that I would like to thank, for contributing through fieldwork, data sharing and sharing of material for the purpose of fieldwork, but also for by sharing a great time in field, such as Julia Boike, Moriz Langer, Gustaf Hugelius, Peter Kuhry, Matthias Siewert and Sasha Niemand. I also want to direct an additional thanks to the local partners and people maintaining the field stations that I have visited for this work. Thank you as well, to all my former colleagues at the Department of Geodesy and Geoinformation, TU Wien, for providing a friendly and inspirational

work environment.

As a part of teams of young researchers (PAGE21 Young Researchers representatives, APECS), I had the opportunity to be part of a motivated team of young researchers, working on several projects, such as outreach, organizing workshops, and scientific publication on the avenues of permafrost research (Fritz et al., 2015). I want to thank everyone involved in these projects for the fun, interesting and efficient exchange and cooperation. In this context, I would like to direct a specific thank you to Matthias Siewert, Stefanie Weege and Michael Fritz.

I also want to thank Helena Bergstedt, Barbara Widhalm, Laurenz Feinig, Willibald Feinig and Isabella Hartmann, for helping me with the German translation of the abstract.

Lastly, I want to thank my father, for reminding me of how important it is to finalize any work that one starts.

Contents

Chapter 1

Problem statement

The Arctic tundra lowlands are to a large extent underlain by perennially frozen ground, known as permafrost. As it is connected to a multitude of climate processes, permafrost counts as one of the 50 essential climate variable (ECV), defined by the Global Climate Observating System (GCOS). In recent decades, the warming in the Arctic has been much faster than in the rest of the world, a phenomenon known as Arctic amplification. Observations show a nearly four-fold faster warming than the rest of globe during the last decades in this area [Pithan and Mauritsen, 2014, Rantanen et al., 2022]. As a result, a degradation of permafrost is already being observed and an increased degradation is predicted [Grosse et al., 2011, Guo and Wang, 2017, IPCC, 2013, Turetsky et al., 2019]. The accelerated release of carbon in teh form of carbon dioxide or methane into the atmosphere from thawing permafrost and its effects on the global climate itself, referred to as permafrost carbon feedback, is of great concern and an important research focus since many years [Friborg et al., 2003, Christensen et al., 2004, Miner et al., 2022].

The soil layer close to the surface, just above the permafrost table, which experiences seasonal freezing and thawing is referred to as the active layer. In summer, the thaw front moves downward from the surface so that the active layer deepens, depending on heat inputs, insulation from vegetation, and soil characteristic, whereas in autumn, the freeze front penetrates both downwards from the surface and upwards from the permafrost table [Painter et al., 2016, Sjöberg et al., 2016].

Knowledge about the amount of water that freezes in this active layer in autumn is of interest, as this water will be available as potentially liquid water for the following spring. Water content in the active layer is a control parameter for carbon exchange with the atmosphere, as well as for the soil thermal properties and surface energy balance [Westermann et al., 2017, Westermann et al., 2022]. Soil moisture data is therefore of high importance for permafrost related applications, specifically for modeling and flux up-scaling studies [Jung et al., 2010, Marchenko et al., 2008, Zhang et al., 2011, Lupascu et al., 2013, Kimball et al., 2009].

The remote nature of large parts of the Arctic means that collected ground data are scarce, which is why availability and applicability of satellite data are crucial here. Global maps of near surface soil moisture are produced using coarse resolution (ca 25-50 km) sensors operating in the microwave frequencies (e.g. ASCAT C-band 5.3 GHz, AMSR-E 6.9, 10.7, 18.7 GHz, SMOS and SMAP L-band 1.4 GH), employing passive as well as active systems. A wide range of global satellite derived soil moisture products are available today from microwave sensors, such as the AMSR-E [Njoku et al., 2003, Owe et al., 2008], TRMM Microwave Imager (TMI) [Owe et al., 2008], Special Sensor Microwave/Imager (SSM/I) [Owe et al., 2008], WindSat Polarimetric Radiometer [Li et al., 2010], European Remote Sensing Satellites ERS 1 and 2 [Wagner et al., 1999, Scipal et al., 2002], and the Advanced Scatterometer (ASCAT) onboard the Meteorological Operational satellite (MetOp)[Bartalis et al., 2007, Wagner et al., 2010]. More recent data collection programs include the Soil Moisture and Ocean Salinity Mission (SMOS) of the European Space Agency and the Soil Moisture Active and Passive (SMAP) [Kerr et al., 2012, Sadri et al., 2020, Colliander et al., 2017] of the United States National Aeronautics and Space Administration (NASA) [Entekhabi et al., 2010], which were specifically designed for the purpose of soil moisture retrieval. Data from the C-band active microwave remote sensing instrument Advanced Scatterometer (ASCAT) has been used since 2008 to produce an operational global coarse scale (25 km) surface soil moisture (SSM) product in near real time

[Bartalis et al., 2007, Wagner et al., 2010]. The method relies on the fact that the grounds dielectric properties change with its moisture level [Ulaby et al., 1986], hence soil moisture variations are assumed to be reflected in the backscatter signal. Surface roughness and volume scattering, which also contribute to the backscatter signal, are parameterized or assumed to be constant under certain conditions [Bartalis et al., 2007, Naeimi et al., 2009a, Naeimi et al., 2009b]. The ASCAT SSM product is suitable for continuous monitoring as it provides an 80 percent daily coverage, and it has been shown to capture the annual cycle as well as fluctuations over shorter time [Naeimi et al., 2009b, Albergel et al., 2012].

However, the retrieval of SSM from satellite data can be particularly challenging at high latitudes because of frozen ground conditions [Zhang et al., 2003], landscape heterogeneity [Fletcher et al., 2010, Bartsch et al., 2016]), seasonal land cover variations and abundant water bodies [Smith et al., 2007], which also contribute to the radar return signal [Bartsch et al., 2011, Wagner et al., 2013]. Freezing of the ground usually results in low backscatter, similar to those attributed to dry soil, which can lead to misinterpretations of the readings as SSM [Naeimi et al., 2012] and snow scattering processes are even more complex [Bartsch, 2010]. Therefore, frozen conditions are flagged and such satellite data are not included in the process.

The Arctic tundra is to a large extent characterized by wetlands, with poorly drained, highly saturated soils and abundant ponds and lakes, with as much as 8% being covered by water bodies [Grosse et al., 2008, Walker et al., 2005]. The existence of surface water within the scatterometer footprint poses a challenge for the ASCAT SSM retrieval [Wagner et al., 2013]. The water surface roughness can quickly increase at rain events or at high wind speeds, causing backscatter variations unrelated to but misinterpreted as SSM variations. This retrieval issue is currently taken into account through a flag that warns for high water fraction, derived from the Global Lake and Wetland Database (GLWD) [Lehner and Döll, 2004] and the Global Selfconsistent, Hierarchical, High-resolution Shoreline Database (GSHHS) [Wessel and Smith, 1996]. This flag does not take wetland dynamics into account or changes in inundation that may occur and it does not capture

small lakes, which is problematic since a large part of the tundra lakes are small and may vary in size with the seasons. The impact that the presence of water bodies through weather events may have on the backscatter and hence on the soil moisture retrieval, was not yet quantified. The potential to correct such bias in lake rich areas is likewise yet to be explored and attempted in this thesis. C-band is expected to provide a means for assessment. A similar strategy was recently used to quantify the impact of lakes on retrieval of freeze/thaw timing from ASCAT [Bergstedt and Bartsch, 2017].

The spatial and temporal resolutions makes global land surface models suitable for comparison with the ASCAT product. One such model is ORCHIDEE (ORganizing Carbon and Hydrology in Dynamic EcosystEms) – a Permafrost Model incorporated into a Land Surface Model (LSM) [Gouttevin et al., 2012]. Such inter-comparisons can be useful in order to evaluate and improve the understanding of limitations associated to the model as well as to the satellite product.

Lastly, in situ measurements are essential for evaluating satellite based soil moisture estimates, and to understand what is represented in the backscatter signal [Ceballos et al., 2005, Wagner et al., 2007]. A multitude of studies have validated soil moisture detection approaches through comparison with in situ measurements (e.g. [Rudiger et al., 2007, Dorigo et al., 2013, Colliander et al., 2017]). Because soil moisture is highly variable in space and time it is a challenge to compare the point observations of measurement stations to large scatterometer footprints of 25-50 km size [Western et al., 2002, Wagner et al., 2013]. Soil moisture measurements have been used for satellite validation purposes since the 1980s [Wang et al., 1980], and the availability of soil moisture in situ data has increased [Krauss et al., 2010], for example through networks such as the International Soil Moisture Network (ISMN) [Robock et al., 2000, Dorigo et al., 2013]. Soil moisture observation networks have been installed and used for calibration/validation activities for the Soil Moisture Active Passive (SMAP) from the National Aeronautics and Space Administration (NASA) [Colliander et al., 2017], the Soil Moisture and Ocean Salinity (SMOS) from the European Space Agency (ESA) [Bircher et al., 2012]

missions, as well as the ESA Climate Change Initiative (CCI) soil moisture product [Ikonen et al., 2016]. Even though these are all highly valuable efforts for quantitative assessments of global remote sensing products, the networks themselves were not always installed for that purpose. Multiple measurements may therefore not exist in one satellite footprint [Crow et al., 2012], meaning that the point measurements might not be representative for a larger area. The large spatial variability in soil moisture [Western et al., 2002] is still challenging, and there is a need to understand the variable satellite derived soil moisture product quality across different environments [Dirmeyer et al., 2004, De Jeu et al., 2008, Sinclair and Pegram, 2010]. Small-scale networks also exist with relatively high spatial density (e.g. 3-5 km^2; [Jackson et al., 2010]) but in-situ data are overall concentrated to the mid-latitudes and scarce in the Arctic.

Even though soil moisture shows high temporal and spatial variability, the spatial variability has been shown to increases with the size of the area up to 10 km^2, thereafter it remains relatively constant. A small number of measurements are actually sufficient to obtain accurate areal measurements [Brocca et al., 2012]. Correlations between satellite and in-situ measurements are usually not very high. Even so, a low correlation does not necessarily mean that the satellite data are wrong. It may, for example, be explained by the fact that the point measured in-situ data are not representative for a larger area, such as that of the satellite footprint. The results simply need to be interpreted in their relative context. It is also necessary to consider the accuracy and quality of the in-situ dataset [Wagner et al., 2013].

par The difference in depth between an in-situ sensor, commonly installed at 10 cm or deeper, and the top layer through which the microwave signal can penetrate is also important to consider. [Bartsch et al., 2012b] demonstrated that Pearson correlations for sensors deeper than 10 cm are below 0.4 in tundra environments. The microwave signal penetration depth also depends on the moisture level itself (deeper penetration in drier soil). The shallow installation of sensors has been shown to be the appropriate choice in tundra environment

[Bartsch et al., 2011, Bartsch et al., 2012a]. The uppermost sensors are more directly affected by the atmospheric conditions than those in deeper soil layers, where changes in moisture and temperature are slower and damped. Prior measurements of in-situ unfrozen water content in tundra over time have been conducted using bulk electrical conductivity and in-situ soil temperature data in Alaska, demonstrating the potential to remotely 'visualize' permafrost via autonomous monitoring over field relevant scales [Dafflon et al., 2017]. Dedicated surveys of near surface soil moisture which specifically advance our understanding of satellite based retrieval issues are, however, still lacking.

Chapter 2

Objectives

Remote sensing is a valuable tool for monitoring and providing useful data products for Arctic research. Meeting the needs for earth observation products in these largely inaccessible regions, this thesis aims to explore the potentials of a coarse scale soil moisture product retrieved from C-band scatterometer for the purpose of permafrost studies. The focus of this thesis lies on soil and surface properties and their connections to the soil dielectric properties, hence their influence on radar C-band backscatter. The interrelations between coarse scale ASCAT backscatter and the medium/finer scale SAR backscatter intensity are explored, in order to understand the origin of potential misreadings of soil moisture in the coarse scale data. In particular, the influence of water surfaces is investigated as well as in-situ data in order to suggest improvements to the satellite product. The intention is to enable circumpolar monitoring of higher quality than available so far.

The following objectives are addressed within the research articles which form the basis of this thesis:

- Investigating the influence of landscape heterogeneity typical for the Arctic environment on C-band backscatter variability other than related to changing soil moisture and delineating the potential impacts on soil moisture retrieval.
- Quantifying the impact of sub-footprint size water bodies on C-band scatterometer observations and understand the specific origin of this bias.
- To lay out path ways for a correction of the soil moisture retrieval through

meteorological data and, in cases when such data are not available, to suggest improved retrieval methods or flags that take typical landscape heterogeneity in the Arctic into account.

- Analyzing the representativity of C-band scatterometer temporal dynamics in tundra landscapes through in-situ soil moisture and temperature data.

Chapter 3

Methodology

The following methods have been used in the course of this thesis:

- Literature review, focusing on microwave remote sensing with emphasis on Arctic regions, land cover (specifically lakes) of the Arctic and their inherent wetness conditions, relations to soil properties and meteorological conditions, as well as literature covering soil moisture validation data availability and monitoring networks.
- Statistical and time series analysis of backscatter intensity with respect to water bodies including Geographical Information Systems (GIS) analyses. Here, the higher spatial resolution SAR data were used to assess the spatial variability and representativity of the coarse scale scatterometer data.
- Statistical and time series analysis of backscatter compared to in-situ soil moisture and temperature data.
- Statistical analyses for assessment of agreement between C-band derived SSM and a Land surface Model (ORCHIDEE (ORganizing Carbon and Hydrology in Dynamic EcosystEms) supporting the evaluation.
- Field survey in a tundra environment including installation of monitoring stations for soil moisture and temperatures, specifically adapted for comparison with C-band backscatter data.
- Statistical analysis of backscatter dependence on meteorological parameters available from external datasets as well as the dedicated field survey.

Chapter 4

Summary of publications

4.1 Publication I: Assessing Seasonal Backscatter Variations with Respect to Uncertainties in Soil Moisture Retrieval in Siberian Tundra Regions

In this study, backscatter variability which is not associated to changing soil moisture, is investigated in order to examine and understand the possible impact on soil moisture retrieval. ENVISAT Advanced Synthetic Aperture Radar(ASAR) Wide Swath (WS, 120 m) data are used to understand and quantify impacts on Metop Advanced Scatterometer (ASCAT, 25 km) soil moisture retrieval during the snowfree period. Sites of interest are chosen according to ASAR WS availability, and by selecting areas where the agreement between outputs from the land surface model ORCHIDEE and ASCAT derived SSM is particularly high or low. ORCHIDEE (ORganizing Carbon and Hydrology in Dynamic EcosystEms) is a Land Surface Model designed to represent terrestrial fluxes of carbon, water and the energy budget, simulating the soil hydrological and thermal dynamics and incorporating a soil freezing scheme necessary for high-latitude processes [Gouttevin et al., 2012]. In each of these sites, backscatter variations are analyzed with respect to the ASCAT footprint area, defined as Regions of Interest (ROI).

The ice free ASAR acquisitions were used to separate land from water through supervised classification (minimum distance). Higher backscatter than what is typical for C-band for smooth water surfaces may be caused by ice cover, or by wind and rain acting by increased surface roughness (e.g. [Bartsch et al., 2012b,

Bartsch et al., 2009]). By replacing the actual backscatter values in all the detected water surface areas by the value 20 dB, which is a typical C-band backscatter value for smooth water surfaces in the used dataset [Bartsch et al., 2012b, Bartsch et al., 2008], a reference dataset with smooth water surfaces was generated. By comparing the actual backscatter from the acquisitions in each ROI with this reference dataset with smooth water, the impact on of C-band backscatter could be derived and was averaged within areas that are approximations of the ASCAT grid cells. This impact is hence referred to as backscatter deviation.

It could be shown that the low agreement with the model output is related to water fraction in most cases. Regions with high backscatter deviations are evidently characterized by a high percentage of total lake area, i.e., many of the ROI in eastern Siberia. The sites in western and central Siberia show low backscatter deviation and are areas with few lakes. In one of the sites (Markovo) the low agreement between the model output and the SSM product is more likely explained by the exceptionally scarce weather data from this area used to force the model [Gouttevin et al., 2013].

The backscatter is seen to be impacted by partial short term surface roughness changes, but no difference could be detected between periods with floating ice (in snow off situation) and ice free periods at the chosen sites. The water fraction does correlate with backscatter deviations within the ASCAT footprint areas (R=0.91-0.97). Backscatter deviations of up to 5 dB can occur in areas with less than 50% water fraction and an assumed soil moisture related range (sensitivity) of 7 dB in the ASCAT data. The sensitivity is also positively correlated with water fraction in regions with low land-surface model agreement (R = 0.68). A precise quantification of the impact on soil moisture retrieval would, however, need to consider actual soil moisture changes and sensor differences. The study demonstrates that the usage of higher spatial resolution data than currently available for SSM is required in lowland permafrost environments.

4.2 Publication II: Impact of Backscatter Variations Over Water Bodies on Coarse-Scale Radar Retrieved Soil Moisture and the Potential of Correcting With Meteorological Data

In this context, satellite-derived soil moisture data are valuable for modeling purposes. Assessing the applicability of such data at high latitudes is essential but has, until recently, been given little attention. [Högström et al., 2014] pointed out that seasonal land cover variations and the presence of small water bodies, which are typical in the Arctic, can cause complications for soil moisture retrieval in tundra environments. Here, it is hypothesized that a bias related to water fraction is caused by variations in the water surface roughness. The impact is quantified for the Metop Advanced Scatterometer by investigations of the higher spatial resolution synthetic aperture radar (SAR) data acquired by ENVISAT Advanced SAR over 11 sites across the Siberian Arctic. The bias calculated as an average over time can be explained by the lake fraction: a water fraction higher than 20% causes a bias of more than 10% relative surface soil moisture. This can to a great extent be attributed to wind, based on which a bias correction was developed. The correction was applied and evaluated with in situ soil moisture data, which were available from one of the sites: the Lena Delta. Weak results are obtained because water surfaces correspond mainly to rivers at this specific site. Variations in discharge, water height, and streams may also affect the water surface roughness, rather than wind only.

4.3 Publication III: Evaluation of MetOp ASCAT-derived surface soil moisture product in tundra environments

Satellite derived surface soil moisture data are available and highly demanded for the Arctic but detailed validation is still lacking. Since early 2000s, soil moisture monitoring networks are being widely established as part of hydrological and meteorological observing capacities. The launch of the ESA mission SMOS in 2009 [Kerr et al., 2012], and the launch of the NASA SMAP mission in 2015 [Entekhabi et al., 2010], lead to the establishment of new research networks [Colliander et al., 2017]. Nevertheless, most of the in-situ soil moisture data available are concentrated to the middle and low latitudes, whereas the representation of the Arctic is still today very limited [Dorigo et al., 2021].

The present study addresses this limit by dedicated soil moisture surveys in the Arctic tundra. In-situ measurements of water content within the active layer at four sites across the Arctic in Alaska (Barrow, Sagwon, Toolik) and Siberia (Tiksi), taken in the spring after thawing and in autumn prior to freezing are investigated and compared with C-band scatterometer SSM data. From these long term monitoring sites already available, but not foreseen for satellite soil moisture validation, only the measurements from shallow depth (5 to 10 cm) were used.

In addition to these relatively deep measurements, additional monitoring stations were set-up for measurements close to the surface in the Lena River Delta, Siberia, in order to account for the limited penetration depth of the radar signal. Volumetric Water Content (VWC) sensors and temperature seonsors were placed in the moss organic layer (depth 1) and in the fibric layer (depth 2), which is an approximately 2 - 3 cm thick water storage layer for the moss [Yoshikawa et al., 2004]. The stations were installed in August 2013 and results collected in August 2014.

It is hypothesized that soil temperature variations after soil thaw impact MetOp ASCAT satellite derived surface soil moisture (SSM) measurements in wet tundra environments as C-band backscatter is sensitive to changes in dielectric properties [Chen et al., 2018]. ASCAT SSM variations are generally very small, in line with the low variability of in situ VWC. Short term changes after complete thawing of

the upper organic layer, however, seem to be mostly related to soil temperature changes. Correlations between SSM and in situ VWC are generally low, or even negative. Mean-standard deviation matching results gives a comparably high RMSE (on average 11%) for predictions of VWC. Further investigations and measurement networks are needed to clarify factors causing temporal variation of C-band backscatter in tundra regions.

Chapter 5

Author's contribution

- **Publication I:** Development of the concept of the study, conducting all data processing and analysis, designing the figures and writing the manuscript.
- **Publication II:** Development of the concept of the study, conducting all data processing and analysis, designing the figures and writing the manuscript.
- **Publication III:** Development of the concept of the study and the concept of the in-situ measurements, conducting the installation of the in-situ measurements, conducting all data processing and analysis, the literature research, and writing the majority of the manuscript.

Chapter 6

Scientific impact and outlook

Following the objectives of this thesis (see section **??**), the key findings and main scientific contributions for microwave remote sensing of surface soil moisture in the Arctic regions are listed below:

- It could be shown that C-band backscatter derived SSM is indeed influenced by landscape heterogeneity typical for the Arctic. Based on comparison with Permafrost Land Surface Model output and investigations of finer resolution C-band SAR data, backscatter deviations originating from surface roughness rather than actual SSM variations could be detected. The findings can be applied to systems relying on similar principles: change detection approaches for C-band backscatter.

- The potential impact of sub-footprint size water bodies on C-band scatterometer retrieved SSM could be quantified for the first time, with special emphasis on wind and rain acting on the water surfaces. The average bias over time, as calculated from finer scale SAR backscatter within areas representing the ASCAT footprint, can be explained by the lake fraction and to a great extent be attributed to wind speed rather than rain.

- A correction was suggested that makes use of meteorological data for lake rich areas. The findings of this study demonstrate the necessity of higher spatial resolution data than currently available for operational global SSM in Arctic environments so that its typical landscape heterogeneity can be taken into account.

- It could be shown that temporal variations of soil moisture across tundra are high, theoretically pointing to applicability of the temporal evolution of C-band backscatter soil moisture products. Soil temperature measurements indicate an influence of temperature variations during the first half of the summer.

Northern latitudes still remain challenging for the retrieval from coarse resolution instruments such as ASCAT [Hahn et al., 2021]. Poor performance in permafrost regions was also shown more recently for soil moisture retrieval from passive microwave records (SMAP), by [Wrona et al., 2017], concluding that this product only should be used with extreme caution in high latitudes. Polarimetric C-band SAR use on the other hand, shows promising results [Zwieback and Berg, 2019]. Investigations of airborne P-band observations in the context of soil moisture and active layer thickness were also recently initiated [Chen et al., 2019]. The future P-band SAR mission BIOMASS is expected to offer further insights on the utility of this frequency. In general, SAR data availability currently still, howver, constraints operational retrieval of time series at the spatial resolution required for permafrost regions.

Bibliography

[Albergel et al., 2012] Albergel, C., de Rosnay, P., Gruhier, C., Muñoz-Sabater, J., Hasenauer, S., Isaksen, L., Kerr, Y., and Wagner, W. (2012). Evaluation of remotely sensed and modelled soil moisture products using global ground-based in situ observations. *Remote Sensing of Environment*, 118:215–226.

[Bartalis et al., 2007] Bartalis, Z., Wagner, W., Naeimi, V., Hasenauer, S., Scipal, K., Bonekamp, H., Figa, J., and Anderson, C. (2007). Initial soil moisture retrieval from the METOP-A advanced scatterometer. *Geophysical Research Letters*, 34(L20401).

[Bartsch, 2010] Bartsch, A. (2010). Ten years of SeaWinds on QuikSCAT for snow applications. *Remote Sensing*, 2(4):1142–1156.

[Bartsch et al., 2016] Bartsch, A., Höfler, A., Kroisleitner, C., and Trofaier, A. M. (2016). Land cover mapping in northern high latitude permafrost regions with satellite data: Achievements and remaining challenges. *Remote Sensing*, 8(12):979.

[Bartsch et al., 2012a] Bartsch, A., Melzer, T., Elger, K., and Heim, B. (2012a). Soil moisture from Metop ASCAT data at high latitudes. *Tenth International Conference on Permafrost (TICOP), Salekhard, Russia*, pages 33–38.

[Bartsch et al., 2008] Bartsch, A., Pathe, C., Wagner, W., and Scipal, K. (2008). Detection of permanent open water surfaces in central Siberia with ENVISAT ASAR wide swath data with special emphasis on the estimation of methane fluxes from tundra wetlands. *Hydrology Research*, 39(2):89–100.

[Bartsch et al., 2011] Bartsch, A., Sabel, D., Wagner, W., and Park, S.-E. (2011). Considerations for derivation and use of soil moisture data from active microwave satellites at high latitudes. In *2011 IEEE International Geoscience and Remote Sensing Symposium (IGARSS), Vancouver, British Columbia, Canada*, pages 3132–3135. IEEE.

[Bartsch et al., 2012b] Bartsch, A., Trofaier, A., Hayman, G., Sabel, D., Schlaffer, S., Clark, D., and Blyth, E. (2012b). Detection of open water dynamics with ENVISAT ASAR in support of land surface modelling at high latitudes. *Biogeosciences*, 9(2).

[Bartsch et al., 2009] Bartsch, A., Wagner, W., Scipal, K., Pathe, C., Sabel, D., and Wolski, P. (2009). Global monitoring of wetlands - the value of ENVISAT ASAR global mode. *Journal of Environmental Management*, 90:2226–2233.

[Bergstedt and Bartsch, 2017] Bergstedt, H. and Bartsch, A. (2017). Surface state across scales; temporal and spatial patterns in land surface freeze/thaw dynamics. *Geosciences*, 7(3):65.

[Bircher et al., 2012] Bircher, S., Skou, N., Jensen, K. H., Walker, J. P., and Rasmussen, L. (2012). A soil moisture and temperature network for SMOS validation in western denmark. *Hydrology and Earth System Sciences*, 16(5):1445–1463.

[Brocca et al., 2012] Brocca, L., Moramarco, T., Melone, F., Wagner, W., Hasenauer, S., and Hahn, S. (2012). Assimilation of surface- and root-zone ASCAT soil moisture products into rainfall-runoff modeling. *IEEE Transactions on Geoscience and Remote Sensing*, 50(7):2542–2555.

[Ceballos et al., 2005] Ceballos, A., Scipal, K., Wagner, W., and Martínez-Fernández, J. (2005). Validation of ERS scatterometer-derived soil moisture data in the central part of the Duero Basin, Spain. *Hydrological processes*, 19(8):1549–1566.

[Chen et al., 2018] Chen, Q., Zeng, J., Cui, C., Li, Z., Chen, K., Bai, X., and Xu, J. (2018). Soil moisture retrieval from SMAP: A validation and error analysis

study using ground-based observations over the little washita watershed. *IEEE Transactions on Geoscience and Remote Sensing*, 56(3):1394–1408.

[Chen et al., 2019] Chen, R. H., Tabatabaeenejad, A., and Moghaddam, M. (2019). Retrieval of permafrost active layer properties using time-series p-band radar observations. *IEEE Transactions on Geoscience and Remote Sensing*, 57(8):6037–6054.

[Christensen et al., 2004] Christensen, T. R., Johansson, T. R., Akerman, H. J., Mastepanov, M., Malmer, N., Friborg, T., Crill, P., and Svensson, B. H. (2004). Thawing sub-arctic permafrost: effects on vegetation and methane emissions. *Geophysical Research Letters*, 31(4).

[Colliander et al., 2017] Colliander, A., Jackson, T., Bindlish, R., Chan, S., Das, N., Kim, S., Cosh, M., Dunbar, R., Dang, L., Pashaian, L., Asanuma, J., Aida, K., Berg, A., Rowlandson, T., Bosch, D., Caldwell, T., Caylor, K., Goodrich, D., al Jassar, H., Lopez-Baeza, E., Martínez-Fernández, J., González-Zamora, A., Livingston, S., McNairn, H., Pacheco, A., Moghaddam, M., Montzka, C., Notarnicola, C., Niedrist, G., Pellarin, T., Prueger, J., Pulliainen, J., Rautiainen, K., Ramos, J., Seyfried, M., Starks, P., Su, Z., Zeng, Y., van der Velde, R., Thibeault, M., Dorigo, W., Vreugdenhil, M., Walker, J., Wu, X., Monerris, A., O'Neill, P., Entekhabi, D., Njoku, E., and Yueh, S. (2017). Validation of smap surface soil moisture products with core validation sites. *Remote Sensing of Environment*, 191:215 – 231.

[Crow et al., 2012] Crow, W. T., Berg, A. A., Cosh, M. H., Loew, A., Mohanty, B. P., Panciera, R., Rosnay, P., Ryu, D., and Walker, J. P. (2012). Upscaling sparse ground-based soil moisture observations for the validation of coarse-resolution satellite soil moisture products. *Reviews of Geophysics*, 50(2).

[Dafflon et al., 2017] Dafflon, B., Oktem, R., Peterson, J., Ulrich, C., Tran, A. P., Romanovsky, V., and Hubbard, S. S. (2017). Coincident aboveground and belowground autonomous monitoring to quantify covariability in permafrost, soil,

and vegetation properties in Arctic tundra. *Journal of Geophysical Research: Biogeosciences*, 122(6):1321–1342. 2016JG003724.

[De Jeu et al., 2008] De Jeu, R., Wagner, W., Holmes, T., Dolman, A., Van De Giesen, N., and Friesen, J. (2008). Global soil moisture patterns observed by space borne microwave radiometers and scatterometers. *Surveys in Geophysics*, 29(4-5):399–420.

[Dirmeyer et al., 2004] Dirmeyer, P. A., Guo, Z., and Gao, X. (2004). Comparison, validation, and transferability of eight multiyear global soil wetness products. *Journal of Hydrometeorology*, 5(6):1011–1033.

[Dorigo et al., 2021] Dorigo, W., Himmelbauer, I., Aberer, D., Schremmer, L., Petrakovic, I., Zappa, L., Preimesberger, W., Xaver, A., Annor, F., Ardö, J., Baldocchi, D., Bitelli, M., Blöschl, G., Bogena, H., Brocca, L., Calvet, J.-C., Camarero, J. J., Capello, G., Choi, M., Cosh, M. C., van de Giesen, N., Hajdu, I., Ikonen, J., Jensen, K. H., Kanniah, K. D., de Kat, I., Kirchengast, G., Rai, P. K., Kyrouac, J., Larson, K., Liu, S., Loew, A., Moghaddam, M., Fernández, J. M., Bader, C. M., Morbidelli, R., Musial, J. P., Osenga, E., Palecki, M. A., Pellarin, T., Petropoulos, G. P., Pfeil, I., Powers, J., Robock, A., Rüdiger, C., Rummel, U., Strobel, M., Su, Z., Sullivan, R., Tagesson, T., Varlagin, A., Vreugdenhil, M., Walker, J., Wen, J., Wenger, F., Wigneron, J. P., Woods, M., Yang, K., Zeng, Y., Zhang, X., Zreda, M., Dietrich, S., Gruber, A., van Oevelen, P., Wagner, W., Scipal, K., Drusch, M., and Sabia, R. (2021). The international soil moisture network: serving earth system science for over a decade. *Hydrology and Earth System Sciences*, 25(11):5749–5804.

[Dorigo et al., 2013] Dorigo, W., Xaver, A., Vreugdenhil, M., Gruber, A., Hegyiová, A., Sanchis-Dufau, A., Zamojski, D., Cordes, C., Wagner, W., and Drusch, M. (2013). Global automated quality control of in situ soil moisture data from the international soil moisture network. *Vadose Zone Journal*, 12(3).

[Entekhabi et al., 2010] Entekhabi, D., Njoku, E. G., O'Neill, P. E., Kellogg, K. H., Crow, W. T., Edelstein, W. N., Entin, J. K., Goodman, S. D., Jackson, T. J.,

Johnson, J., et al. (2010). The soil moisture active passive (SMAP) mission. *Proceedings of the IEEE*, 98(5):704–716.

[Fletcher et al., 2010] Fletcher, B. J., Press, M. C., Baxter, R., and Phoenix, G. K. (2010). Transition zones between vegetation patches in a heterogeneous arctic landscape: how plant growth and photosynthesis change with abundance at small scales. *Oecologia*, 163(1):47–56.

[Friborg et al., 2003] Friborg, T., Soegaard, H., Christensen, T., Lloyd, C., and Panikov, N. (2003). Siberian wetlands: where a sink is a source. *Geophysical Research Letters*, 30(21).

[Gouttevin et al., 2013] Gouttevin, I., Bartsch, A., Krinner, G., and Naeimi, V. (2013). A comparison between remotely-sensed and modelled surface soil moisture (and frozen status) at high latitudes. *Hydrology & Earth System Sciences Discussions*, 10(8).

[Gouttevin et al., 2012] Gouttevin, I., Krinner, G., Ciais, P., Polcher, J., Legout, C., et al. (2012). Multi-scale validation of a new soil freezing scheme for a land-surface model with physically-based hydrology. *The Cryosphere*, 6:407–430.

[Grosse et al., 2011] Grosse, G., Romanovsky, V., Jorgenson, T., Valter Anthony, K., Brown, J., and Overduin, P. P. (2011). Vulnerability and feedbacks of permafrost to climate change. *EOS Transactions, American Geophysical Union*, (9):73–80.

[Grosse et al., 2008] Grosse, G., Romanovsky, V., Walter, K., Morgenstern, A., Lantuit, H., and Zimov, S. (2008). Distribution of thermokarst lakes and ponds at three yedoma sites in siberia. *Proc. 9th Int. Conf. Permafrost, Fairbanks, AK, USA*, pages 551–556.

[Guo and Wang, 2017] Guo, D. and Wang, H. (2017). Permafrost degradation and associated ground settlement estimation under 2c global warming. *Climate Dynamics*, (49):2569–2583.

[Hahn et al., 2021] Hahn, S., Wagner, W., Steele-Dunne, S. C., Vreugdenhil, M., and Melzer, T. (2021). Improving ASCAT soil moisture retrievals with an enhanced spatially variable vegetation parameterization. *IEEE Transactions on Geoscience and Remote Sensing*, 59(10):8241–8256.

[Högström et al., 2014] Högström, E., Trofaier, A. M., Gouttevin, I., and Bartsch, A. (2014). Assessing seasonal backscatter variations with respect to uncertainties in soil moisture retrieval in Siberian tundra regions. *Remote Sensing*, 6(9):8718–8738.

[Ikonen et al., 2016] Ikonen, J., Vehviläinen, J., Rautiainen, K., Smolander, T., Lemmetyinen, J., Bircher, S., and Pulliainen, J. (2016). The Sodankylä in situ soil moisture observation network: An example application of ESA CCI soil moisture product evaluation. *Geosci. Instrum. Methods Data Syst*, 5:95–108.

[IPCC, 2013] IPCC (2013). Observations: Cryosphere. In Stocker, T., Qin, D., Plattner, G.-K., Tignor, M., Allen, S., Boschung, J., Nauels, A., Xia, Y., Bex, V., and Midgley, P., editors, *Climate Change 2013: The Physical Science Basis. Contribution of Working Group I to the Fifth Assessment Report of the Intergovernmental Panel on Climate Change*, pages 362–364. Cambridge University Press, Cambridge, United Kingdom and New York, NY, USA.

[Jackson et al., 2010] Jackson, T. J., Cosh, M. H., Bindlish, R., Starks, P. J., Bosch, D. D., Seyfried, M., Goodrich, D. C., Moran, M. S., and Du, J. (2010). Validation of advanced microwave scanning radiometer soil moisture products. *IEEE Transactions on Geoscience and Remote Sensing*, 48(12):4256–4272.

[Jung et al., 2010] Jung, M., Reichstein, M., Ciais, P., Seneviratne, S. I., Sheffield, J., Goulden, M. L., Bonan, G., Cescatti, A., Chen, J., De Jeu, R., et al. (2010). Recent decline in the global land evapotranspiration trend due to limited moisture supply. *Nature*, 467(7318):951.

[Kerr et al., 2012] Kerr, Y. H., Waldteufel, P., Richaume, P., Wigneron, J. P., Ferrazzoli, P., Mahmoodi, A., Bitar, A. A., Cabot, F., Gruhier, C., Juglea, S. E., Leroux, D., Mialon, A., and Delwart, S. (2012). The SMOS soil moisture

retrieval algorithm. *IEEE Transactions on Geoscience and Remote Sensing*, 50(5):1384–1403.

[Kimball et al., 2009] Kimball, J. S., Jones, L. A., Zhang, K., Heinsch, F. A., McDonald, K. C., and Oechel, W. C. (2009). A satellite approach to estimate land–atmosphere exchange for boreal and arctic biomes using modis and amsr-e. *Geoscience and Remote Sensing, IEEE Transactions on*, 47(2):569–587.

[Krauss et al., 2010] Krauss, L., Hauck, C., and Kottmeier, C. (2010). Spatio-temporal soil moisture variability in Southwest Germany observed with a new monitoring network within the COPS domain. *Meteorologische Zeitschrift*, 19(6):523–537.

[Lehner and Döll, 2004] Lehner, B. and Döll, P. (2004). Development and validation of a global database of lakes, reservoirs and wetlands. *Journal of Hydrology*, 296(1):1–22.

[Li et al., 2010] Li, L., Gaiser, P. W., Gao, B.-C., Bevilacqua, R. M., Jackson, T. J., Njoku, E. G., Rudiger, C., Calvet, J.-C., and Bindlish, R. (2010). WindSat global soil moisture retrieval and validation. *IEEE Transactions on Geoscience and Remote Sensing*, 48(5):2224–2241.

[Lupascu et al., 2013] Lupascu, M., Welker, J., Seibt, U., Maseyk, K., Xu, X., and Czimczik, C. (2013). High arctic wetting reduces permafrost carbon feedbacks to climate warming. *Nature Climate Change*.

[Marchenko et al., 2008] Marchenko, S., Romanovsky, V., and Tipenko, G. (2008). Numerical modeling of spatial permafrost dynamics in Alaska. In *Proceedings of the ninth international conference on permafrost*, volume 29, pages 1125–1130. Institute of Northern Engineering, University of Alaska Fairbanks.

[Miner et al., 2022] Miner, K. R., Turetsky, M. R., Malina, E., Bartsch, A., Tamminen, J., McGuire, A. D., Fix, A., Sweeney, C., Elder, C. D., and Miller, C. E. (2022). Permafrost carbon emissions in a changing arctic. *Nature Reviews Earth &amp Environment*, 3(1):55–67.

[Naeimi et al., 2009a] Naeimi, V., Bartalis, Z., and Wagner, W. (2009a). ASCAT Soil Moisture: An assessment of the Data Quality and consistency with the ERS Scatterometer Heritage. *Journal Of Hydrometeorology*, 10(2):555–563.

[Naeimi et al., 2012] Naeimi, V., Paulik, C., Bartsch, A., Wagner, W., Kidd, R., Park, S.-E., Elger, K., and Boike, J. (2012). ASCAT surface state flag (SSF): Extracting information on surface freeze/thaw conditions from backscatter data using an empirical threshold-analysis algorithm. *IEEE Transactions on Geoscience and Remote Sensing*, 50(7):2566–2582.

[Naeimi et al., 2009b] Naeimi, V., Scipal, K., Bartalis, Z., Hasenauer, S., and Wagner, W. (2009b). An improved soil moisture retrieval algorithm for ERS and METOP scatterometer observations. *IEEE Transactions on Geoscience and Remote Sensing*, 47(7):1999–2013.

[Njoku et al., 2003] Njoku, E. G., Jackson, T. J., Lakshmi, V., Chan, T. K., and Nghiem, S. V. (2003). Soil moisture retrieval from AMSR-E. *Geoscience and Remote Sensing, IEEE Transactions on*, 41(2):215–229.

[Owe et al., 2008] Owe, M., de Jeu, R., and Holmes, T. (2008). Multisensor historical climatology of satellite-derived global land surface moisture. *Journal of Geophysical Research: Earth Surface*, 113(F1).

[Painter et al., 2016] Painter, S., Coon, E., Atchley, A., Berndt, M., Garimella, R., Moulton, J., Svyatskiy, D., and Wilson, C. (2016). Integrated surface/subsurface permafrost thermal hydrology: Model formulation and proof-of-concept simulations. *Water Resources Research*, 52:6062–6077.

[Pithan and Mauritsen, 2014] Pithan, F. and Mauritsen, T. (2014). Arctic amplification dominated by temperature feedbacks in contemporary climate models. *Nature Geoscience*, 7(10).

[Rantanen et al., 2022] Rantanen, M., Karpechko, A., and Lipponen, A. e. a. (2022). The arctic has warmed nearly four times faster than the globe since 1979. *Communications Earth Environment*, 3(168).

[Robock et al., 2000] Robock, A., Vinnikov, K. Y., Srinivasan, G., Entin, J. K., Hollinger, S. E., Speranskaya, N. A., Liu, S., and Namkhai, A. (2000). The global soil moisture data bank. *Bulletin of the American Meteorological Society*, 81(6):1281–1299.

[Rudiger et al., 2007] Rudiger, C., Calvet, J.-C., Brut, A., Wigneron, J.-P., Berthelot, B., Chanzy, A., Cros, S., and Berger, M. (2007). Aggregation and disaggregation of synthetic l-band soil moisture data over south-western france in preparation of SMOS. In *Geoscience and Remote Sensing Symposium, 2007. IGARSS 2007. IEEE International*, pages 1853–1856. IEEE.

[Sadri et al., 2020] Sadri, S., Pan, M., Wada, Y., Vergopolan, N., and et al. (2020). A global near-real-time soil moisture index monitor for food security using integrated smos and smap. *Remote Sensing of Environment*, 246.

[Scipal et al., 2002] Scipal, K., Wagner, W., Trommler, M., and Naumann, K. (2002). The global soil moisture archive 1992-2000 from ERS scatterometer data: First results. In *Geoscience and Remote Sensing Symposium, 2002. IGARSS'02. 2002 IEEE International*, volume 3, pages 1399–1401. IEEE.

[Sinclair and Pegram, 2010] Sinclair, S. and Pegram, G. (2010). A comparison of ASCAT and modelled soil moisture over South Africa, using TOPKAPI in land surface model. *Hydrology and Earth System Sciences*, 14(4):613.

[Sjöberg et al., 2016] Sjöberg, Y., Coon, E., Sannel, A., Pannetier, R., Harp, D., Frampton, A., S.L., P., and Lyon, S. (2016). Thermal effects of groundwater flow through subarctic fens: A case study based on field observations and numerical modeling. *Water Resources Research*, 3(52):1591–1606.

[Smith et al., 2007] Smith, L. C., Sheng, Y., and MacDonald, G. M. (2007). A first pan-arctic assessment of the influence of glaciation, permafrost, topography and peatlands on northern hemisphere lake distribution. *Permafrost and Periglacial Processes*, 18(2):201–208.

[Turetsky et al., 2019] Turetsky, M. R., Abbott, B. W., Jones, M. C., Anthony, K. W., Olefeldt, D., Schuur, E. A. G., Koven, C., McGuire, A. D., Grosse, G.,

Kuhry, P., Hugelius, G., Lawrence, D. M., Gibson, C., and Sannel, A. B. K. (2019). Permafrost collapse is accelerating carbon release. *Nature*, 569(7754):32–34.

[Ulaby et al., 1986] Ulaby, F. T., Moore, R. K., and Fung, A. K. (1986). Microwave remote sensing, active and passive, iii, radar remote sensing and surface scattering and emission theory. *Artech House, Norwood, Mass.*

[Wagner et al., 2010] Wagner, W., Bartalis, Z., Naeimi, V., Park, S.-E., Figa-Saldaña, J., and Bonekamp, H. (2010). Status of the METOP ASCAT soil moisture product. In *Geoscience and Remote Sensing Symposium (IGARSS), 2010 IEEE International*, pages 276–279. IEEE.

[Wagner et al., 2013] Wagner, W., Hahn, S., Kidd, R., Melzer, T., Bartalis, Z., Hasenauer, S., Figa-Saldaña, J., de Rosnay, P., Jann, A., Schneider, S., Komma, J., Kubu, G., Brugger, K., Aubrecht, C., Züger, J., Gangkofner, U., Kienberger, S., Brocca, L., Wang, Y., Blöschl, G., Eitzinger, J., Steinnocher, K., Zeil, P., and Rubel, F. (2013). The ASCAT soil moisture product: A review of its specifications, validation results, and emerging applications. *Meteorologische Zeitschrift*, 22(1):5–33.

[Wagner et al., 1999] Wagner, W., Lemoine, G., and Rott, H. (1999). A method for estimating soil moisture from ERS scatterometer and soil data. *Remote Sensing of Environment*, 70(2):191–207.

[Wagner et al., 2007] Wagner, W., Naeimi, V., Scipal, K., de Jeu, R., and Martínez-Fernández, J. (2007). Soil moisture from operational meteorological satellites. *Hydrogeology Journal*, 15(1):121–131.

[Walker et al., 2005] Walker, D., Raynolds, M., Daniëls, F., Einarson, E., A., E., et al. (2005). The Circumpolar Arctic Vegetation Map. *Journal of Vegetation Science*, 6(3):267–282.

[Wang et al., 1980] Wang, J. R., Shiue, J. C., and McMurtrey, J. E. (1980). Microwave remote sensing of soil moisture content over bare and vegetated fields. *Geophysical Research Letters*, 7(10):801–804.

[Wessel and Smith, 1996] Wessel, P. and Smith, W. (1996). A global, self-consistent, hierarchical, high-resolution shoreline database. *Journal of Geophysic Research*, 101(B4):8741–8743.

[Westermann et al., 2022] Westermann, S., Ingeman-Nielsen, T., Scheer, J., Aalstad, K., Aga, J., Chaudhary, N., Etzelmüller, B., Filhol, S., Kääb, A., Renette, C., Schmidt, L. S., Schuler, T. V., Zweigel, R. B., Martin, L., Morard, S., Ben-Asher, M., Angelopoulos, M., Boike, J., Groenke, B., Miesner, F., Nitzbon, J., Overduin, P., Stuenzi, S. M., and Langer, M. (2022). The CryoGrid community model (version 1.0) – a multi-physics toolbox for climate-driven simulations in the terrestrial cryosphere.

[Westermann et al., 2017] Westermann, S., Peter, M., Langer, M., Schwamborn, G., Schirrmeister, L., Etzelmüller, B., and Boike, J. (2017). Transient modeling of the ground thermal conditions using satellite data in the lena river delta, siberia. *The Cryosphere*, 11(3):1441–1463.

[Western et al., 2002] Western, A. W., Grayson, R. B., and Blöschl, G. (2002). Scaling of soil moisture: A hydrologic perspective. *Annual Review of Earth and Planetary Sciences*, 30(1):149–180.

[Wrona et al., 2017] Wrona, E., Rowlandson, T. L., Nambiar, M., Berg, A. A., Colliander, A., and Marsh, P. (2017). Validation of the soil moisture active passive (SMAP) satellite soil moisture retrieval in an arctic tundra environment. *Geophysical Research Letters*, 44(9):4152–4158.

[Yoshikawa et al., 2004] Yoshikawa, K., Overduin, P. P., and Harden, J. W. (2004). Moisture content measurements of moss (Sphagnum spp.) using commercial sensors. *Permafrost and Periglacial Processes*, 15(4):309–318.

[Zhang et al., 2011] Zhang, N., Yasunari, T., and Ohta, T. (2011). Dynamics of the larch taiga–permafrost coupled system in siberia under climate change. *Environmental Research Letters*, 6(2):024–003.

[Zhang et al., 2003] Zhang, T., Barry, R., Knowles, K., Ling, F., and Armstrong, R. (2003). Distribution of seasonally and perennially frozen ground in the northern

hemisphere. In *Proceedings of the 8th International Conference on Permafrost*, volume 2, pages 1289–1294. AA Balkema Publishers.

[Zwieback and Berg, 2019] Zwieback, S. and Berg, A. A. (2019). Fine-scale SAR soil moisture estimation in the subarctic tundra. *IEEE Transactions on Geoscience and Remote Sensing*, 57(7):4898–4912.

Appendices

Appendix A

Publication 1

Högström, E.; Trofaier, A.M.; Gouttevin, I.; Bartsch, A. Assessing Seasonal Backscatter Variations with Respect to Uncertainties in Soil Moisture Retrieval in Siberian Tundra Regions. Remote Sens. 2014, 6, 8718-8738.

Remote Sens. **2014**, *6*, 8718-8738; doi:10.3390/rs6098718

OPEN ACCESS

remote sensing

ISSN 2072-4292

www.mdpi.com/journal/remotesensing

Article

Assessing Seasonal Backscatter Variations with Respect to Uncertainties in Soil Moisture Retrieval in Siberian Tundra Regions

Elin Högström [1,2,*], Anna Maria Trofaier [1,2,3], Isabelle Gouttevin [4,5] and Annett Bartsch [1,2,6,7]

[1] Research Group Remote Sensing, Department of Geodesy and Geoinformation (GEO), Vienna University of Technology, Gußhausstraße 27-29, A-1040 Vienna, Austria; E-Mails: amat2@cam.ac.uk (A.M.T.); annett.bartsch@lmu.de (A.B.)

[2] Research Group Remote Sensing, Austrian Polar Research Institute, Vienna University, Althanstraße 14, A-1090 Vienna, Austria

[3] Scott Polar Research Institute, University of Cambridge, Lensfield Road, Cambridge, CB2 1ER, UK

[4] Institut National de Recherche en Sciences et Technologies pour l'Environnement et l'Agriculture, Unité de Recherche Hydrologie-Hydraulique, 5 rue de la Doua, CS 70077, F-69626 Villeurbanne Cedex, France; E-Mail: isabelle.gouttevin@gmail.com

[5] CRYOS School of Architecture, Civil and Environmental Engineering, Ecole Polytechnique Federale de Lausanne, Batiment GR, Station 2, CH-1015 Lausanne, Switzerland

[6] Department of Geography, Ludwig-Maximilians-Universität München, Luisenstraße 37, D-80333 Munich, Germany

[7] IFFB Geoinformatik-Z GIS, Universität Salzburg, Hellbrunner Str, 35, A-5020 Salzburg, Austria

* Author to whom correspondence should be addressed; E-Mail: Elin.Hoegstroem@geo.tuwien.ac.at; Tel.: +43-1-58801-12266; Fax: +43-1-58801-12299.

Received: 30 June 2014; in revised form: 26 August 2014 / Accepted: 2 September 2014 / Published: 17 September 2014

Abstract: Knowledge of surface hydrology is essential for many applications, including studies that aim to understand permafrost response to changing climate and the associated feedback mechanisms. Advanced remote sensing techniques make it possible to retrieve a range of land-surface variables, including radar retrieved soil moisture (SSM). It has been pointed out before that soil moisture retrieval from satellite data can be challenging at high latitudes, which correspond to remote areas where ground data are scarce and the applicability of satellite data of this type is essential. This study investigates backscatter variability other than associated with changing soil moisture in order to examine the possible impact on soil moisture retrieval. It focuses on issues specific to SSM retrieval in the Arctic,

notably variations related to tundra lakes. ENVISAT Advanced Synthetic Aperture Radar (ASAR) Wide Swath (WS, 120 m) data are used to understand and quantify impacts on Metop (AAdvanced Scatterometer (ASCAT, 25 km) soil moisture retrieval during the snow free period. Sites of interest are chosen according to ASAR WS availability, high or low agreement between output from the land surface model ORCHIDEE and ASCAT derived SSM. Backscatter variations are analyzed with respect to the ASCAT footprint area. It can be shown that the low model agreement is related to water fraction in most cases. No difference could be detected between periods with floating ice (in snow off situation) and ice free periods at the chosen sites. The mean footprint backscatter is however impacted by partial short term surface roughness change. The water fraction correlates with backscatter deviations (relative to a smooth water surface reference image) within the ASCAT footprint areas ($R = 0.91-0.97$). Backscatter deviations of up to 5 dB can occur in areas with less than 50% water fraction and an assumed soil moisture related range (sensitivity) of 7 dB in the ASCAT data. The sensitivity is also positively correlated with water fraction in regions with low land-surface model agreement ($R = 0.68$). A precise quantification of the impact on soil moisture retrieval would, however, need to consider actual soil moisture changes and sensor differences. The study demonstrates that the usage of higher spatial resolution data than currently available for SSM is required in lowland permafrost environments.

Keywords: permafrost; soil moisture; Arctic; high latitudes; water bodies; radar; remote sensing; land surface model

1. Introduction

The pan-Arctic tundra lowlands are underlain by perennially frozen ground known as permafrost. Permafrost warming is ongoing and predicted to increase in magnitude over the course of the 21st century [1]. The potential impact that thawing permafrost may have on the global climate system through the release of greenhouse gases has been a concern and a research focus since many years (e.g., [2,3]). Changes to the thermal state of permafrost are linked to rising air temperatures and variations in the precipitation. These changes to the ground thermal regime are also modifying hydrological and biogeochemical dynamics [4] which are closely coupled with active layer processes [5]. The soil water content (SWC) of the active layer is a driving factor of ecosystem respiration [6] and therefore soil moisture may be seen as a control parameter for carbon exchange with the atmosphere [7]. Soil moisture is highly variable in space and time, controlled by precipitation, redistribution and evapotranspiration. Attempts to address this spatio-temporal variability have led to the development of remote sensing techniques employing surface soil moisture (SSM) retrieval algorithms (e.g., [8–11]). The availability and applicability of satellite data in the Arctic is in addition crucial because of the remote nature of this region. Both passive and active microwave sensors are used to produce SSM data, including global coarse resolution (25–50 km) datasets [12]. Past studies have often focused on

developing methods using active microwave sensors. Scatterometer data have become central to SSM retrieval studies. The ERS scatterometer derived SSM datasets have been used in a number of studies (e.g., [13,14]). More recently the Advanced Scatterometer (ASCAT) data (e.g., [15,16]), including an operational retrieval method implemented by the European Organization for the Exploitation of Meteorological Satellites (EUMETSAT), is used for the same purpose. The ASCAT sensor, which is onboard the polar-orbiting meteorological satellite MetOp (A and B), is well suited for continuous monitoring, providing 80% daily global coverage [17,18] undertook a validation study that compares soil moisture products from ASCAT as well as from the passive microwave Soil Moisture Ocean Salinity (SMOS) radiometer with in situ observations. They found that the remotely-sensed SSM products show a significant correlation with the in situ data, capturing the annual cycle as well as trends in short term fluctuations in SSM.

Furthermore, the feasibility of using synthetic aperture radar (SAR) data to extract soil moisture patterns at higher spatial resolution (1 km) have been investigated (e.g., [19,20]). There are limitations to SSM retrieval from active microwave sensors in cold regions where frozen ground conditions, landscape heterogeneity and seasonal land cover variations all contribute to the radar's return signal [21]. Each of these factors impacts on the radar scattering mechanism and hence complicates the SSM retrieval methods that rely on relating differences in the ground's dielectric properties to soil moisture levels according to the empirical relationship established by [22]. Particularly challenging for the SSM retrieval procedure are frozen ground conditions. In fact, the soil water index (SWI) method entirely relies on unfrozen and snow-free ground conditions [23]. Phase changes between the liquid and solid states of water have a significant effect on its dielectric properties [24–26]. Freezing of the ground usually results in low backscatter values that are similar to those attributed to dry soils, which in turn may lead to misinterpretation [27]. Furthermore, snow scattering processes are even more complex, depending on depth, density and grain size of the snowpack, as well as wet or dry snow conditions [28]. Information on snowmelt timings and duration, as well as freeze/thaw cycles can be extracted from the radar signal itself [27,29]. However, they still pose a considerable problem for SSM retrieval in cold regions. The future Soil Moisture Active Passive (SMAP) mission, due to launch in late 2014, will try to address all of the aforementioned limitations by combining both radar and radiometer measurements [30].

Precipitation records from the field are sparse in remote areas such as the Arctic. Satellite data provide input data with high temporal and spatial coverage, which in addition can be obtained considerably more frequently than the field measurements can be collected, which makes it valuable for e.g., real-time flood forecasting. Thus, to predict precipitation runoff and infiltration, remotely-sensed SSM data are used as input and/or as validation data for hydrological models [31,32]. In cold regions, the hydrological system is interconnected to the frozen ground, as it hampers the infiltration capacity and percolation. Therefore, permafrost hydrology and active layer processes need to be taken into account for accurate modeling [33]. While permafrost models primarily consider the extent of snow cover and land surface temperatures, simulations of active layer processes rely on soil composition including the active layer's water retention capability [4]. Permafrost models are either developed as stand-alone algorithms or as modules that are incorporated into Land Surface Models (LSMs) and General Circulation Model (GCMs) [34]. One such LSM is ORCHIDEE (ORganizing Carbon and Hydrology in Dynamic EcosystEms). This model is designed to represent terrestrial fluxes (carbon,

water and energy budget). As such, it is a physically-based model that simulates the soil hydrological and thermal dynamics, incorporating a soil freezing scheme necessary for appropriately modeling high-latitude processes [35]. This present study comes in support of a comparison study between modeling results and satellite-derived surface soil moisture [36], by putting effort in the evaluation of the limitations associated with the radar backscatter behavior. In [36] ORCHIDEE output is compared to an ASCAT SSM product, derived using the algorithm put forward by [17], aggregated on weekly time steps and adjusted to polar regions [27].

In the present study, we take advantage of the higher spatial resolution data from the European Space Agency's Envisat Advanced Synthetic Aperture Radar (ASAR) operating in Wide Swath (WS, 120 m) mode, to investigate how seasonal dynamics other than surface soil moisture changes can affect the radar backscatter within proportions of the ASCAT footprints. The focus is on open water surfaces, whose backscatter signal will be altered by winter lake ice covers and weather conditions, e.g., rain or wind. The open water surfaces are defined by supervised classification (see methods). Previous studies of coarse scale scatterometer data from Siberia have concluded that the contribution of lakes and rivers to the overall normalized radar backscatter is negligible [37]. However, weather induced changes on the open water surface and seasonal changes of its extent may be impacting on the dry and wet references which are used as input for relative surface soil moisture retrieval [38] and the impact on coarse resolution backscatter has so far not been quantified with respect to water fraction and water body size.

Gouttevin [36] formulates several hypotheses to explain the low agreement between ORCHIDEE and ASCAT SSM, including the topographical impact (for which both the modeling and the SSM retrieval algorithm are not suited), surface ponding (coarsely represented in ORCHIDEE) and unreliable meteorological forcing data for land-surface modelling in remote, Arctic regions like North-Eastern Siberia. The present study examines whether the presence of permanent open water surfaces may be an additional source of disagreement between the SSM product and the model output.

2. Data and Methods

2.1. Study Sites

Across Siberia, 10 sites were selected (Figure 1). These sites were chosen in order to represent the diversity of landscapes in the Arctic region and because of their proximity to meteorological stations. Furthermore, among the sites, Kytalyk, Cherski, Vorkuta and Nadym are long-term permafrost monitoring sites [39]. Lastly, an essential criterion for choosing the sites was the ASAR data availability (several acquisitions per month). Kharampur and Vorkuta are underlain by sporadic permafrost and Nadym by discontinuous permafrost, whereas all other sites are underlain by continuous permafrost, with the exception of Muzi, which is not underlain by permafrost [40]. The site locations include lake-rich as well as lake-poor areas. The flat and low altitude areas where the sites are located are generally wet. The Western Siberian Lowlands, the coastal plains and the Taimyr Peninsula largely consist of tundra landscapes with predominating wet conditions (e.g., [41,42]).

Figure 1. Site overview indicating the locations of the 10 Arctic sites. Three of the site names are abbreviated: Cherski (CHE), Kytalyk (KYT) and Andryuskino (AND). A simplification (not including sub-classes for ground ice content) of the Circum-Arctic map of permafrost and ground ice conditions [40] is shown as background. The extent of continuous, discontinuous, sporadic and isolated patches of permafrost (PF), as well as glaciers, land and ocean is indicated. Projection: Lambert Azimuthal.

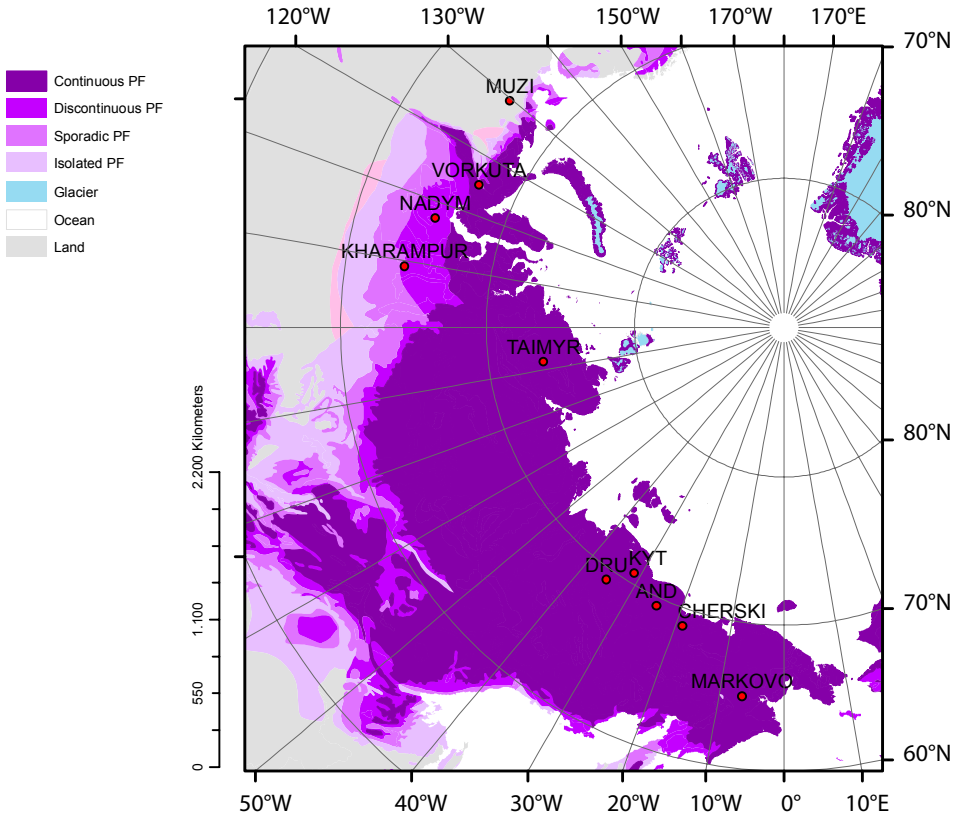

2.2. Satellite and in Situ Data

Both the ASCAT and ASAR instruments are active microwave sensors operating in C-band (frequency 5.2 GHz), which is suitable for SSM applications due to the contrasts in dielectric properties between dry and wet soils [24–26]. This forms the basis for SSM retrieval methods from microwave remote sensing. In the method by [8,43], instantaneous backscatter measurements are firstly normalized to a reference incidence angle (40°) and corrected for vegetation influences by making use of the scatterometer multi-incidence angle viewing capacities. The values are thereafter scaled between the so called dry (σ^0-dry, 0%) and wet (σ^0-wet, 100%) backscatter references, which correspond to the locally obtained historical minimum and maximum backscatter. The resulting soil moisture product is a percentage-index that relates to the uppermost 5 cm of the soil or (in the case of high water content) less. The relative soil moisture is thus calculated as [8,43]:

$$\theta s(t) = \frac{\sigma^0(40,t) - \sigma^0 dry(40,t)}{\sigma^0 wet(40,t) - \sigma^0 dry(40,t)} \quad (1)$$

where $\theta s(t)$ s(t) is the relative measure of the water content in the uppermost soil layer, ranging between zero and one (1%–100%). The difference between the wet and dry reference is defined as the sensitivity.

MetOp-A ASCAT (launched 2006, C-Band, VV polarization) together with its predecessors onboard ERS1 and ERS2 (European Remote Sensing Satellite) allows to obtain such references over a time period reaching back to 1991 [9]. The ASCAT incidence angle ranges from 25° to 65° and the backscatter is normalized to a standard incidence angle of 40° [44]. The MetOp ASCAT derived dataset which has been used for this study is available globally from TU Wien [8,9,27,43]. The high global coverage (approximately 2 days for mapping the entire globe) and coarse spatial resolution (25 km) makes it appropriate for comparison with global models, such as the ORCHIDEE land surface model.

Since the retrieval algorithm makes use of a change detection technique [12,19] it may be sensitive to other dynamics than those truly related to soil moisture, such as seasonal water body dynamics. In addition, the SSM values can only be derived under unfrozen conditions. Therefore, an algorithm for detecting the surface status and if necessary masking frozen surfaces (creating a surface status flag) has already been implemented for high-latitude applications [17,27]. The ASCAT time series data are available for a predefined discrete global grid (DGG; for definition see [17]). The grid format is based on the assumption that the Earth can be modeled as a rotated ellipsoid. Each grid cell over land is attributed a timeseries of backscatter values which are spatially resampled with an equal spacing of 12.5 km in latitude and longitude. The cells are identified by a unique grid cell index (GPI) [17]. For this study the global original dataset (without temporal aggregation) has been used, except for the model to remotely-sensed data comparison, where a weekly composite of the ASCAT data was used [45]. This specific dataset was developed as requested by users from the global modeling community within the DUE-permafrost project. The weekly composite consists in daily records where the retrieved SSM values from the preceding week are averaged.

The ASAR WS (C-band) dataset has a higher spatial resolution than ASCAT. ASAR was a ScanSAR instrument on board ENVISAT. Its spatial resolution in wide swath (WS) mode is 120 m for all sub-swaths [46]. ASAR had a revisit period of 35 days. Data availability is considerably constraint compared to scatterometer data. Suitable time series can be obtained for a range of locations across Siberia for selected years [47]. For this study, an ASAR WS dataset which was pre-processed over Northern Eurasia for the time period 2007–2008 within the framework of the European Space Agency (ESA) Support To Science Element (STSE) project ALANIS Methane [47–49] was used. Since the backscatter signal decreases with increasing incidence angle of the radar beam relative to the surface, the backscatter measurements are normalized to a common reference angle (30°) using the SAR Geophysical Retrieval Toolbox (SGRT), which is a scripting chain developed by the Institute of Photogrammetry and Remote Sensing (IPF). The scripting chain calls the commercial SARscape or the free NEST software, allowing for the automatization of the entire preprocessing procedure [47,50]. Single images are split up into predefined subsets and stored as time series stacks. In addition, the surface status flag developed for ASCAT [27] is used for masking the frozen ground condition and melting snow from the ASAR data. Point-station data measurements of maximum- and minimum temperature, precipitation and wind speed was obtained from the harmonized Global Summary of the Day and Month Observations dataset from the Global Precipitation Climatology Center [51].

2.3. Land Surface Model

The land surface model ORCHIDEE combines a multi-layer hydrological scheme recently improved for high-latitude processes [35], with a detailed representation of the energy and carbon cycles and the interface between soil and atmosphere. Of more relevance here is the hydrological scheme, which relies on a vertical discretization of the Richards equation allowing for physically-based diffusion of liquid water within the soil, up to a depth of 2 m. Soil freezing, vertical soil compaction and the effect of root water uptake, are also accounted for [52]. When rainfall of meltwater exceed the infiltration capacity of the uppermost soil layers, exceeding water either ponds or flows as surface runoff, depending on the local topography. The model uses as input standard meteorological data (precipitation, air humidity, pressure, temperature, and thermal and solar radiations), which are usually referred to as "forcing data". It produces several hydrological outputs, including vertically discretized soil moisture content, subsurface and surface runoff and evapotranspiration. The ORCHIDEE land surface model has proven able to reproduce observed hydrological features even in high-latitude regions [36].

The present study uses the model's output for vertically discretized volumetric SSM of daily resolution. In order to compare the average volumetric soil moisture calculated by the model to the weekly aggregated ASCAT SSM data, a number of adaptations were made. The modeled soil moisture from the uppermost 5 cm of the soil was masked out for frozen conditions and snow cover. For each model grid cell, the local historical maximum and minimum references were found so that the SWI of the model output could be established, rescaling between 0% and 100%. A weekly composite of the model output from the second step was then produced on a daily basis for consistent comparison with the ASCAT high-latitudes product from the DUE-permafrost project (see Sections 2.1 and 2.2) [36]. On average, the agreement between ORCHIDEE SSM and ASCAT SSM, as measured by the daily correlation coefficient of the model and ASCAT weekly composites, is however quite low over our study areas. Possible reasons for this outcome have been mentioned in the introduction.

2.4. Methodology

ASCAT SSM time series were retrieved for each DGG cell. For comparability, these DGG extents were used to define regions of interest (ROI) within each ASAR grid stack. For each study site, a 3100 km^2 large area was divided into meshes of hexagons using the GPI as center points. This resulted in 9–11 hexagonal ROI within each of the ten sites (Figure 2 shows the 11 ROI in Cherski).

A supervised classification (minimum distance) was performed on ice free ASAR acquisitions with summer maximal lake expansion and water/land contrasts, to separate land from water. Higher backscatter than the typical C-band backscatter for smooth water surfaces may be caused by (1) ice covers on water surfaces and (2) wind and rain action. Wave ripples on the water body surface due to wind and rain increase the surface roughness and hence lead to diffuse scattering and high backscatter values [47,53]. The persistence of lake ice on large lakes well into the summer and the associated water body classification issues have already been pointed out by [47]. To identify any water surface effects, the water areas identified by the classification were replaced by the value −20 dB, which is a typical C-band backscatter value for smooth water surfaces in the used dataset [47,54]. This builds the reference dataset.

Figure 2. ASAR acquisitions from Cherski, 2008. (**A**) shows a time with high wind speed and precipitation (11 August 2007); (**B**) shows a time with prevailing ice cover (17 June 2007); (**C**) illustrates an acquisition from 6 July 2007 when there is no disturbances on the water surface. The overlain hexagon mesh shows the ROI and their grid point index number.

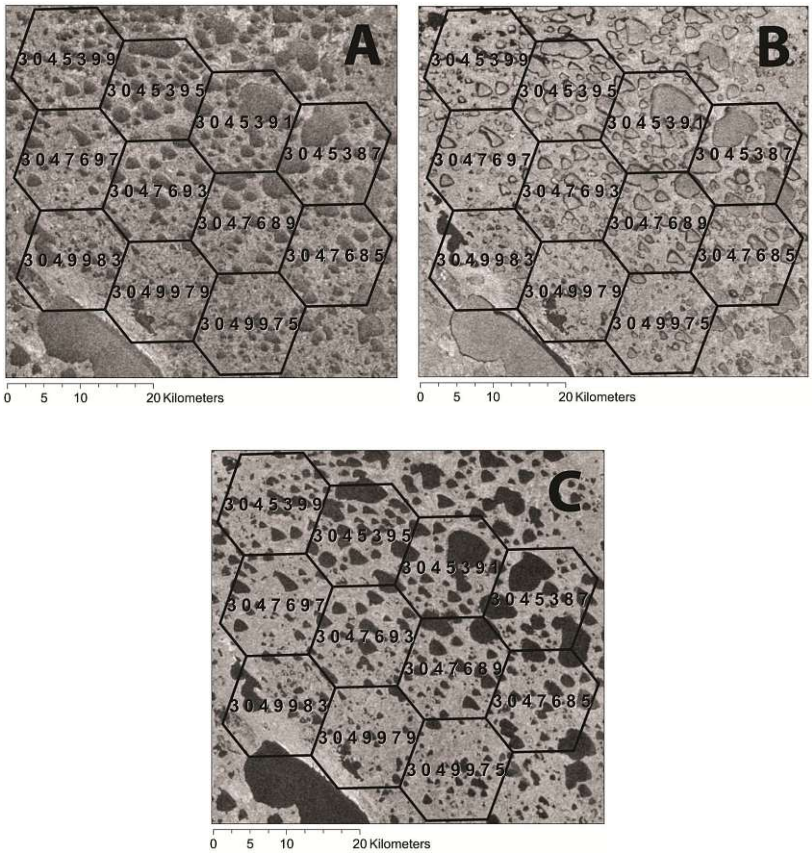

The mean backscatter result of the masking and replacement by a reference value, henceforth referred to as refilling, was calculated for each ROI and for each available acquisition. This average from the reference datasets was plotted against the original dataset. The mask effect, $\Delta\overline{\sigma^0}$, is the difference between the original and the reference ROI average for each available acquisition. The acquisitions were also visually interpreted together with meteorological data in order to identify any rain, ice and wind conditions. In addition to the above described specific examination of the surface effects (potentially from ice, rain and/or wind) it was investigated whether the level of agreement between the ASCAT and ORCHIDEE SSM results could be related to the abundance of lakes. For this purpose, open water fraction and lake size were calculated for each ROI from the ASAR WS data by converting the previously described water classification to polygons. Criteria related to total water cover and lake size were defined and used to separate ROI into three categories:

(A) More than 20% lake area per total area including only lakes larger than 10 km^2
(B) More than 20% lake area per total area including only lakes smaller than 10 km^2
(C) Less than 20% lake area per total area.

The fractional area of lake, lake count, $\Delta\overline{\sigma^0}$, ASCAT sensitivity and ASCAT-ORCHIDEE agreement and the correlation thereof, were computed and analysed for each category. Here, the correlation is

meant to determine whether significant relationships exist between lake characteristics, identified lake effect on backscatter ($\Delta\overline{\sigma^0}$) and ASCAT SSM retrieval characteristics (sensitivity) or performance (here assessed by the ASCAT-ORCHIDEE agreement). Since ice is assumed more likely to be present in early summer than the high summer months, the $\Delta\overline{\sigma^0}$ during June was calculated separately from that during July-August, to isolate eventual impacts of prevailing ice cover. For the same reason, a two sampled t-test of the $\Delta\overline{\sigma^0}$ from June in relation to that in July-August was done in order to know if there was a significant difference between these two time periods. Analyses of higher temporal resolution than monthly could not be done due to the irregular acquisition intervals by ENVISAT ASAR WS [47].

3. Results

The original mean backscatter for the ROIs is always higher than or equal to the mean backscatter from the reference image since frozen ground conditions and spring snowmelt events have been excluded. Figure 3A shows the backscatter for one of the ROI in Cherski during 2007, including the mean unmasked backscatter (black diamonds) and the mean of the backscatter after having applied the water mask and replaced the backscatter values with the smooth water surface reference value (-20 dB) (red crosses). It can be seen in Figure 3A and that the difference is in the order of more than 2 dB during several occasions during the warm months of the year. Note that the winter months are excluded since ASCAT soil moisture is derived only under unfrozen conditions (see Section 2.2). Figure 3B–D shows the temperature, wind speed and precipitation for the same site and time period.

In three of the acquisitions from Cherski in 2007 where $\Delta\overline{\sigma^0}$ was found to be high, either precipitation or high wind speed was identified by visual interpretation of the ASAR data and in the meteorological record. One example is the acquisition from 11 August 2007, illustrated in Figure 2A (see Figure 3D for precipitation data). Figure 2B shows the same area but an acquisition with presumed ice cover. One occasion with presumed prevailing ice cover (17 June 2007) was visually identified for this site during 2007, but strong effects were not recognized compared to the reference (smooth surface). Figure 2C shows relatively smooth water surface conditions for Cherski (6 July 2007), as well as the limits of the hexagonal ROI for this site and their GPI numbers. For Kytalyk, Andryuskino and partly for Druzhina, the results were similar to those from Cherski. In Kharampur, Muzi, Nadym, Taimyr and Vorkuta, $\Delta\overline{\sigma^0}$ is generally low and no significant backscatter change that could be related to weather conditions was observed in the ASAR data. Scatterplots of the reference values as a function of the original data for one of the ROI in Cherski (subject to high $\Delta\overline{\sigma^0}$) and one of the ROI in Kharampur (not subject to a high $\Delta\overline{\sigma^0}$) are shown in the left and right panel of Figure 4, respectively.

To isolate the potential effect from prevailing ice cover the early summer months are separated from the late summer months: the acquisitions from June are plotted as black diamonds whereas those from July and August as red crosses. Figure 4B shows that the mean from the unmasked backscatter in the case of Kharampur is similar to that of the masked (reference dataset). A clear difference between $\Delta\overline{\sigma^0}$ in the low agreement sites compared to the high agreement sites can be seen. It can not be concluded that $\Delta\overline{\sigma^0}$ is different during the early summer months from the later summer months. When statistically testing the null hypothesis that the $\Delta\overline{\sigma^0}$ is not significantly different in June compared to that in July–August over

all ROIs, the *p*-value is 0.616, which is insufficient for rejecting the hypothesis (regardless if choosing any of the common levels of significance: 0.10, 0.05 or 0.01) and supports our visual analysis.

Figure 3. (**A**) Time seriesof averaged backscatter Cherski 2007, ROI 3045391. Red crosses correspond to the reference dataset, black diamonds show the original mean backscatter; (**B**) The maximum (black) and minimum (red) temperature over 24 h); (**C**) wind speed at 03h00 (black), 09h00 (red) and 15h00 (blue); and (**D**) total precipitation for 24 h. Meteorological data from the harmonized CPC Global Summary of the Day and Month Observations data set [51]. Dates are given in BE standard.

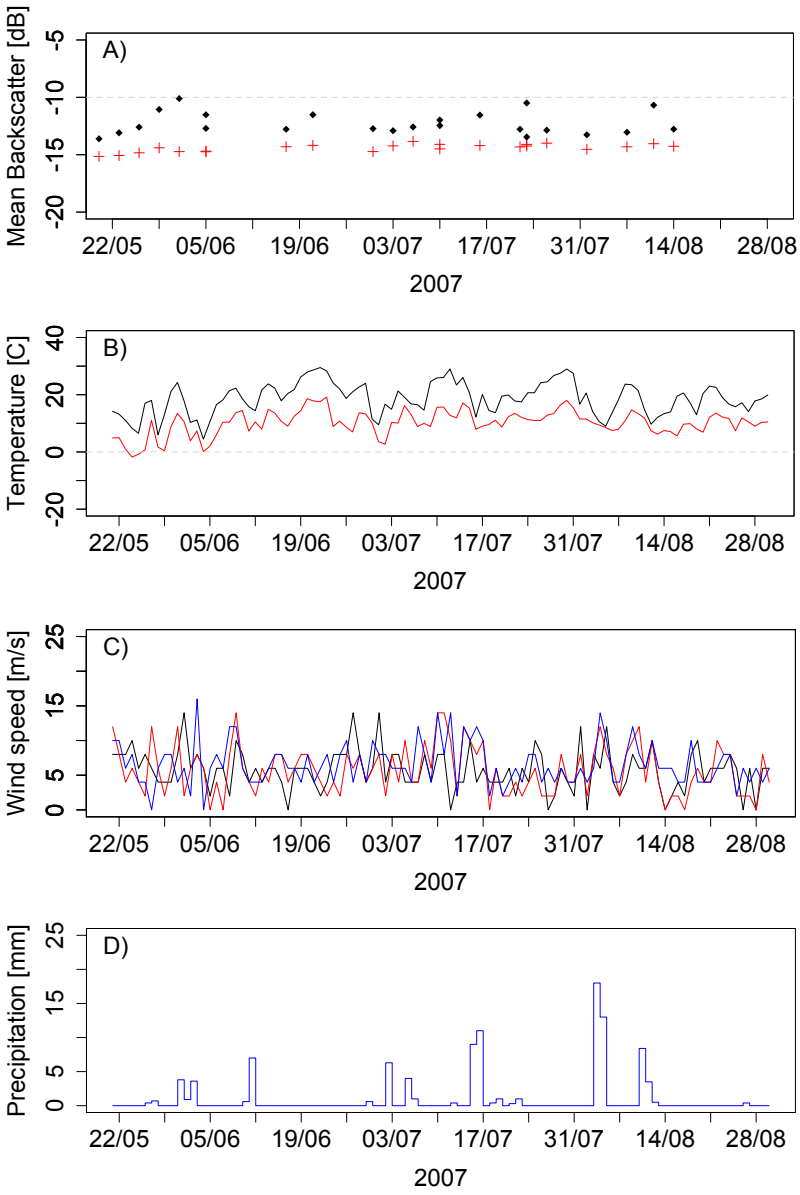

Figure 4. Scatterplots of masked against unmasked ASAR backscatter for (**A**) Cherski (ROI 3045387) and (**B**) Kharampur (ROI 2950873). The masking implies that lakes have been masked and re-filled by −20 dB, as a reference backscatter value for smooth water surfaces. Red crosses represent acquisitions in June and black represent acquisitions from July–August. The zero difference line is shown as a black line.

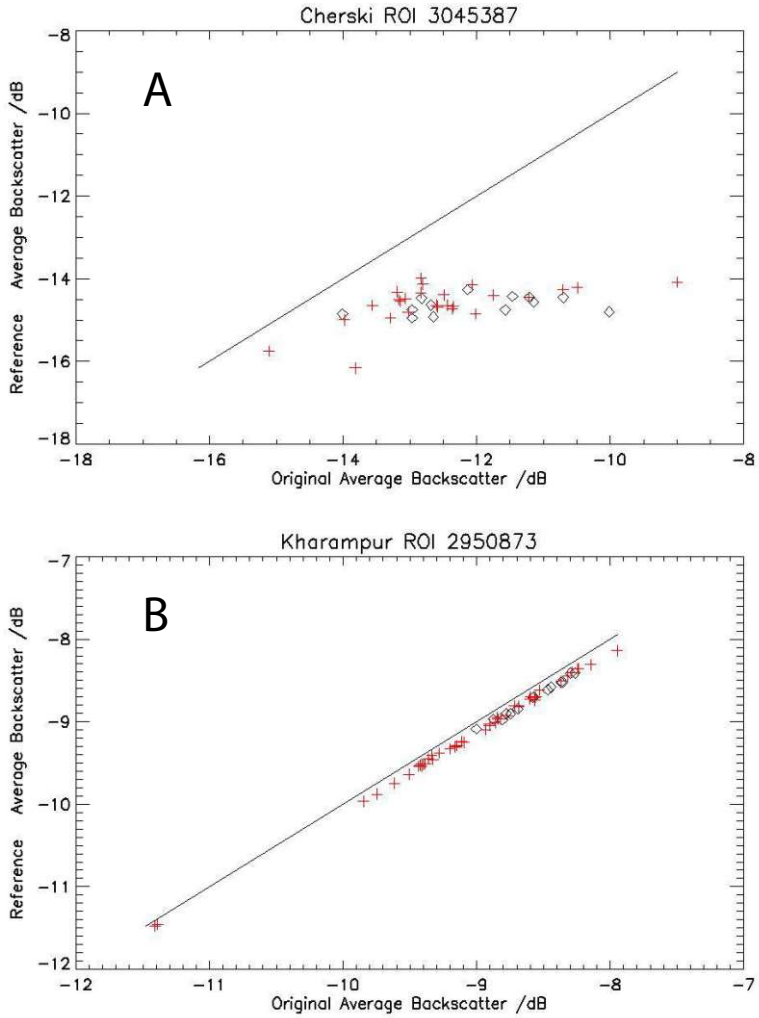

The extracted data for each ROI, including $\Delta\overline{\sigma^0}$, lake count, lake area, ASCAT sensitivity and daily correlation with ORCHIDEE from [36] are given in Table 1. This last value is a measure of agreement between the modeled and remotely-sensed surface soil moistures in terms of temporal dynamics. Out of the total 95 ROI, this table includes the 15 ROI with the maximum and the 15 with minimum $\Delta\overline{\sigma^0}$ in June, respectively. Further, Table 2 shows the correlation matrix for the parameters from Table 1, calculated from all the 95 ROI, and separately for the low (including negative high correlation) and the high agreement sites.

For the low agreement sites only (including negative correlation), the sensitivity correlates positively with the total lake area (0.55) and the total number of lakes (0.68) and shows a strong correlation with $\Delta\overline{\sigma^0}$, in June (0.71) slightly more so than in July–August (0.68). The ASCAT-ORCHIDEE agreement correlates negatively with the sensitivity (−0.68) but, regarding $\Delta\overline{\sigma^0}$, displays similar agreement in June (−0.53) and in July–August (−0.57). Further, it correlates moderately with the lake area (−0.55) and

only weakly with the lake count (−0.30). That is to say, the areas with a low ASCAT-ORCHIDEE agreement correspond to areas with a high water fraction, although they are not linked to a high number of lakes. It is found that the ROI within the lake size group A and B are almost exclusively located within areas of low agreement between the model output and the remote sensing product. This is the case for the majority of the ROI in Andryuskino, Cherski and Druzhina. For Kytalyk, only the ROI with large lakes present are related to low agreement between the model output and remote sensing product. A few ROI within the site Muzi also fall within the group B but the daily correlation here is positive. Muzi contains no lakes but the low $\Delta\overline{\sigma^0}$ seen here is related to the masking out of a river rather than lakes. The ROI within the lake size group A and B also show a strong $\Delta\overline{\sigma^0}$, ranging from 0.55 to 2.61 dB in the case of group A, from 0.14 to 2.38 for group B, whereas no more than from 0.00 to 0.94 for group C. Lake area is more strongly correlated to the $\Delta\overline{\sigma^0}$ (0.92 in June, 0.91 in July–August) than the lake count is to the $\Delta\overline{\sigma^0}$ (0.46 in June, 0.39 in July–August). Considering the correlation matrix for the high agreement sites, only weak correlation if any at all are found, the caveat being the correlation between lake area and $\Delta\overline{\sigma^0}$.

Table 1. Characteristics of the 15 ROIs with the highest $\Delta\overline{\sigma^0}$ and the 15 lowest, respectively (separated by the dashed line). The number of lakes, lake area percentage per total ROI area, sensitivity (ASCAT dry-wet reference) in decibel, $\Delta\overline{\sigma^0}$ in decibel and the daily correlation between the ORCHIDEE model and ASCAT SSM are presented in the columns. The ROIs in group A are written in bold, B in italic and C as plain text. The site names in the table are Cherski (CHE), Kytalyk (KYT), Taimyr (TAI), Andryuskino (AND), Druzhina (DRU), Voruta (VOR), Muzi (MUZ) and Kharampur (KHA).

Site Name	GPI	June $\Delta\overline{\sigma^0}$ (dB)			July–August $\Delta\overline{\sigma^0}$ (dB)			Lake		Sensitivity	Daily
		Min	Max	Mean	Min	Max	Mean	Count	Area (%)	Mean (dB)	Correlation
CHE	**3045387**	**0.85**	**4.78**	**2.61**	**1.01**	**5.09**	**2.44**	**34**	**44.84**	**7.29**	**−0.35**
CHE	**3045391**	**0.41**	**4.62**	**2.60**	**0.67**	**4.50**	**2.22**	**36**	**40.82**	**7.49**	**−0.35**
KYT	**3084867**	**1.43**	**4.16**	**2.46**	**1.09**	**3.98**	**2.46**	**12**	**39.48**	**6.27**	**−0.17**
CHE	*3045395*	*0.69*	*4.25*	*2.38*	*0.02*	*4.05*	*1.80*	*35*	*41.83*	*7.08*	*−0.35*
TAI	3120067	0.94	4.12	2.25	0.42	3.85	2.97	3	41.17	5.22	0.10
CHE	**3047693**	**1.96**	**2.37**	**2.19**	**1.46**	**2.45**	**1.95**	**27**	**23.84**	**7.65**	**−0.35**
TAI	3118181	0.83	3.53	2.08	0.38	3.33	2.70	1	32.44	6.01	0.10
CHE	**3047689**	**0.49**	**3.21**	**1.82**	**0.59**	**3.53**	**1.66**	**41**	**32.19**	**7.73**	**−0.35**
CHE	*3047685*	*0.21*	*3.33*	*1.81*	*0.49*	*4.01*	*1.70*	*42*	*31.99*	*7.85*	*−0.21*
CHE	*3047697*	*1.54*	*1.88*	*1.74*	*1.31*	*2.06*	*1.59*	*35*	*17.26*	*6.89*	*−0.35*
AND	**3049899**	**0.62**	**2.60**	**1.72**	**0.36**	**2.05**	**1.19**	**43**	**23.83**	**6.06**	**−0.13**
AND	*3052177*	*0.49*	*2.24*	*1.47*	*0.05*	*1.91*	*1.01*	*27*	*23.44*	*5.89*	*0.00*
DRU	*3033509*	*0.21*	*2.92*	*1.46*	*0.47*	*2.85*	*1.28*	*22*	*18.91*	*5.74*	*−0.26*
AND	*3047609*	*0.61*	*2.32*	*1.46*	*0.41*	*1.86*	*1.08*	*45*	*22.26*	*6.36*	*0.00*
CHE	*3045399*	*0.38*	*2.25*	*1.42*	*0.20*	*2.35*	*1.04*	*45*	*30.09*	*6.41*	*−0.35*
KHA	2948131	0.00	0.01	0.01	0.01	0.01	0.01	0	0.00	5.26	0.34
TAI	3120063	0.00	0.01	0.00	0.00	0.01	0.00	0	0.00	5.18	0.10
KHA	2945369	0.00	0.00	0.00	0.00	0.01	0.00	0	0.00	5.40	0.34
VOR	3013089	0.00	0.00	0.00	0.00	0.00	0.00	5	0.61	5.91	0.45
MUZ	2961321	0.00	0.00	0.00	0.00	0.00	0.00	0	0.00	4.50	0.23

Table 2. Correlation matrix including the number of lakes, lake area percentage per total ROI area, sensitivity (ASCAT dry-wet reference) in decibel, $\Delta\overline{\sigma^0}$ in decibel and the daily correlation between the ORCHIDEE model and ASCAT SSM. The correlation is retrieved for all the 95 ROI in total. The correlations for ROI with lower agreement than or equal to zero (47 ROI) are presented separated from those with higher agreement than zero (48 ROI). See legend below the table for explanation of bold, italic and asterisk.

Low Agreement Sites

	Lake count	Lake area	Sensitivity	June $\Delta\overline{\sigma^0}$	July–August $\Delta\overline{\sigma^0}$	Daily correlation
Lake count			***	***	***	**
Lake area			***	***	***	***
Sensitivity	*0.55*	*0.68*		***	***	***
June $\Delta\overline{\sigma^0}$	0.46	**0.92**	**0.71**			***
July–August $\Delta\overline{\sigma^0}$	0.39	**0.91**	*0.68*			***
Daily correlation	−0.30	*−0.55*	*−0.68*	*−0.53*	*−0.57*	

High Agreement Sites

	Lake count	Lake area	Sensitivity	June $\Delta\overline{\sigma^0}$	July–August $\Delta\overline{\sigma^0}$	Daily correlation
Lake count			|	|	|	|
Lake area			|	***	***	|
Sensitivity	0.03	−0.04		|	|	|
June $\Delta\overline{\sigma^0}$	0.16	**0.97**	0.00			|
July–August $\Delta\overline{\sigma^0}$	0.10	**0.96**	0.00			|
Daily correlation	0.01	−0.25	0.38	−0.25	−0.30	

| = *p*-value insufficient; **bold = strong correlation**; *italic = moderate correlation*; ** = *p*-value < 0.01; *** = *p*-value < 0.001.

Figure 5 shows $\Delta\overline{\sigma^0}$ from June in dB plotted against the ASCAT-ORCHIDEE agreement. It can be seen that the $\Delta\overline{\sigma^0}$ increases with daily correlation, notably so for group A and B. The R^2 can not be said to be strong for any of the groups. However, R^2 for group A is notably stronger than both B and C. Results are similar for the two investigated time periods, e.g., June as well as July–August.

Figure 5. Spatially (within each ROI) and temporally (June only) averaged backscatter ($\Delta\overline{\sigma^0}$) in dB plotted against the ASCAT-ORCHIDEE agreement. The regions of interest with high total lake area percentage and notably large lakes (group A) are shown as blue diamonds and those with high lake area including small lakes (group B) are shown as red squares. Regions with generally little lake area (group C) are shown as green triangles. This plot includes all the 95 ROI.

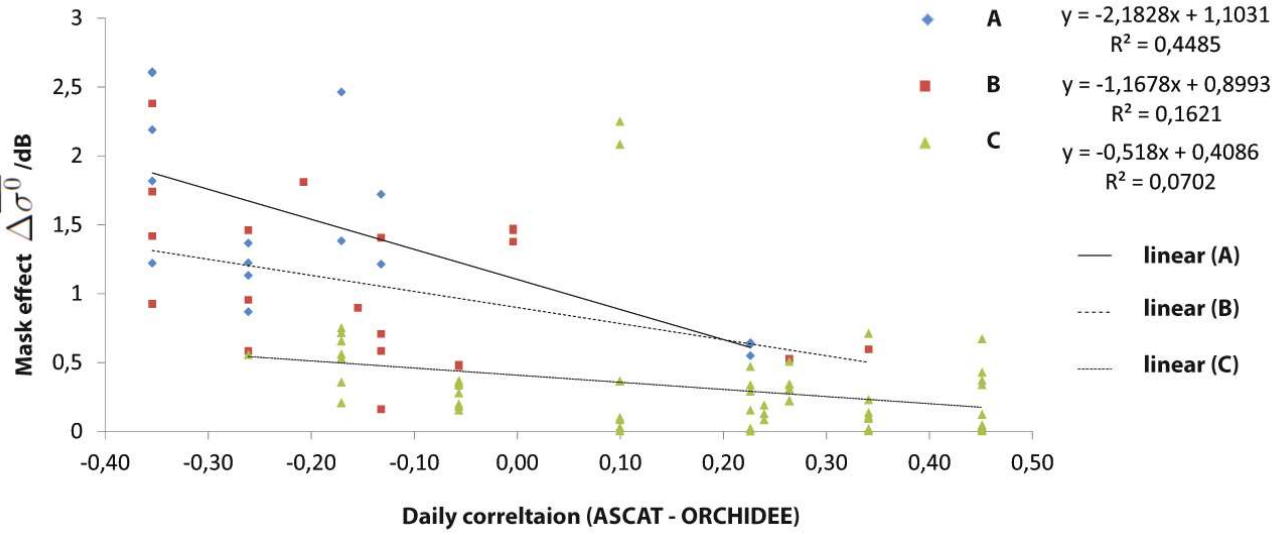

4. Discussion

The results confirm that open water surfaces of tundra lakes are typically rough with respect to the used wavelength (C-band). Indeed, authors have previously estimated an on average −4.9 dB higher backscatter (same preprocessing) than under calm conditions [50]. Spatially averaged backscatter deviations for the ROIs which represent the ASCAT cells and include both water and land area reach up to 5 dB. High $\Delta\overline{\sigma^0}$ correspond with times of high wind speed or precipitation. It is here hypothesized that locations with low (including negative) agreement between the ASCAT and ORCHIDEE SSM correspond to areas that have many and/or large lakes and that the $\Delta\overline{\sigma^0}$ at the same locations is high. At sites with positive correlation between ASCAT and the landsurface model SSM (Kharampur, Muzi, Nadym, Taimyr and Vorkuta), $\Delta\overline{\sigma^0}$ is generally low (<0.71 dB). There are two exceptions in Taimyr, where the mask effect is as large as 2.08 and 2.25 dB. These cases correspond to the only ROI in Taimyr with a large total water area (32.44% and 41.17%, respectively). This is however not reflected in the the daily correlation between ASCAT and ORCHIDEE, which is 0.10 for all of the ROI in Taimyr. This could thus be explained by reasons other than water bodies but related to the model, brought up in the Section 2.3.

At Markovo (eastern Siberia), the model-SSM retrieval agreement is low (−0.06). Here, the $\Delta\overline{\sigma^0}$ is less pronounced. It is in fact comparable to the high agreement sites, although the site is located in an area of low agreement. For Markovo, the low agreement between the model output and the ASCAT data could be explained by other reasons than water bodies; it is more likely due to the exceptionally scarce forcing weather data from this part of Siberia [36].

Figure 5 further confirms that there is a difference between the water fraction and lake size classes (groups A, B and C) regarding the dependency of the ASCAT-ORCHIDEE agreement and $\Delta\overline{\sigma^0}$. Results are similar for the two investigated time periods (June, July-Aug). Although there is some scatter among the categories and the R^2 value is moderate, it is found that the magnitude of $\Delta\overline{\sigma^0}$ for group C appears to be independent from the ASCAT-ORCHIDEE correlation whereas it explains 16%–44 % of the variation for group A and B.

At sites with an ASCAT-ORCHIDEE correlation lower than −0.21, the average June $\Delta\overline{\sigma^0}$ ranges from 0.56–2.26 dB. This corresponds to 10%–35% of the overall ASCAT sensitivity to soil moisture, which in turn would translate into as much as 35% higher relative soil moisture value if the difference in ASAR backscatter ($\Delta\overline{\sigma^0}$) would be directly comparable to the ASCAT soil moisture product. For single acquisitions it amounts to 60%–70% in areas of 40%–45% water fraction. A direct comparison to ASCAT backscatter and quantification of impact on soil moisture retrieval is however limited. One would need to make the assumption that the averaged ASAR WS backscatter over the ROI corresponds to the ASCAT backscatter. The hexagonal grid of ROI generated in this study is merely an approximation of the ASCAT grid cells. Furthermore, the absolute backscatter values may deviate due to incidence angle differences (ranging from 25° to 65°) and differences in signal contribution over the footprint for ASCAT [44] as well as actual soil moisture changes. In the cases when the high backscatter events coincide with precipitation events, the impact of dielectric properties changes would need to be taken into account.In the cases when the high backscatter events coincide with precipitation events, the impact of dielectric properties changes would need to be taken into account: it is difficult to separate the backscatter variations due to the actual increase in soil moisture from the action that the rain causes on the surface. Furthermore, it should be considered that the ASCAT dataset which has been used for comparison with ORCHIDEE has been aggregated to weekly time steps. One can expect a smoothing of the backscatter variations in this case, so the actual disagreement with the model may be higher when compared on a daily basis.

For soil moisture retrieval the signal is impacted if the area covered by open water surface within the footprint is large [38]. A surface water fraction flag, derived from the Global Lakes and Wetlands Database [55], exists but it does not take wetland dynamics, temporary inundation and small lakes into account [54]. An improved flag of this kind could be derived from ASAR data [13,56]. Tundra lakes can be considerably smaller than the ASAR WS resolution [57]. The impact of these small lakes would need to be analyzed in addition for the development of a correction algorithm of the scatterometer soil moisture datasets, e.g., by taking into account subpixel-scale fraction of water cover [57].

5. Conclusions

This study examines backscatter variabilities other than related to soil moisture in order to address challenges in radar soil moisture retrieval that are specific for in the Arctic. The impact on the soil moisture retrieval is investigated for sites across Siberia, including permafrost longterm monitoring sites. Satellite derived surface soil moisture datasets would provide valuable additional information to point measurements in these regions. Envisat ASAR WS imaging radar data are investigated in order to identify seasonal variations in backscatter that are not related to SSM but to lake cover surface status.

This gives an indication for the magnitude of the impact of such features on the coarser spatial resolution ASCAT SSM retrieval, and cast some light on the model-to-ASCAT low agreement in SSM, highlighted by a previously published study [36]. Different techniques and sensors can be used for SSM retrieval from satellites [7,8,10]. The findings of this study can be applied to systems relying on similar principles: change detection approach in a backscattered signal that is impacted by surface soil moisture but also by surface conditions, e.g., water surface roughness or frozen conditions. Most importantly, these specific findings are applicable to C-band sensors.

Identified backscatter difference is in the order of 2 dB on the mean backscatter over several weeks and up to 5 dB on specific acquisitions in the areas with low ORCHIDEE-ASCAT agreement (no or negative correlation). In comparison, the assumed ASCAT sensitivity for soil moisture changes reaches approximately 7 dB in these areas. A direct translation of the identified difference to deviations of the soil moisture values from the actual values would need to take sensor and data processing differences into account.

Regions with high backscatter deviations (averaged over ASCAT grid cell) from the reference dataset representing smooth water surfaces ($\Delta\overline{\sigma^0}$) are however evidently characterized by a high percentage of total lake area, *i.e.*, many of the ROI in eastern Siberia: Cherski, Andryuskio, Druzhina and Kytalyk. The sites Kharampur, Taimyr, Nadym, Vorkuta and Muzi (western and central Siberia), show low $\Delta\overline{\sigma^0}$ and are areas with few lakes. In the case of Markovo (far eastern Siberia) the low agreement between the model output and the SSM product is more likely explained by the exceptionally scarce weather data from this area used to force the model [36]. Although events of wind and precipitation identified by the meteorological data only occurred infrequently for each site, the correlation between the backscatter deviation and the ASCAT-ORCHIDEE agreement together with the lake size distribution lead to the conclusion that water body fraction and water body size is one explanation for the disagreement between the ASCAT and ORCHIDEE SSM. In this context, it should be considered that the ORCHIDEE model does not represent ephemeral lakes (*i.e.*, normally dry lakes that fills with water for short periods), which are an additional source of error for ORCHIDEE in lake-rich areas.

The low and negative correlation sites compared to the high agreement sites clearly show different results for the $\Delta\overline{\sigma^0}$ in relation to the total lake expansion and size distribution. However, no significant difference was shown between the early and late summer months. The presence of ice cover on lakes does not give strong effect on the $\Delta\overline{\sigma^0}$ in this study.

In addition to the above and other model-related issues as discussed by [36], the low agreement between ORCHIDEE and ASCAT SSM in the Siberian lowlands is likely related to the existence of water bodies. Therefore, it should be noted that in circumpolar lowland permafrost areas, where ponds and lakes are common features, the presence of water bodies has an impact on the ASCAT SSM retrieval. This supports what has previously been pointed out about open water having a disturbing influence on the signal and thus for the surface soil moisture retrieval if the area covered by open water surface within the footprint is large [38]. In Siberia, an improved surface flag product that takes into account wetland dynamics could be derived from Synthetic Aperture Radar (SAR) imagery [32,53]. The usage of higher spatial resolution data for SSM retrieval as available from Sentinel-1 is required in regions with large water fractions, including lowland permafrost environments.

Acknowledgments

The authors acknowledge financial support by the European Union FP7-ENV project PAGE21 (Changing Permafrost in the Arctic and its Global effects in the 21st century) under contract No. GA282700. The ALANIS project was funded by the European Space Agency (ESA) Support to Science Element (STSE) program (ESRIN Contr. No. 4000100647/10/I-LG).

Author Contributions

All co-authors have substantially contributed to the writing of the manuscript. In addition, Elin Högström has carried out all analyses and prepared the first draft. Anna Maria Trofaier has set the study into a wider context including SAR applications, took care of layout and provided native English editing. All items related to land surface modelling have been prepared by Isabella Gouttevin. Annett Bartsch developed the concept for the study and provided expertise in EO data handling.

Conflicts of Interest

The authors declare no conflict of interest.

References

1. IPCC. Observations: Cryosphere. In Proceedings of the Climate Change 2013: The Physical Science Basis. Contribution of Working Group I to the Fifth Assessment Report of the Intergovernmental Panel on Climate Change, Stockholm, Sweden, 23–26 September 2013; pp. 362–364.
2. Friborg, T.; Soegaard, H.; Christensen, T.; Lloyd, C.; Panikov, N. Siberian wetlands: Where a sink is a source. *Geophys. Res. Lett.* **2004**, *30*, doi:10.1029/2003GL017797
3. Christensen, T.R.; Johansson, T.R.; Akerman, H.J.; Mastepanov, M.; Malmer, N.; Friborg, T.; Crill, P.; Svensson, B H. Thawing sub-arctic permafrost: Effects on vegetation and methane emissions. *Geophys. Res. Lett.* **2004**, *31*, doi:10.1029/2003GL018680
4. Langer, M.; Westermann, S.; Heikenfeld, M.; Dorn, W.; Boike, J. Satellite-based modeling of permafrost temperatures in a tundra lowland landscape. *Remote Sens. Environ.* **2013**, *135*, 12–24.
5. Swenson, S.; Lawrence, D.; Lee, H. Improved simulation of the terrestrial hydrological cycle in permafrost regions by the Community Land Model. *J. Adv. Model. Earth Syst.* **2012**, *4*, doi:10.1029/2012MS000165.
6. Lupascu, M.; Welker, J.; Seibt, U.; Maseyk, K.; Xu, X.; Czimczik, C. High Arctic wetting reduces permafrost carbon feedbacks to climate warming. *Nat. Clim. Chang.* **2013**, *4*, 51–55.
7. Kimball, J.S.; Jones, L.A.; Zhang, K.; Heinsch, F.A.; McDonald, K.C.; Oechel, W.C. A satellite approach to estimate land—Atmosphere exchange for boreal and arctic biomes using MODIS and AMSR-E. *IEEE Trans. Geosci. Remote Sens.* **2009**, *47*, 569–587.
8. Wagner, W.; Noll, J.; Borgeaud, M.; Rott, H. Monitoring soil moisture over the Canadian prairies with the ERS scatterometer. *IEEE Trans. Geosci. Remote Sens.* **1999**, *37*, 206–216.

9. Naeimi, V.; Bartalis, Z.; Wagner, W. ASCAT soil moisture: An assessment of the data quality and consistency with the ERS scatterometer heritage. *J. Hydrometeorol.* **2009**, *10*, 555–563.
10. Njoku, E.G.; Jackson, T.J.; Lakshmi, V.; Chan, T.K.; Nghiem, S.V. Soil moisture retrieval from AMSR-E. *IEEE Trans. Geosci. Remote Sens.* **2003**, *41*, 215–229.
11. Koike, T.; Nakamura, Y.; Kaihotsu, I.; Davva, G.; Matsuura, N.; Tamagawa, K.; Fujii, H. Development of an Advanced Microwave Scanning Radiometer (AMSR-E) algorithm of soil moisture and vegetation water content. *Annu. J. Hydraul. Eng. JSCE* **2004**, *48*, 217–222.
12. Wagner, W.; Bloschl, G.; Pampaloni, P.; Calvet, J.C.; Bizzarri, B.; Wigneron, J.P.; Kerr, Y. Operational readiness of microwave remote sensing of soil moisture for hydrologic applications. *Nord. Hydrol.* **2007**, *38*, 1–20.
13. Bartsch, A.; Balzter, H.; George, C. The influence of regional surface soil moisture anomalies on forest fires in Siberia observed from satellites. *Environ. Res. Lett.* **2009**, *4*. doi:10.1088/1748-9326/4/4/045021.
14. Künzer, C.; Zhao, D.; Scipal, K.; Sabel, D.; Naeimi, V.; Bartalis, Z.; Hasenauer, S.; Mehl, H.; Dech, S.; Wagner, W. El Niño influences represented in ERS scatterometer derived soil moisture data. *Appl. Geogr.* **2009**, *29*, 463–477.
15. Paulik, C.; Dorigo, W.; Wagner, W.; Kidd, R. Validation of the ASCAT soil water index using *in situ* datafrom the international soil moisture network. *Int. J. Appl. Earth Obs. Geoinf.* **2014**, *30*, 1–8.
16. Brocca, L.; Melone, F.; Moramarco, T.; Wagner, W.; Hasenauer, S. ASCAT soil wetness index validation through *in situ* and modeled soil moisture data in central Italy. *Remote Sens. Environ.* **2010**, *114*, 2745–2755.
17. Naeimi, V.; Scipal, K.; Bartalis, Z.; Hasenauer, S.; Wagner, W. An improved soil moisture retrieval algorithm for ERS and METOP scatterometer observations. *IEEE Trans. Geosci. Remote Sens.* **2009**, *47*, 1999–2013.
18. Albergel, C.; de Rosnay, P.; Gruhier, C.; Muñoz-Sabater, J.; Hasenauer, S.; Isaksen, L.; Kerr, Y.; Wagner, W. Evaluation of remotely sensed and modelled soil moisture products using global ground-based *in situ* observations. *Remote Sens. Environ.* **2012**, *118*, 215–226.
19. Wagner, W.; Pathe, C.; Doubkova, M.; Sabel, D.; Bartsch, A.; Hasenauer, S.; Blöschl, G.; Scipal, K.; Martínez-Fernández, J.; Löw, A. Temporal stability of soil moisture and radar backscatter observed by the Advanced Synthetic Aperture Radar (ASAR). *Sensors* **2008**, *8*, 1174–1197.
20. Doubkova, M.; van Dijk, A.I.J.M.; Sabel, D.; Wagner, W.; Blöschl, G. Evaluation of the predicted error of the soil moisture retrieval from C-band SAR by comparison against modelled soil moisture estimates over Australia. *Remote Sens. Environ.* **2012**, *120*, 188–196.
21. Bartsch, A.; Sabel, D.; Wagner, W.; Park, S.E. Considerations for derivation and use of soil moisture data from active microwave satellites at high latitudes. In Proceedings of the 2011 IEEE International Geoscience and Remote Sensing Symposium (IGARSS), Vancouver, BC, Canada, 24–29 July 2011; pp. 3132–3135.

22. Ulaby, F.T.; Moore, R.K.; Fung, A.K. *Microwave Remote Sensing, Active and Passive, III, Radar Remote Sensing and Surface Scattering and Emission Theory*; Artech House Publishers: London, UK/Boston, MA, USA, 1986.
23. Scipal, K.; Drusch, M.; Wagner, W. Assimilation of a ERS scatterometer derived soil moisture index in the ECMWF numerical weather prediction system. *Adv. Water Resour.* **2008**, *31*, 1101–1112.
24. Ulaby, F.T.; Moore, R.K.; Fung, A.K. *Microwave Remote Sensing, Active and Passive, II, Radar Remote Sensing and Surface Scattering and Emission Theory*; Artech House Publishers: London, UK/Boston, MA, USA, 1982.
25. Way, J.; Zimmermann, R.; Rignot, E.; McDonald, K.; Oren, R. Winter and spring thaw as observed with imaging radar at BOREAS. *J. Geophys. Res. Atmos. (1984–2012)* **1997**, *102*, 29673–29684.
26. Wegmüller, U. The effect of freezing and thawing on the microwave signatures of bare soil. *Remote Sens. Environ.* **1990**, *33*, 123–135.
27. Naeimi, V.; Paulik, C.; Bartsch, A.; Wagner, W.; Kidd, R.; Park, S.E.; Elger, K.; Boike, J. ASCAT Surface State Flag (SSF): Extracting information on surface freeze/thaw conditions from backscatter data using an empirical threshold-analysis algorithm. *IEEE Trans. Geosci. Remote Sens.* **2012**, *50*, 2566–2582.
28. Bartsch, A. Ten years of SeaWinds on QuikSCAT for snow applications. *Remote Sens.* **2010**, *2*, 1142–1156.
29. Bartsch, A.; Kidd, R.A.; Wagner, W.; Bartalis, Z. Temporal and spatial variability of the beginning and end of daily spring freeze/thaw cycles derived from scatterometer data. *Remote Sens. Environ.* **2007**, *106*, 360–374.
30. Entekhabi, D.; Njoku, E.G.; O'Neill, P.E.; Kellogg, K.H.; Crow, W.T.; Edelstein, W.N.; Entin, J.K.; Goodman, S.D.; Jackson, T.J.; Johnson, J.; *et al.* The soil moisture active passive (SMAP) mission. *IEEE Proc.* **2010**, *98*, 704–716.
31. Brocca, L.; Moramarco, T.; Melone, F.; Wagner, W.; Hasenauer, S.; Hahn, S. Assimilation of surface- and root-zone ASCAT soil moisture products into rainfall-runoff modeling. *IEEE Trans. Geosci. Remote Sens.* **2012**, *50*, 2542–2555.
32. Schumann, G.; Bates, P.D.; Horritt, M.S.; Matgen, P.; Pappenberger, F. Progress in integration of remote sensing—Derived flood extent and stage data and hydraulic models. *Rev. Geophys.* **2009**, *47*, doi:10.1029/2008RG000274.
33. Woo, M.K.; Kane, D.L.; Carey, S.K.; Yang, D. Progress in permafrost hydrology in the new millennium. *Permafr. Periglac. Process.* **2008**, *19*, 237–254.
34. Marchenko, S.; Romanovsky, V.; Tipenko, G. Numerical modeling of spatial permafrost dynamics in Alaska. In Proceedings of the Ninth International Conference on Permafrost, Institute of Northern Engineering, University of Alaska Fairbanks, Fairbanks, AK, USA, 29 June–3 July 2008; Volume 29, pp. 1125–1130.
35. Gouttevin, I.; Krinner, G.; Ciais, P.; Polcher, J.; Legout, C. Multi-scale validation of a new soil freezing scheme for a land-surface model with physically-based hydrology. *Cryosphere* **2012**, *6*, 407–430.

36. Gouttevin, I.; Bartsch, A.; Krinner, G.; Naeimi, V. A comparison between remotely-sensed and modelled surface soil moisture (and frozen status) at high latitudes. *Hydrol. Earth Syst. Sci. Discuss.* **2013**, *10*, doi:10.5194/hessd-10-11241-2013.
37. Wismann, V. Monitoring of seasonal thawing in Siberia with ERS scatterometer data. *IEEE Trans. Geosci. Remote Sens.* **2000**, *38*, 1804–1809.
38. Wagner, W.; Hahn, S.; Kidd, R.; Melzer, T.; Bartalis, Z.; Hasenauer, S.; Figa-Saldaña, J.; de Rosnay, P.; Jann, A.; Schneider, S.; *et al.* The ASCAT soil moisture product: A review of its specifications, validation results, and emerging applications. *Meteorol. Z.* **2013**, *22*, 5–33.
39. Romanovsky, V.E.; Smith, S.L.; Christiansen, H.H. Permafrost thermal state in the polar Northern Hemisphere during the international polar year 2007–2009: A synthesis. *Permafr. Periglac. Process.* **2010**, *21*, 106–116.
40. Brown, J.; Ferrians, O.J.; Heginbottom, J.; Melnikov, E. *Circum-Arctic Map of Permafrost and Ground-Ice Conditions*; National Snow and Ice Data Center; Digital Media. Available online: http://nsidc.org/data/docs/fgdc/ggd318_map_circumarctic/ (accessed on 17 September 2014).
41. Serreze, M.C.; Etringer, A.J. Precipitation characteristics of the Eurasian Arctic drainage system. *Int. J. Climatol.* **2003**, *23*, 1267–1291.
42. Boike, J.; Wille, C.; Abnizova, A. Climatology and summer energy and water balance of polygonal tundra in the Lena River Delta, Siberia. *J. Geophys. Res. Biogeosci. (2005–2012)* **2008**, *113*, doi:10.1029/2007JG000540.
43. Wagner, W.; Lemoine, G.; Borgeaud, M.; Rott, H. A study of vegetation cover effects on ERS scatterometer data. *IEEE Trans. Geosci. Remote Sens.* **1999**, *37*, 938–948.
44. Bartalis, Z.; Wagner, W.; Naeimi, V.; Hasenauer, S.; Scipal, K.; Bonekamp, H.; Figa, J.; Anderson, C. Initial soil moisture retrieval from the METOP—A Advanced Scatterometer (ASCAT). *Geophys. Res. Lett.* **2007**, *34*, doi:10.1029/2007GL031088.
45. Paulik, C.; Melzer, T.; Hahn, S.; Bartsch, A.; Heim, B.; Elger, K.; Wagner, W. *Circumpolar Surface Soil Moisture and Freeze/Thaw Surface Status Remote Sensing Products (Version 2) with Links to Geotiff Images and NetCDF Files (2007-01 to 2010-09)*; TU Vienna: Vienna, Austria, 2012.
46. Closa, J.; Rosich, B.; Monti-Guarnieri, A. The ASAR wide swath mode products. In Proceedings of the 2003 IEEE International Geoscience and Remote Sensing Symposium (IGARSS'03), Toulouse, France, 21–25 July 2003; Volume 2, pp. 1118–1120.
47. Bartsch, A.; Trofaier, A.; Hayman, G.; Sabel, D.; Schlaffer, S.; Clark, D.; Blyth, E. Detection of open water dynamics with ENVISAT ASAR in support of land surface modelling at high latitudes. *Biogeosciences* **2012**, *9*, 703–714.
48. Reschke, J.; Bartsch, A.; Schlaffer, S.; Schepaschenko, D. Capability of C-Band SAR for operational wetland monitoring at high latitudes. *Remote Sens.* **2012**, *4*, 2923–2943.
49. Trofaier, A.; Bartsch, A.; Rees, W.; Leibman, M. Assessment of spring floods and surface water extent over the Yamalo-Nenets Autonomous District. *Environ. Res. Lett.* **2013**, *8*, doi:10.1088/1748-9326/8/4/045026.

50. Sabel, D.; Bartsch, A.; Schlaffer, S.; Klein, J.P.; Wagner, W. Soil moisture mapping in permafrost regions—An outlook to Sentinel-1. In Proceedings of the 2012 IEEE International Geoscience and Remote Sensing Symposium (IGARSS), Munich, Germany, 22–27 July 2012; pp. 1216–1219.
51. Climate Prediction Center/National Centers for Environmental Prediction/National Weather Service/NOAA/U.S. Dpt. of Commerce. 1987, Updated Half-Yearly. *CPC Global Summary of Day/Month Observations, 1979-Continuing.* Research Data Archive at the National Center for Atmospheric Research, Computational and Information Systems Laboratory. Dataset. Available online: http://rda.ucar.edu/datasets/ds512.0/ (accessed on 27 July 2011).
52. de Rosney, P.; Polcher, J. Modelling root water uptake in a complex land surface scheme coupled to a GCM. *Hydrol. Earth Syst. Sci.* **1998**, *2*, 239–255.
53. Bartsch, A.; Wagner, W.; Scipal, K.; Pathe, C.; Sabel, D.; Wolski, P. Global monitoring of wetlands—The value of ENVISAT ASAR Global mode. *J. Environ. Manag.* **2009**, *90*, 2226–2233.
54. Bartsch, A.; Pathe, C.; Wagner, W.; Scipal, K. Detection of permanent open water surfaces in central Siberia with ENVISAT ASAR wide swath data with special emphasis on the estimation of methane fluxes from tundra wetlands. *Hydrol. Res.* **2008**, *39*, 89–100.
55. Lehner, B.; Döll, P. Development and validation of a global database of lakes, reservoirs and wetlands. *J. Hydrol.* **2004**, *296*, 1–22.
56. Schumann, G.; Lunt, D.; Valdes, P.; de Jeu, R.; Scipal, K.; Bates, P. Assessment of soil moisture fields from imperfect climate models with uncertain satellite observations. *Hydrol. Earth Syst. Sci.* **2009**, *13*, 1545–1553.
57. Muster, S.; Langer, M.; Heim, B.; Westermann, S.; Boike, J. Subpixel heterogeneity of ice-wedge polygonal tundra: A multi-scale analysis of land cover and evapotranspiration in the Lena River Delta, Siberia. *Tellus B* **2012**, *64*, doi:10.3402/tellusb.v64i0.17301.

Appendix B

Publication 2

Högström, E.; Bartsch, A.: Impact of Backscatter Variations Over Water Bodies on Coarse-Scale Radar Retrieved Soil Moisture and the Potential of Correcting With Meteorological Data. IEEE Transactions on Geoscience and Remote Sensing. 2017, 55(1), 3-13.

Impact of Backscatter Variations Over Water Bodies on Coarse-Scale Radar Retrieved Soil Moisture and the Potential of Correcting With Meteorological Data

Elin Högström and Annett Bartsch

***Abstract*—The Northern Hemisphere is, to a large extent, underlain by permafrost, which is prone to thawing due to rapid warming in the Arctic during the 21st century. In this context, satellite-derived soil moisture data are valuable for modeling purposes. Assessing the applicability of such data at high latitudes is essential but has, until recently, been given little attention. Recent studies have pointed out that seasonal land cover variations and the presence of small water bodies, which are typical in the Arctic, can cause complications for soil moisture retrieval. Here, it is hypothesized that a bias related to water fraction is caused by variations in the water surface roughness. The impact is quantified for the Metop Advanced Scatterometer by investigations of the higher spatial resolution synthetic aperture radar (SAR) data acquired by ENVISAT Advanced SAR over 11 sites across the Siberian Arctic. The bias calculated as an average over time can be explained by the lake fraction: a water fraction higher than 20% causes a bias of more than 10% relative surface soil moisture. This can, to a great extent, be attributed to wind, based on which a bias correction was developed. The correction was applied and evaluated with *in situ* soil moisture data, which were available from one of the sites: the Lena Delta. Weak results are obtained because water surfaces correspond mainly to rivers at this site. Variations in discharge, water height, and streams may therefore also affect the water surface roughness.**

***Index Terms*—Arctic, C-band, lakes, microwave measurement, moisture, radar remote sensing, scatterometer, surface waves, synthetic aperture radar (SAR).**

I. Introduction and Motivation

A. Remote Sensing of Soil Moisture in the Arctic

APPROXIMATELY 25% of the Northern Hemisphere is underlain by permafrost [1]. Permafrost temperatures have risen significantly over the past two to three decades [2], and the Arctic is expected to warm more rapidly than the global mean temperature until the end of the 21st century [3]. The Arctic is also, to a large extent, characterized by remote areas which are difficult to access for ground measurements. There is, thus, a particular need for accurate measurements from satellite data in these regions. Soil moisture is one of the main controllers of the exchange of water, energy, and carbon between the land surface and the atmosphere, and it is an essential variable for studies of permafrost, including modeling and upscaling [1], [4], [5].

B. Microwave Remote Sensing of Soil Moisture

A range of retrieval algorithms have been developed in order to obtain soil moisture from the uppermost surface from radar satellite data, including passive and active microwave sensors (e.g., [6] and [7]). From the active microwave remote sensing instrument Advanced Scatterometer (ASCAT), successor to ERS-1/2 scatterometer (ESCAT), a global coarse-scale (25-km) surface soil moisture (SSM) product is derived through a method implemented by the European Organization for the Exploitation of Meteorological Satellites. This is a near-real-time service which has been implemented in cooperation with the Vienna University of Technology and been in operation since 2008 [5], [8]. Numerous studies have shown the applicability of the product (e.g., [9] and [10]), including recent operational use for numerical weather forecasts [11]. The ASCAT data only reflect the moisture of the upper few centimeters of the soil, and there are uncertainties for regions of dense vegetation ([12]), but large moisture patterns are captured well [13]. The retrieval method relies on the fact that the ground's dielectric properties vary with changes in soil moisture levels [14]. The dielectric properties of the soil change also when freezing. Soil moisture retrieval is only applied to unfrozen conditions. Frozen conditions are flagged and not included in the processing.

C. Technical Challenges for Soil Moisture Retrieval Related to Land/Water Fraction

Limitations to the retrieval that are typical for high latitudes include landscape heterogeneity and seasonal land cover variations, which also contribute to the satellite return signal [15]. It has been pointed out in the literature that too much open water within the footprint may have a disturbing influence on the ASCAT backscatter signal and thus for the surface soil moisture retrieval [13]. The Arctic tundra includes, to a

Manuscript received April 30, 2015; revised September 15, 2015 and November 29, 2015; accepted January 5, 2016. Date of publication September 27, 2016; date of current version November 29, 2016. This work was supported in part by the European Commission (FP7-ENV-2011) through the project Changing Permafrost in the Arctic and its Global Effects in the 21st Century (PAGE21) under Grant 282700 and in part by the International Network for Terrestrial Research and Monitoring in the Arctic (INTERACT), under the European Community's Seventh Framework Programme, under Grant 262693.

E. Högström is with the Department of Geodesy and Geoinformation (GEO), Vienna University of Technology (TUW), 1040 Vienna, Austria, and also with Austrian Polar Research Institute, 1090 Vienna, Austria (e-mail: Elin.Hoegstroem@geo.tuwien.ac.at).

A. Bartsch is with the Department of Geodesy and Geoinformation (GEO), Vienna University of Technology (TUW), 1040 Vienna, Austria, with the Austrian Polar Research Institute, 1090 Vienna, Austria, and also with Zentralanstalt für Meteorologie und Geodynamik (ZAMG), 1190 Vienna, Austria.

Color versions of one or more of the figures in this paper are available online at http://ieeexplore.ieee.org.

Digital Object Identifier 10.1109/TGRS.2016.2530845

large, part wetlands, which are characterized by poorly drained highly saturated soils and abundant ponds (< 100 m^2) and lakes [16]–[18]. Eight percent of the unglaciated tundra in the Arctic is covered by water bodies [18]. It is therefore expected that there are retrieval issues in the Arctic, where this type of satellite-derived product is particularly needed. The retrieval issue related to water fraction is currently taken into account for the ASCAT soil moisture product by providing the user with a flag that warns for high water fraction. The flag has been derived from coarse-scale data sets: the Global Lakes and Wetlands Database (GLWD) [19] and the Global Self-consistent, Hierarchical, High-resolution Shoreline Database (GSHHS) [20]. This flag does not take wetland dynamics into account, nor does it account for any changes in inundation that may occur, nor does it capture small lakes. The potential bias through backscatter variations unrelated to soil moisture has been assessed based on intercomparison with Land Surface Model output (ORCHIDEE, 25 km) for the coarse-scale ASCAT product [21], [22]. Högström *et al.* [22] utilized medium-resolution satellite data [ASAR wide swath (WS), 75 km] in order to describe the effects from smaller water bodies within areas corresponding to the ASCAT footprint. Backscatter differences related to water bodies were assessed. Disagreements between the model (ORCHIDEE)-derived SSM and the remote sensing ASCAT SSM [21] could, to a large extent, be explained by the presence of open water ($R^2 = 0.45$ for areas with high water fraction and large lakes) [22]. The backscatter variability could be partially attributed to changes in roughness on the water surfaces rather than variations over land. It remains to be answered how this difference translates to the ASCAT soil moisture. Furthermore, it has not yet been determined to what extent the water roughness relates to wind, rain, or ice cover and snow on the lakes compared with a smooth surface.

D. Water Fraction Related Bias and Potential Correction With Wind Data

This study quantifies the water body related potential bias in the ASCAT soil moisture product and investigates how this bias relates to *in situ* meteorological data. It further investigates how this bias could be corrected. It is expected that wind or rain acting on the water surface causes a higher backscatter than during calm weather conditions, an issue which is currently not considered in the retrieval algorithm. We make use of the medium-resolution synthetic aperture radar (SAR) data acquired by the ENVISAT Advanced SAR (ASAR) in WS mode (120-m resolution) to investigate backscatter variations unrelated to soil moisture within regions of interest (ROIs) that correspond to the ASCAT footprints over 11 sites across the Russian Arctic (Table I). The bias is quantified by generating an ASAR data set with a virtually smooth water surface and subsequently comparing it with the original ASAR data set. The average difference during the summers 2007 and 2008 is considered with respect to the total water body area in all the selected study sites across the Arctic. At sites where *in situ* data are available, the ASAR-derived bias for specific dates during the time period is analyzed using meteorological data, such as wind speed (Table I, column 5). We hypothesize that if the bias is related to water surface roughness variations caused by wind or rain, a correction of ASCAT SSM should be possible with meteorological data. A correction for wind speed is tested, and the outcome is evaluated with *in situ* soil moisture measurements in the Lena Delta.

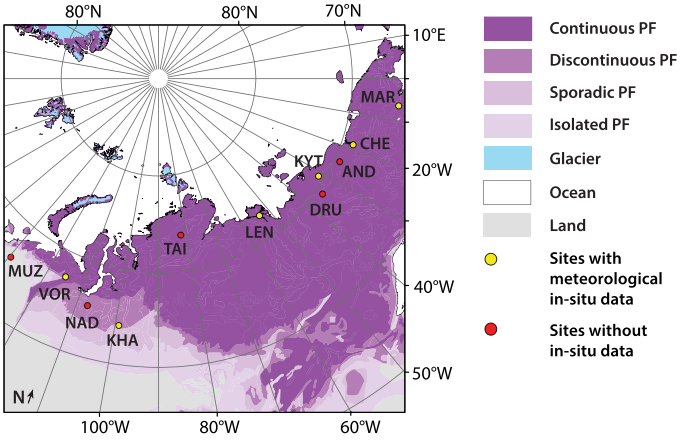

Fig. 1. Site overview showing the location of the 11 sites across the Siberian Arctic. The site names are abbreviated according to Table I. The sites where meteorological data are available are indicated with yellow color. The underlying permafrost conditions are shown as background as a simplification (not including subclasses for ground ice content) of the Circum-Arctic map of permafrost and ground ice conditions [23]. Projection: Lambert azimuthal.

TABLE I
SITE NAMES, ABBREVIATIONS, TYPE OF AVAILABLE *in situ* DATA, AND TOTAL ENVISAT ASAR WS DATA AVAILABILITY FOR THE SNOW-FREE PERIODS IN 2007 AND 2008

site name	site acronym	PF zone /vegetation	lat, lon	in-situ data	number of ASAR WS acquisitions
Andruyoskino	AND	continuous, tundra	69.18, 154.45	-	35
Cherski	CHE	continuous, tundra	68.8, 161.28	meteo	22
Druzhina	DRU	continuous, tundra	68.23, 145.3	-	16
Kharampur	KHA	discontinuous, boreal forest	64.28, 78.15	-	39
Kytalyk	KYT	continuous, tundra	70.62, 147.9	meteo	37
Lena Delta	LEN	continuous, tundra	72.37, 126.5	meteo, soil moisture	34
Markovo	MAR	continuous, tundra	64.68, 170.42	meteo	20
Muzi	MUZ	none, boreal forest	65.38, 64.72	-	32
Nadym	NAD	discontinuous, boreal forest	65.6, 72.7	-	51
Taimyr	TAI	continuous, tundra	71.98, 102.45	-	52
Vorkuta	VOR	discontinuous, boreal forest	67.48, 64.02	meteo	72

II. SITE DESCRIPTION

Eleven sites across the Russian Arctic were selected for the study (see Table I and Fig. 1). They are underlain by different types of permafrost, from continuous to sporadic (as defined in [23]), and they cover a variety of land covers, including tundra and boreal forest, as well as lake-rich and lake-poor areas. Fig. 1 shows an overview of all sites and the underlying permafrost conditions according to [23]. Kytalyk, Cherski, Vorkuta, Nadym, and the Lena River Delta are long-term permafrost monitoring sites [2]. The selected locations coincide

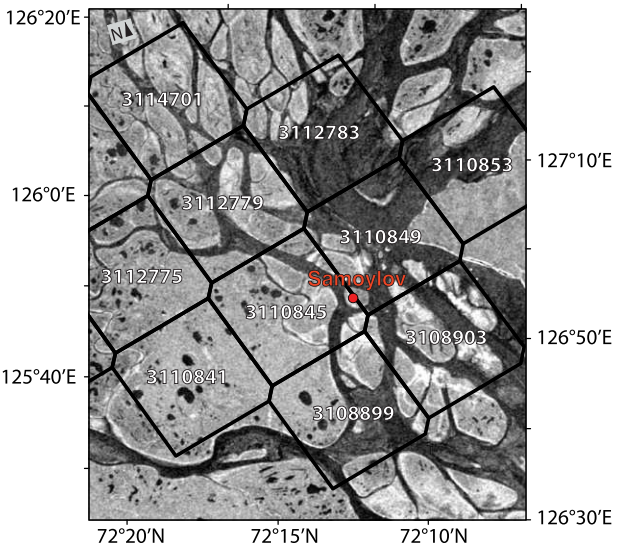

Fig. 2. ENVISAT ASAR WS image of the central Lena Delta from June 31, 2007. The location of the *in situ* measurements on the Samoylov Island is shown in red. Black hexagons represent the ROIs corresponding to the ASCAT footprints and are labeled with the ASCAT product ID. Projection: UPS North Stereographic.

with the areas of interest in [22], except for the Lena River Delta. The latter has been added since *in situ* meteorological and soil moisture data are available for the time period of the investigated ASAR archive data. Within the ASCAT footprints in the Lena River Delta, the water fraction ranges from 14% to 79%. To a great extent, the water includes rivers with sandy banks and partially very shallow depth. The *in situ* data themselves have been collected at the Samoylov Island in the Lena River [24]. The island is one of the 1500 islands that make up the Lena River Delta (see Fig. 1). It is located within one of the main river channels at 72°22′ N, 126°28′ E and lies within the zone of continuous permafrost, which reaches down to 600 m below the surface [54]. The western part of the Samoylov Island consists of a flood plain and the eastern part of an elevated river terrace, which, to a large extent, is covered with sphagnum moss. The total size of the island is 4.38 km^2. The terrace is characterized by polygonal tundra (average polygonal pond size $= 54$ m^2) and smaller lakes (average thermokarst lake size $= 26\,884$ m^2) [17], [24]. The polygons take the form of dry ridges and wet depressed centers. Numerous multidisciplinary studies with a focus on climate, land cover, ecology, hydrology, limnology, and permafrost have been conducted here since 1993. Automatic stations for soil and climate measurements have been installed in 1998 [24]. Fig. 2 shows a part of the Lena River Delta. The location of the *in situ* stations where wind speed and soil moisture are measured is indicated in red. The ROIs located closest to the *in situ* stations are shown as black hexagons.

III. Material and Method

A. In Situ Meteorological and Soil Moisture Data

Meteorological data from the harmonized CPC Global Summary of the Day and Month Observations data set [25] were available from five of the ten sites (Cherski, Kytalyk, Lena Delta, Markovo, and Vorkuta), including wind speed and precipitation. Networks with *in situ* soil moisture data exist, such as the International Soil Moisture Network, with a high global coverage, but data are still scarce in the Arctic [55]. From the Samoylov Island in the Lena River Delta, meteorological and soil moisture *in situ* data were available for this study [17]. Fig. 2 shows the Lena River Delta and the ASCAT grid points that were located closest to the *in situ* measurements of wind speed and soil moisture. The soil moisture sensors are located at the ridge and slope within a low centered polygon, which is a typical feature in polygonal tundra. One sensor is placed in the rim at a depth of 5 cm and another in the slope at a depth of 5 cm. At the depth of 5 cm, the sensor is normally placed within the fibric layer. This layer consists of dead moss and peat and is located just underneath the living material. In the case of sphagnum, the lower part of the dead moss can store significant amounts of water [26].

B. Satellite Data and Preprocessing

1) Satellite Sensors: The ASCAT is an active microwave remote sensing instrument that is well calibrated, stable over time, and has high radiometric accuracy [5], [27], which means that the signal-to-noise ratio is expected to be high enough to achieve acceptable retrieval accuracy [13]. It was originally designed to monitor winds over the oceans to support, e.g., numerical weather forecasting [28]. Although no terrestrial applications were foreseen, the ASCAT predecessor instrument, i.e., the ERS-1/2 scatterometer (ESCAT), has been shown suitable for monitoring soil moisture [7], [29].

The ASAR was a ScanSAR instrument carried on the satellite ENVISAT, which operated until 2012. The ASAR WS archive data analyzed here have a spatial resolution of 120 m, and the revisit time is 35 days [30]. The data availability is thus considerably lower than for the ASCAT data, but the spatial resolution is higher. The ASAR WS was preprocessed for Northern Eurasia for 2007–2008 within the framework of the European Space Agency Support to Science Element project ALANIS Methane [31]–[33]. This was done using the SAR Geophysical Toolbox (SGRT), which is a scripting chain that calls the commercial SARscape or the free NEST software, thus allowing for the automatization of the processing [34], [56]. The data were resampled to a fixed grid to allow efficient spatial and temporal analysis. The 15-arc-second grid was divided into blocks of $0.5^\circ \times 0.5^\circ$ boxes (denoted "gridboxes"), resulting in 720 columns and 360 rows globally, to be used for efficient referencing of the data. To remove influences of the local incidence angle, the data were normalized to a reference angle of 30° [34], Sabel *et al.*, 2007. The ASCAT and ASAR satellite sensors are both operating in C-band (center frequency of 5.2 GHz), which has been shown suitable for soil moisture retrieval through the dielectric properties of water, making it possible to build the retrieval technique on backscatter contrasts between dry and wet soil. The polarization is vertical (VV) in both cases. The available data sets differ, however, in reference incidence angle for the normalization.

2) ASCAT Soil Moisture Retrieval: The retrieval algorithm for the ASCAT soil moisture products is based on a change

detection method implemented for ESCAT but later transferred to ASCAT [8], [29], [35], [36], [57], [58]. Dry soil gives a contrasting radar backscatter signal to that of wet soil. A linear relationship between the backscattering coefficient (dB) and the surface soil moisture content is assumed [14], [36], [37]. Because vegetation has a significant effect on the radar backscatter, the ASCAT soil moisture algorithm uses a vegetation correction that depicts vegetation scattering at large incidence angles and a reduced sensitivity to soil moisture during the peak of the vegetation season ([38] [39]). The ASCAT backscatter is normalized to a reference angle incidence of 40°, and a vegetation correction through the scatterometer multiincidence angle capacities is applied. Thereafter, the backscatter is scaled to its local historical maximum and minimum, which are referred to as the wet (σ^0wet) and dry (σ^0dry) references [7]. The scaling results in a soil moisture product in the form of a saturation percentage, which is referred to as SSM. The relative soil moisture is thus calculated as

$$\Theta s(t) = \frac{\sigma 0(40,t) - \sigma 0\text{dry}(40,t)}{\sigma 0\text{wet}(40,t) - \sigma 0\text{dry}(40,t)} \quad (1)$$

where $\Theta s(t)$ is the relative measure of the water content in the uppermost soil layer, and $\sigma^0(40,t)$ is the backscatter at 40° incidence angle. The absolute difference in decibels between σ^0wet and σ^0dry is the sensitivity and can be seen as a measure of local historical backscatter range. The ASCAT data are available for a predefined discrete global grid where each grid cell is identified by its unique grid cell point index (GPI). Over land, each GPI is attributed a time series of data which is spatially resampled with an equal spacing of 12.5 km in the latitude and longitude directions [40]. A surface state flag (SSF) exists for each backscatter measurement, which shows whether the surface is frozen/unfrozen and if there are thaw conditions or snow melt. This SSF is derived from ASCAT backscatter time series and is used for masking ASCAT and ASAR data for this study. External (nonscatterometer derived) advisory flags also exist, which are calculated from several sources and provided to identify problematic areas. The records start in 2007. The advisory flags include inundation/wetland fractions derived from the GLWD and the GSHHS [19], [20].

C. Method for Bias Quantification and Wind Correction

For this study, a supervised classification (parallelepiped) was performed on ice-free ASAR acquisitions under calm conditions and with maximal lake extension in the summer, as well as maximal water/land contrasts, in order to separate land from water. This was done for all the areas. The water bodies were masked out and replaced by −20 dB in accordance with [22], which is a backscatter value typical for smooth water surfaces for the applied preprocessing (see Section III-B) Sabel *et al.*, 2007; [31], [41]. This data set is hereby referred to as the smooth water data set.

The ASCAT time series of backscatter and SSM were retrieved for each grid point index (GPI) cell. In order to create a data set comparable with the ASCAT data, a mesh of hexagons with the GPI as center points was generated to define ROIs within each ASAR data stack following the method of [22]. For the 11 sites, this resulted in a total of 100 ROIs. To avoid frozen ground conditions, the ASCAT SSF (see Section III-B) was used for the selection of the ASAR acquisitions. The site Lena Delta turned out to have the shortest season of unfrozen ground conditions (June 21 to September 2), and this time period was applied for all sites during the years 2007 and 2008.

A saturation index (SI), which is comparable with ASCAT SSM [see (2)] and expressed as saturation in percentage, was calculated from the ASAR backscatter. The SI was derived by scaling the backscatter values to the local historical (ASAR) minimum (σ^0dry) (respectively, maximum (σ^0wet)). The dry reference values were delineated from ASAR WS acquisitions from December 2007 or 2008 depending on data availability [31], [51]. The backscatter in winter represents the minimum backscatter during frozen conditions, which is similar to that of dry conditions [42], [43]. The wet reference was obtained from the summer periods 2007 and 2008, representing the local maximum backscatter values. The smooth water data sets (masking with smooth water) were also derived for the wet and dry references. The ASAR SI was thus calculated as

$$\text{SI}(t)\frac{\sigma 0(30,t) - \sigma 0\text{dry}(30,t)}{\sigma 0\text{wet}(30,t) - \sigma 0\text{dry}(30,t)} \times 100 \quad (2)$$

where $\sigma^0(30,t)$ is the average ASAR backscatter at a 30° incidence angle within the ASCAT footprint, and σ^0dry is the ASAR average dry reference retrieved from December only.

In order to investigate the comparability of ASCAT and ASAR with respect to the difference in incidence angle, the average backscatter was calculated within four pairs of ROIs across nonnormalized ASAR imagery in a homogenous area with close-to-zero water fraction located near the Lena Delta site. The four ROI pairs were located opposite to each other, separated by 30°. The average backscatter at these ROIs and the resulting backscatter difference per 10° incidence angle were calculated and compared with the direct difference in backscatter between the ASCAT and ASAR time series.

To quantify the impact of water surface roughness at ASCAT scale, the average backscatter within each ROI of the smooth water data set was subtracted from that of the original data set, i.e.,

$$\Delta\sigma^0 = \text{ASAR}\overline{\sigma^0}_{\text{ORIG.}} - \text{ASAR}\overline{\sigma^0}_{\text{SMOOTH.}}. \quad (3)$$

In the same manner, the bias was also calculated in the form of ΔSI, which compares to the ASCAT SSM. The ASAR ΔSI was derived as follows:

$$\Delta\text{SI} = \overline{\text{SI}}_{\text{ORIG.}} - \overline{\text{SI}}_{\text{SMOOTH.}}. \quad (4)$$

For all the sites and each ROI, $\Delta\sigma^0$ and ΔSI were thus calculated, and they are referred to as the bias. First, this bias was compared with the water fraction in order to assess the linear dependence of water fraction. Second, the bias was compared with the *in situ* meteorological data in order to understand to what extent the difference is caused by water surface roughness due to wind or precipitation. This was done for all sites where meteorological data were available

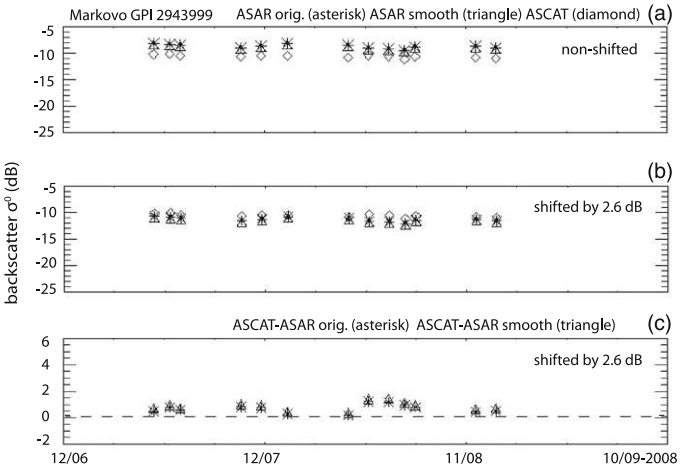

Fig. 3. (Diamond) ASCAT backscatter, (asterisk) ASAR original, and (triangle) ASAR smooth water average backscatter in decibels for ROI 2943999 in Markovo. The water fraction in this ROI is 0.05%. (a) Unshifted ASAR backscatter. (b) Values shifted by 2.6 dB for improved comparability with ASCAT. (c) Difference between the (asterisk) ASCAT-ASAR original and the (triangle) ASCAT-ASAR smooth water.

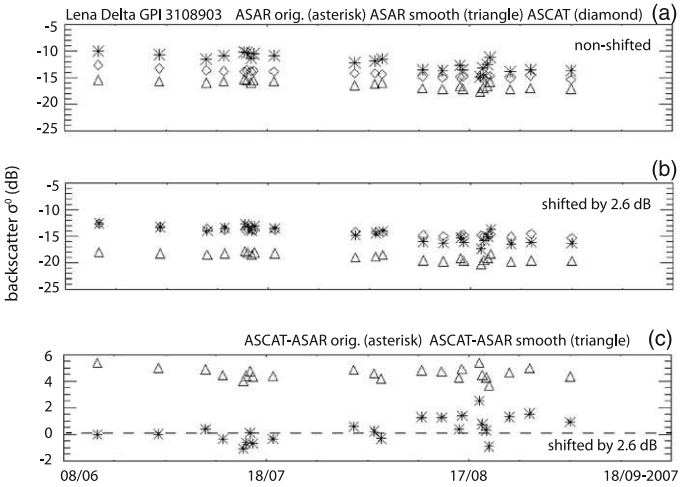

Fig. 4. (Diamond) ASCAT backscatter, (asterisk) ASAR original, and (triangle) ASAR smooth water average backscatter in decibels for ROI 3110849 in the Lena Delta. The water fraction in this ROI is 77%. (a) Unshifted ASAR backscatter. (b) Values shifted by 2.6 dB for improved comparability with ASCAT. (c) Difference between the (asterisk) ASCAT-ASAR original and the (triangle) ASCAT-ASAR smooth water.

(Cherski, Kytalik, Lena Delta, Markovo, Vorkuta). The Pearson correlation and covariance of wind speed and precipitation with the bias during the summer (June 21 to September 2) 2007–2008 were calculated (see Table III). A linear fit was applied, and the resulting linear equations based on wind data and the ASAR ΔSI bias were used for the correction of ASCAT SSM, according to the following equation:

$$\mathrm{ASCAT}_{\mathrm{corr}}(t) = \mathrm{ASCAT}_{\mathrm{orig}}(t) - (k\,U(t) + m) \qquad (5)$$

where U is the wind speed, $\mathrm{ASCAT}_{\mathrm{orig}}$ is the original ASCAT-derived soil moisture, and $\mathrm{ASCAT}_{\mathrm{corr}}$ is the corrected ASCAT soil moisture. The constants (k = slope, m = y-intercept), which are derived from the linear regression between ASAR ΔSI and the wind, remain specific for each ROI. The resulting time series with corrected ASCAT SSM were evaluated using the *in situ* soil moisture data from the Samoylov Island in the Lena Delta—the only site where both *in situ* meteorological data and soil moisture data were available. The ASAR- and ASCAT-derived sensitivity (see Section III-B) is discussed in the context of the applicability of the ASAR-derived correction for the wind-related SI bias on the ASCAT SSM.

IV. Results

The time series (summers 2007 and 2008) of the ASCAT backscatter were plotted together with the ASAR-derived original and smooth water average backscatter (see Figs. 3 and 4). The low water fraction (2%) of ROI 2943999 in Markovo corresponds to a low difference between the original and smooth water ASAR data sets (see Fig. 3). The time series of the backscatter from ROI 3108903 in the Lena River Delta, with a high water fraction (50%), show a large difference between the original and smooth water ASAR data sets (see Fig. 4). In Markovo, it can be seen that the ASAR data set generally is a few decibels higher than the ASCAT backscatter [see Fig. 3(a)], and in the Lena Delta, the same is valid for the original ASAR backscatter, but not for the smooth water data set [see Fig. 4(a)]. This difference between ASCAT and ASAR is related to the incidence angle: a 40° incidence angle should give a 2.6 dB lower backscatter value than a 30° incidence angle. This is demonstrated in Table II, which shows the resulting average backscatter within the four subset pairs from different incidence angle regions (see Section III-C). It also shows the backscatter difference per 10° incidence angle. The average is 2.6 dB. We can see that the smooth water ASAR backscatter remains lower than the ASCAT backscatter for an area with a high water fraction such as the Lena Delta [see Fig. 4(b)] in the time series of ASAR and ASCAT backscatter after applying a 2.6-dB offset to the ASAR data. This is also clearly shown by the difference between the ASCAT and ASAR backscatter, which is below 1 dB in the ROI in Markovo [see Fig. 3(c)], whereas in the Lena Delta [see Fig. 4(c)], the difference is close to zero for the original ASAR and up to 6 dB for the smooth water data. The absolute SI is thus not directly comparable to the absolute ASCAT-derived SSM due to the incidence angle. However, we assume that the relative difference $\Delta\sigma^0$ and ΔSI can be considered independent of this angle difference and thus be applied to ASCAT, although retrieved from ASAR.

TABLE II
Difference per 10° Incidence Angle Across an ASAR Acquisition in the Lena Delta, Before Normalization (Column 4). The Difference Is Calculated From the Average Backscatter Within Four ROI Pairs (Column 1) Separated by 30° Incidence Angle (Columns 2 and 3). The Backscatter Average in These ROIs Was Calculated From Nonnormalized Radar Imagery Over a Homogeneous Area Close to the Lena Delta

ROI pair	sub W average backscatter (dB)	sub E average backscatter (dB)	difference per 10° incidence angle (dB)
1	-3.12	-12.43	3.10
2	-3.21	-11.49	2.76
3	-3.49	-9.66	2.06
4	-2.63	-9.75	2.37

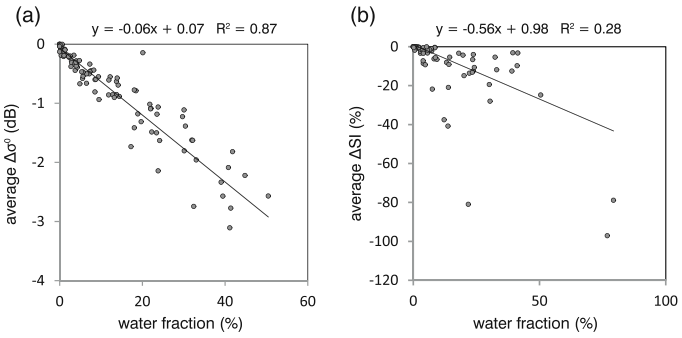

Fig. 5. Bias in the form of (a) backscatter $\Delta\sigma^0$ and (b) saturation index ΔSI, for each ROI averaged over time, as a function of water fraction. The values are averages for the summer season in 2007 and 2008 for each ROI of all the 11 sites. The bias is shown as negative values, since the smooth water data set results in a reduction in relation to the original data set.

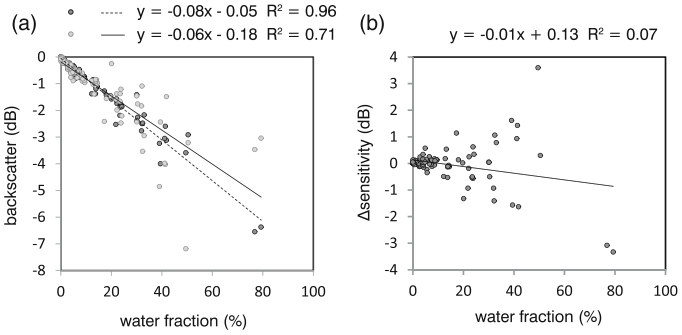

Fig. 6. (a) Impact of the bias on σ^0wet (Δwet original–smooth water-R) and σ^0dry (Δdry original–smooth water) in backscatter as a function of water fraction. (b) Difference in sensitivity (Δsensitivity) between the original and smooth water ASAR data sets, as a function of water fraction. All ROIs are included, and the backscatter is averaged over the summer period in 2007 and 2008.

The impact of water surface roughness ($\Delta\sigma^0$ and ΔSI) for each ROI was calculated as an average over time, plotted against water fraction (see Fig. 5). In terms of backscatter, this ranges from 1 to 3.1 dB for ROIs with high water fraction, such as the sites Lena Delta, Cherski, Kytalyk, Andryoskino, and Druzhina. The linear relationship between the water fraction and the bias in the form of backscatter $\Delta\sigma^0$ ($R^2 = 0.87$) is shown in Fig. 5(a), and that between the water fraction and the bias in the form of ΔSI ($R^2 = 0.28$) is shown in Fig. 5(b). Five outliers with sensitivity lower than 1 dB and which thus cause an exceptionally high (negative) scaled bias were excluded from Fig. 5(b). It can be seen that, in areas with more than, e.g., 40% water bodies, higher than 2 dB is to be expected, which translates to a bias of 20% in terms of ΔSI. The impact of water surface roughness ($\Delta\sigma^0$) on σ^0wet (Δwet) and σ^0dry (Δdry) plotted against the water fraction is shown in Fig. 6(a). The same impact on the sensitivity (Δsensitivity) is shown in Fig. 6(b). Both the σ^0dry and σ^0wet are affected similarly, and the difference between the masked ASAR sensitivity and the original is, on average, close to zero. A significant impact of wind on the ASCAT sensitivity is therefore not expected.

The ASCAT backscatter is further plotted with ASAR sensitivity [see Fig. 7(a)], with the ASAR wet reference σ^0wet [see Fig. 7(b)] and with the ASAR dry reference σ^0dry [see Fig. 7(c)]. The ASAR shows almost exclusively lower values than ASCAT with respect to the sensitivity. σ^0dry is similar, but the ASAR smooth water data set shows about 2–4 dB higher σ^0wet values than ASCAT. The ASAR original data set shows σ^0wet values more similar to ASCAT. The σ^0dry reference from the ASAR smooth water data set is relatively well in line with that of ASCAT, whereas the ASAR original shows up to 4 dB lower values than ASCAT.

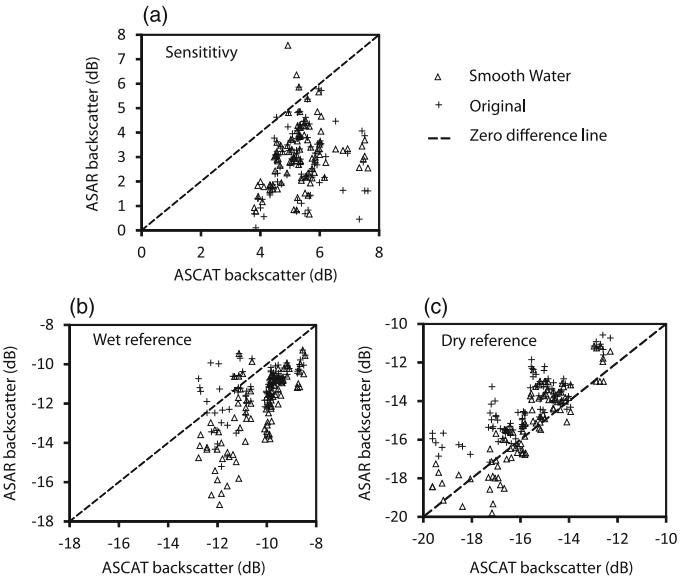

Fig. 7. (a) ASCAT plotted with ASAR sensitivity. (b) ASCAT plotted with ASAR σ^0wet. (c) ASCAT plotted with ASAR σ^0dry. The ASAR smooth water data set is shown as triangles, and the ASAR original is shown as crosses.

At each of the five sites where meteorological data were available (Cherski, Kytalyk, Lena Delta, Markovo, and Vorkuta), 20–72 ASAR acquisitions, depending on the coverage at each site, were matched with the dates of the *in situ* measurements. The meteorological data from the Lena Delta were daily averaged for comparability with the other sites. Days with rain, as well as ROI with a water fraction lower than 5%, were excluded for all scatterplots and Pearson correlation analysis between wind speed and the backscatter or SI bias. Scatterplots of the backscatter bias $\Delta\sigma^0$ and the wind speed for the ROIs located closest to the meteorological station in the Lena Delta are shown in Fig. 8. The meteorological data from the Lena Delta were measured on an hourly basis and could therefore be matched with the ASAR data according to the timing of acquisitions of ASAR with a difference of less than 4 h. The ROIs 3108903 and 310889 are areas with a high water fraction (50% and 39%, respectively), and they show the strongest dependence on wind for the backscatter bias. The ROI 3110849 has a water fraction as high as 77%, but it is found to show less strong dependence on wind speed than expected (see Section V). Results from all the five sites with meteorological data, including the Lena Delta, are shown in Fig. 9(a) and (b). The slope in a linear regression between the bias and the wind speed is clearly highest for the sites with high water fraction [see Fig. 9(a)]. The Pearson correlation between the wind speed and the bias is the highest for the ROI located closest to the meteorological stations [see Fig. 9(b)]. Correlations between

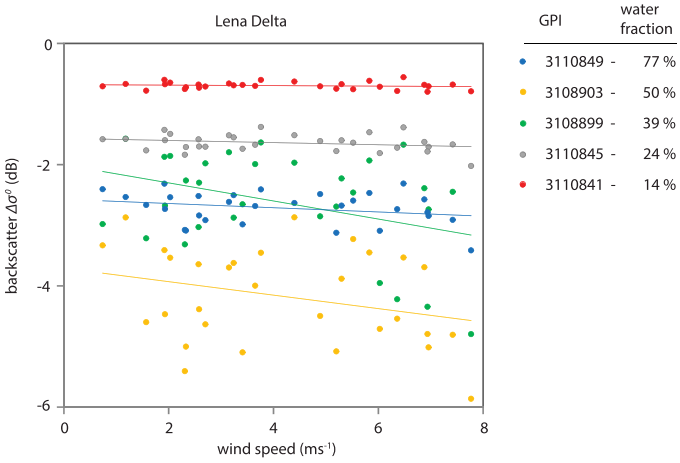

Fig. 8. Scatterplots of $\Delta\sigma^0$ and wind speed for the ROIs located closest to the meteorological station in the Lena Delta. The wind data are available on an hourly basis. The ASCAT GPI and water fraction for each ROI are indicated in the table to the right.

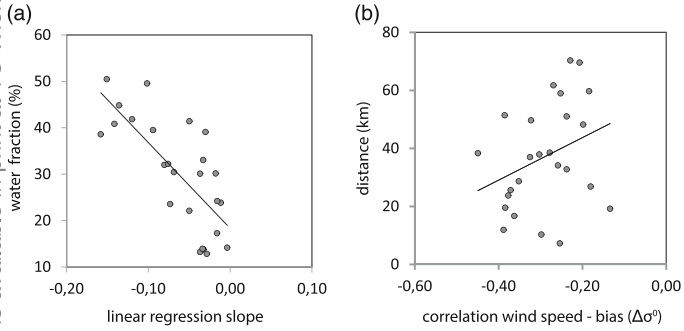

Fig. 9. (a) Scatterplot of water fraction and the slope from linear regressions between wind speed and the bias from all five sites from which meteorological data are available. (b) Scatterplot of the correlation between the wind speed and the bias, plotted together with the distance from the *in situ* measurements and the center point of each ROI where meteorological data were available. Dates with any precipitation are excluded. The wind data are obtained averaged as a diurnal average.

TABLE III
MINIMUM, MAXIMUM, MEAN, AND MEDIAN CORRELATION AND COVARIANCE BETWEEN THE ASAR-DERIVED BACKSCATTER BIAS ($\Delta\sigma^0$) AND THE WIND SPEED AND BETWEEN THE SAME BIAS AND THE PRECIPITATION. THE VALUES WERE CALCULATED AS AVERAGES FROM THE ROIS WHERE METEOROLOGICAL DATA WERE AVAILABLE

	wind speed correlation	covariance	precipitation correlation	covariance
min	0.06	0.01	-0.31	-0.01
max	0.48	1.00	0.29	0.27
mean	0.30	0.35	0.00	0.07
median	0.30	0.28	0.04	0.03

the bias and the precipitation showed almost exclusively low values, ranging from −0.31 to 0.29 (see Table III).

The wind correction was derived based on regression with ΔSI and applied to the ASCAT SSM. The results of the correction for ROIs 3110841 and 3110845 are shown in Fig. 10. The SI bias calculation and its relation with wind were limited to the dates for which ASAR acquisitions are available. The correction was applied to all dates during this period of

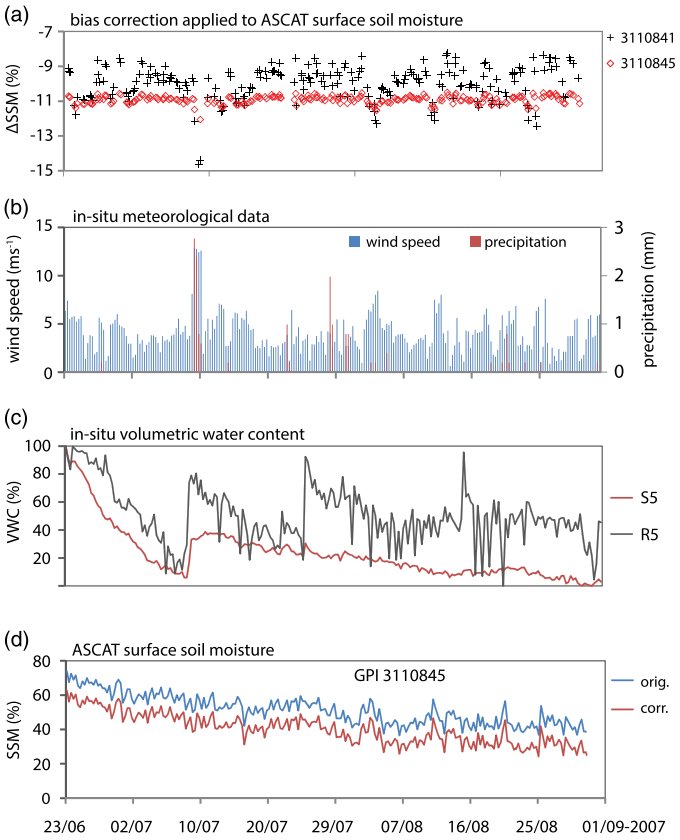

Fig. 10. (a) Wind correction, calculated from the linear regression between wind speed and soil moisture bias, for GPIs 3110841 (black) and 3110845 (red). (b) *In situ* wind speed data ($m \cdot s^{-1}$) (blue) and precipitation (mm) (red) from Samoylov Island [24]. (c) *In situ* soil moisture data (VWC) from the Samoylov Island [17]. The sensors are located within a polygon: at a depth of 5 cm in the slope (S5) and in the rim (R5). The *in situ* soil moisture has been scaled to its respective maximum and minimum. (d) ASCAT surface soil moisture for GPI 3110845: original (blue) and wind corrected (red). All three time series show values for June to September 2007.

time according to the ASCAT availability. The actual wind corrections, i.e., ΔSSM, for ROIs 3110841 and 3110845 to be applied on the ASCAT SSM are shown in Fig. 10(a). The ROI 3110845 includes the Samoylov Island, where the *in situ* data were collected. This ROI has a water fraction of 24.19%, which mostly corresponds to rivers. The ROI 3110841 is located next to 3110845, has a water fraction of 14%, and includes no river at all (see Fig. 2). The *in situ* wind speed ($m \cdot s^{-1}$) and precipitation (mm) are shown in Fig. 10(b), whereas the *in situ* soil moisture as volumetric water content (VWC) from sensors at three different locations within a polygon (ridge, slope) at a depth of 5 cm is shown in Fig. 10(c). The ASCAT original soil moisture and the wind-corrected ASCAT soil moisture are shown in Fig. 10(d). The correction for 3110845 is rather steadily close to a reduction of 11%, whereas the correction for 3110841 generally ranges from −9% to −11% but even reaches −12% and close to −15% [see Fig. 10(a)] on occasions with high wind speed [see Fig. 10(b)]. Although the impact of water surface roughness is large for ROI 3110845, it is less controlled by wind speed here than for ROI 3110841. The high wind speed from the meteorological data can only be matched with high ASCAT soil moisture in few cases (e.g., 30/06, 20/07,

TABLE IV
PEARSON CORRELATIONS AND COVARIANCE OF *in situ* SSM AND THE ORIGINAL ASCAT SSM (ORIG. SSM) AND WIND-CORRECTED ASCAT SSM (CORR. SSM) FOR THE SUMMER OF 2007. ONLY THE RESULTS FROM THE SENSORS WHICH GAVE THE STRONGEST CORRELATION AND COVARIANCE WITH ASCAT ARE INCLUDED, AS INDICATED IN COLUMN 2 ($R5$ = POLYGON RIDGE 5-cm DEPTH; $S5$ = POLYGON SLOPE 5-cm DEPTH)

ROI	in-situ	correlation		covariance	
		orig. SSM	corr. SSM	orig. SSM	corr. SSM
3108899	R5	0.39	0.41	0.91	12.30
3108903	S5	0.69	0.66	17.65	18.24
3110841	S5	0.68	0.67	15.57	15.29
3110845	S5	0.71	0.71	18.01	17.93
3110849	R5	0.62	0.69	1.18	16.40

12/08, and 18/08); at other times, they cannot be matched (e.g., 10/07 and 13/07). The *in situ* measured soil moisture obviously does not increase on occasions with high wind speed, with the exception of 10/07, when there is a peak in wind speed and precipitation simultaneously and what therefore likely means there is an actual increase in soil moisture in addition to the increase in roughness on the water surfaces. The covariance and Pearson correlation calculated between the *in situ* SSM and the ASCAT SSM, i.e., the original and wind-corrected data, are presented in Table IV. Due to strong differences between the years 2008 and 2007 of the *in situ* and ASCAT soil moisture correlation and because of the scarce ASAR data availability from 2008, only results from 2007 are shown here. Furthermore, only the results from the sensors which gave the strongest Pearson correlation and covariance with ASCAT are shown. The wind correction leads to a decrease or an improvement of the correlation ranging from -0.02 to $+0.07$, whereas the change in covariance ranges from -0.30 to $+15$. For the ROI 3110841, which is the only ROI in the table which does not include any river, the correction leads to a weak improvement of the correlation and a decrease of the covariance.

V. DISCUSSION

From the literature, we know that the water surfaces of tundra lakes in the Arctic are typically rough with respect to the wavelength in question (C-band) [22], [34]. The typical bimodal histogram of backscatter under calm conditions cannot be detected in more than 60% of ASAR WS acquisitions [32]. The average bias due to water surface roughness during the summer (June 21 to September 2) in 2007 and 2008 is up to 4 dB for the selected sites. There is a clear linear relationship between the bias ($\Delta\sigma^0$ and ΔSI) and the water fraction within each ROI (summers 2007 and 2008) for all sites, with the exception of the outliers. For areas with more water than 40%, we can expect a bias of almost 2 dB, which translates to a ΔSI close to 20%. Outliers with a very high ΔSI have been derived by scaling of the backscatter to a very low sensitivity (see Section III-B), i.e., the difference between the dry and wet references is very small. The backscatter bias does not only affect the average backscatter in each ROI but also the dry and wet references which are used for the scaling of the ASAR ΔSI. The impact is on the order of 3 to 7 dB in areas with higher water fraction than 40%. The bias leads to an offset of both the wet and dry references of approximately the same magnitude, which means that the sensitivity is not much affected. The wind is thus not expected to have any major impact on the sensitivity.

The Pearson correlations between the bias and the wind speed in the Lena Delta for specific dates during the time period of interest are low but notably higher than between the bias and the precipitation (see Table III). If the correlation is unexpectedly low with respect to the high water fraction in an ROI, this could be related to shallow water depth. There can be substantial changes in river discharge, which means that the water depth can fluctuate seasonally [24]. Relatively large areas in the Lena River around the Samoylov Island are flat and shallow, and seasonal changes in water depth are noticeable. Shallow water depth could contribute to unexpectedly low bias, since waves cannot develop the same height/amplitude as in deep water, even with high wind speed [44]. A low correlation could be also explained by other roughness effects on the surface than the wind, such as flow patterns in the river.

When the SI and the wind-derived bias correction are applied to the ASCAT SSM, the correction only improves the measurements partially, which can be seen when the original SSM and the corrected SSM are compared with the evaluation data (see Table IV). The applied correction improves the Pearson correlation for some of the ROIs. The ROIs included in Table IV are located in the proximity of the *in situ* data. However, there are differences between these ROIs with regard to the distance to the Samoylov Island, where the *in situ* wind and soil moisture measurements were collected. Local wind conditions can be further reasons to explain unexpectedly low correlation coefficients that we see in Table IV. For an optimal comparison between the different ROIs and in order to truly isolate the effects of wind on the water surface on the bias, wind data would need to be collected from each of these ROI or at least from more than one location. Such meteorological data are unfortunately not available for this study during the time period of the ASAR WS acquisitions. Constraints were the ASAR satellite failure in 2012 and the low availability of ASAR data compared with ASCAT (see Section III-B1). However, networks of meteorological data are expanding, and without the limitation to archive data but with data from the recently launched Sentinel-1, examination of wind data and subsequent ASCAT footprint specific determination of parameters for the correction could be applied. The distance to the *in situ* measurement as described earlier is thus one limitation, but there is also the scaling issue to take into consideration (25 km compared with point *in situ* measurements). Due to variable soil properties, vegetation, and fine-scale topography, the soil moisture may vary strongly in space, making it difficult to match the satellite measurements [45]. Previous studies have, however, concluded that the ASCAT SSM product shows a significant correlation with the *in situ* data and that the annual cycle and trends in short-term fluctuations are captured [5], [9].

A direct comparison between the ASAR and ASCAT absolute backscatter is constrained due to the 10° difference in normalization incidence angle between the available ASAR and ASCAT backscatter products, which translates to a shift of

2.6 dB in homogenous terrain without water. The bias, however, which is a relative difference, is assumed independent from the incidence angle correction under the assumption that noticeable volume scattering (which differs by incidence angle) does not occur in tundra where trees are not present. A parameterization based on SAR is thus applicable to ASCAT backscatter. It should be also considered that the averaged ASAR WS backscatter over the ROI is assumed to correspond to the ASCAT backscatter, although the hexagonal grid generated for the ROI in this study is merely an approximation of the ASCAT grid cells. There are also differences in signal contribution over the footprint for ASCAT to take into account, as well as actual soil moisture changes [8] during times with high wind speed. Finally, the limited time period of this study means that few data are used for defining the wet reference from ASAR here in comparison with when it is derived from ASCAT. Comparisons of ASAR with ASCAT show that the dry reference is relatively comparable but that the wet reference is notably lower for ASAR than for ASCAT, which, in turn, also gives a low sensitivity for ASAR compared with ASCAT. The short time period used for ASAR may be insufficient for defining the appropriate wet reference.

Finally, there are limitations of the ORCHIDEE model with regard to the representation of ephemeral lakes, i.e., which are commonly dry but seasonally water filled, and scarce forcing weather data in certain regions [59]. In addition to that, water body fraction and water body size can cause a problem for the remote sensing retrieval and thus explain the disagreement between ASCAT and model-derived (ORCHIDEE) SSM [22]. This study shows that wind can be a reason for the aforementioned disagreement, which has already been shown attributed to water bodies in the Arctic. This is essential information for studies in high-latitude landscapes, which are indeed rich in lake and in streams and rivers, and where remote sensing data of this kind are needed.

VI. Conclusion

The applicability and quality of the soil moisture product derived from ASCAT have been studied extensively since it was put in operation in 2008 (e.g., [9] and [10]). Potential limitations which are specific for high latitudes have so far been given little attention, although this type of satellite product is of great interest in these regions. Recent studies have concluded that disagreements between the land surface model ORCHIDEE and ASCAT SSM can be explained by the presence of water bodies [21], [22]. Here, we hypothesize and test whether this difference can be explained in terms of variations in the water surface roughness due to rain or wind. Furthermore, we test whether this bias can be corrected with meteorological data.

Medium-resolution ASAR WS data were used to quantify the average bias from water surface roughness within ROIs corresponding to the coarse-scale ASCAT footprint in 11 sites across the Siberian Arctic. The hexagonal grid generated for the ROI in this study is merely an approximation of the ASCAT grid cells, and there are differences in signal contribution over the footprint for ASCAT to take into account, as well as actual soil moisture changes. These aspects need to be considered as limitations. The bias was quantified in the form of backscatter and as SI for improved comparison with the ASCAT SSM data. In support of previous statements that too much water within the ASCAT footprint can disturb the SSM retrieval [13], [22], the results show that the average bias over time can be explained by the lake fraction. For the five sites where meteorological *in situ* data were available, the bias could clearly be better explained by the wind speed than by precipitation.

Low correlations with wind were likely due to a large distance between the ROI and the *in situ* station or to the presence of river; shallow floodplains combined with changes in discharge can give only low wave height even with high wind speeds, or oppositely, streams can give high wave height even when there is no wind. The evaluation of the correction with *in situ* soil moisture data in the Lena River Delta did not give a satisfying result to support the stated hypothesis. However, *in situ* SSM data were only available from the Lena River Delta during this time period when the ASAR archive data were analyzed for this study. It should be considered that this site in many ways is a special case, due to the previously discussed river issues. Future studies can hopefully be expanded by making use of satellite data from the recently launched Sentinel-1, as well as through more recently established *in situ* networks in several sites across the Arctic. The findings of this study are applicable to systems that rely on similar principles, notably the change detection approach for a backscatter signal impacted by soil moisture or other surface conditions.

Acknowledgment

In situ data sharing was made possible through the project Changing Permafrost in the Arctic and its Global Effects in the 21st Century (PAGE21) and in part by the International Network for Terrestrial Research and Monitoring in the Arctic (INTERACT).

References

[1] T. Zhang, J. A. Heginbottom, R. G. Barry, and J. Brown, "Further statistics on the distribution of permafrost and ground ice in the Northern Hemisphere," *Polar Geography*, vol. 24, no. 2, Dec. 2000, doi: 10.1080/10889370009377692.

[2] V. E. Romanovsky, S. L. Smith, and H. H. Christiansen, "Permafrost thermal state in the polar Northern Hemisphere during the international polar year 2007–2009: A synthesis," *Permafrost Periglacial Process.*, vol. 21, pp. 106–116, 2010.

[3] "The physical science basis. Contribution of working group I to the fifth assessment report of the intergovernmental panel on climate change," in *Proc. IPCC Observ., Cryosphere*, Stockholm, Sweden, Sep. 23–26, 2013, pp. 362–364.

[4] S. Marchenko, V. Romanovsky, and G. Tipenko, "Numerical modeling of spatial permafrost dynamics in Alaska," in *Proc. 9th Int. Conf. Permafrost, Inst. Northern Eng., Univ. Alaska Fairbanks*, Fairbanks, AK, USA, Jul. 2008, vol. 29, pp. 1125–1130.

[5] W. Wagner, Z. Bartalais, V. Naemi, S. E. Park, J. Figa-Saladana, and H. Bonekamp, "Status of the Metop ASCAT soil moisture product," in *Proc. IEEE IGARSS*, Honolulu, HI, USA, 2010, pp. 276–279.

[6] E. G. Njoku, T. J. Jackson, V. Lakshimi, T. K. Chan, and V. Nghiem, "Soil moisture retrieval from AMSR-E," *IEEE Trans. Geosci. Remote Sens.*, vol. 41, no. 2, pp. 215–229, Feb. 2003.

[7] W. Wagner *et al.*, "Operational readiness of microwave remote sensing of soil moisture for hydrologic applications," *Nordic Hydrol.*, vol. 38, pp. 1–20, Jul. 2007.

[8] Z. Bartalis *et al.*, "Initial soil moisture retrievals from the METOP-A Advanced Scatterometer (ASCAT)," *Geophys. Res. Lett.*, vol. 34, Oct. 2007, Art. no. L20401.

[9] C. Albergel *et al.*, "Evaluation of remotely sensed and modelled soil moisture products using global ground-based in situ observations," *Remote Sens. Environ.*, vol. 118, pp. 215–226, Mar. 2012.

[10] A. Bartsch, H. Balzter, and C. George, "The influence of regional surface soil moisture anomalies on forest fires in Siberia observed from satellites," *Environ. Res. Lett.*, vol. 4, no. 4, Oct. 2009, doi: 10.1088/1748-9326/4/4/045021.

[11] I. Dharssi, K. J. Bovis, B. Macpherson, and C. P. Jones, "Operational assimilation of ASCAT surface soil wetness at the Met Office," *Hydrol. Earth Syst. Sci.*, vol. 15, pp. 2729–2746, Aug. 2011.

[12] K. Scipal, M. Drusch, and W. Wagner, "Assimilation of ERS scatterometer derived soil moisture index in the ECMWF numerical weather prediction system," *Adv. Water Resources*, vol. 31, no. 8, pp. 1101–1112, Aug. 2008.

[13] W. Wagner *et al.*, "The ASCAT soil moisture product: A review of its specifications, validation results, and emerging applications," *Meteorol. Zeitschrift*, vol. 22, no. 1, pp. 5–33, Feb. 2013.

[14] F. T. Ulaby, R. K. Moore, and A. K. Fung, "Microwave remote sensing: Active and passive-volume III: From theory to applications," in *Advanced Systems and Applications*, ser. Volume Scattering and Emission Theory. Dedham, MA, USA: Artech House, 1986.

[15] A. Bartsch, D. Sabel, W. Wagner, and S. E. Park, "Considerations for derivation and use of soil moisture data from active microwave satellites at high latitudes," in *Proc. IEEE IGARSS*, Vancouver, BC, Canada, Jul. 2011, pp. 3132–3135.

[16] G. Grosse, V. Romanovsky, K. Walter, A. Morgenstern, H. Lantuit, and S. Zimov, "Distribution of thermokarst lakes and ponds at three Yedoma sites in Siberia," in *Proc. 9th Int. Conf. Permafrost*, Fairbanks, AK, USA, Jul. 2008, pp. 551–556.

[17] S. Muster, M. Langer, B. Heim, S. Westermann, and J. Boike, "Subpixel heterogeneity of ice-wedge polygonal tundra: A multi-scale analysis of land cover and evapotranspiration in the Lena River Delta, Siberia," *Tellus B, Chem. Phys. Meteorol.*, vol. 64, Mar. 2012, Art. no. 17301, doi: 10.3402/tellusb.v64i0.17301.

[18] D. A. Walker *et al.*, "The circumpolar Arctic vegetation map," *J. Vegetation Sci.*, vol. 16, pp. 267–282, Jun. 2005.

[19] B. Lehner and P. Döll, "Development and validation of a global database of lakes, reservoirs and wetlands," *J. Hydrol.*, vol. 296, no. 1–4, pp. 1–22, Aug. 2004, doi: 10.1016/j.jhydrol.2004.03.028.

[20] P. Wessel and W. H. F. Smith, "A global, self-consistent, hierarchical, high-resolution shoreline database," *J. Geophys. Res.*, vol. 101, no. B4, pp. 8741–8743, Apr. 1996, doi: 10.1029/96JB00104.

[21] I. Gouttevin, A. Bartsch, G. Krinner, and V. Naeimi, "A comparison between remotely-sensed and modelled surface soil moisture (and frozen status) at high latitudes," *Hydrol. Earth Syst. Sci. Discuss.*, vol. 10, pp. 11 241–11 291, Aug. 2013, doi: 10.5194/hessd-10-11241-2013.

[22] E. Högström, A. M. Trofaier, I. Gouttevin, and A. Bartsch, "Assessing seasonal backscatter variations with respect to uncertainties in soil moisture retrieval in Siberian tundra regions," *Remote Sens.*, vol. 6, pp. 8718–8738, Sep. 2014.

[23] W. J. Brown, O. J. Ferrians, J. Heginbottom, and E. Melnikov, "Circumarctic map of permafrost and ground-ice conditions," Nat. Snow Ice Data Center, Digit. Media, Boulder, CO, USA, 1998, accessed on Sep. 17, 2014. [Online]. Available: http://nsidc.org/data/docs/fgdc/ggd318_map_circumarctic/

[24] J. Boike *et al.*, "Baseline characteristics of climate, permafrost and land cover from a new permafrost observatory in the Lena River Delta, Siberia (1998–2011)," *Biogeoscinece*, vol. 10, pp. 2105–2128, Mar. 2013, doi: 10.5194/bg-10-2105-2013.

[25] Climate Prediction Center/Nat. Centers Environ. Predict./Nat. Weather Service/NOAA/U.S. Dept. Commerce, "Updated half-yearly. CPC global summary of day/month observations, 1979-Continuing," Res. Data Archive Nat. Center Atmos. Res., Comput. Inf. Syst. Lab., Washington, DC, USA, 1987, accessed on Jul. 27, 2011. [Online]. Available: http://rda.ucar.edu/datasets/ds512.0/

[26] K. Yoshikawa, P. P. Overduin, and J. W. Harden, "Moisture content measurements of moss (Sphagnum spp.) using commercial sensors," *Permafrost Periglacial Process.*, vol. 15, no. 4, pp. 309–318, Oct./Dec. 2004, doi: 10.1002/ppp.505.

[27] C. Anderson *et al.*, "Validation of backscatter measurements from the advanced scatterometer on MetOp-A," *J. Atmos. Ocean. Technol.*, vol. 29, pp. 77–88, Jan. 2012.

[28] L. Isaksen and A. Stoffelen, "ERS scatterometer wind data impact on ECMWF's tropical cyclone forecasts," *IEEE Trans. Geosci. Remote Sens.*, vol. 38, no. 4, pp. 1885–1892, Jul. 2000.

[29] W. Wagner, J. Noll, M. Borgeaud, and H. Rott, "Monitoring soil moisture over the Canadian prairies with the ERS scatterometer," *IEEE Trans. Geosci. Remote Sens.*, vol. 37, no. 1, pp. 206–216, Jan. 1999.

[30] J. Closa, B. Rosich, and A. Monti-Guarnieri, "The ASAR wide swath mode products," in *Proc. IEEE IGARSS*, Toulouse, France, Jul. 2003, vol. 2, pp. 1118–1120.

[31] A. Bartsch *et al.*, "Detection of open water dynamics with ENVISAT ASAR in support of land surface modelling at high latitudes," *Biogeosciences*, vol. 9, pp. 703–714, Feb. 2012, doi: 10.5194/bg-9-703-2012.

[32] J. Reschke, A. Bartsch, S. Schlaffer, and D. Schepaschenko, "Capability of C-band SAR for operational wetland monitoring at high latitudes," *Remote Sens.*, vol. 4, no. 10, pp. 2923–2943, Oct. 2012.

[33] A. Trofaier, A. Bartsch, W. Rees, and M. Leibman, "Assessment of spring floods and surface water extent over the Yamalo-Nenets Autonomous District," *Environ. Res. Lett.*, vol. 8, no. 4, pp. 1–9, Nov. 2013, doi: 10.1088/1748-9326/8/4/045026.

[34] D. Sabel, A. Bartsch, S. Schlaffer, J. P. Klein, and W. Wagner, "Soil moisture mapping in permafrost regions—An outlook to Sentinel-1," in *Proc. IEEE IGARSS*, Munich, Germany, Jul. 2012, pp. 1216–1219.

[35] Z. Bartalis, K. Scipal, and W. Wagner, "Azimuthal anisotropy of scatterometer measurements over land," *IEEE Trans. Geosci. Remote Sens.*, vol. 44, pp. 2083–2092, Aug. 2006, doi: 10.1109/TGRS.2006.872084.

[36] W. Wagner, K. Scipal, C. Pathe, D. Gerten, W. Lucht, and B. Rudolf, "Evaluation of the agreement between the first global remotely sensed soil moisture data with model and precipitation data," *J. Geophys. Res. Atmos.*, vol. 108, no. D19, p. 4611, Oct. 2003, doi: 10.1029/2003JD003663.

[37] U. Wegmüller, "The effect of freezing and thawing on the microwave signatures of bare soil" *Remote Sens. Environ.*, vol. 33, no. 2, pp. 123–135, Aug. 1990.

[38] W. Wagner, "Vegetation as observed with the AVHRR and the ERS Scatterometer: A case study over the Iberian Peninsula," in *Proc. Joint ESA-EUMETSAT Workshop Emerg. Scatterometer Appl. Res. Oper.*, Noordwijk, The Netherlands, 1998, vol. 424, pp. 51–56.

[39] W. Wagner, G. Lemoine, M. Borgeaud, H. Rott, "A study of vegetation cover effects on ERS scatterometer data," *IEEE Trans. Geosci. Remote Sens.*, vol. 37, no. 2, pp. 938–948, Jan. 1999.

[40] V. Naeimi, K. Scipal, Z. Bartalis, S. Hasenauer, and W. Wagner, "An improved soil moisture retrieval algorithm for ERS and METOP scatterometer observations," *IEEE Trans. Geosci. Remote Sens.*, vol. 47, no. 7, pp. 1999–2013, Jul. 2009.

[41] A. Bartsch, C. Pathe, W. Wagner, and K. Scipal, "Detection of permanent open water surfaces in central Siberia with ENVISAT ASAR wide swath data with special emphasis on the estimation of methane fluxes from tundra wetlands," *Hydrol. Res.*, vol. 39, pp. 89–100, Aug. 2008.

[42] M. C. Dobson, F. T. Ulaby, M. T. Hallikainen, and M. A. El-Rayes, "Microwave dielectric behavior of wet soil—Part II: Dielectric mixing models," *IEEE Trans. Geosci. Remote Sens.*, vol. GE-23, no. 1, pp. 35—46, Jan. 1985.

[43] J. R. Wang and T. J. Schmugge, "An empirical model for the complex dielectric permittivity of soils as a function of water content," *IEEE Trans. Geosci. Remote Sens.*, vol. GE-18, no. 4, pp. 288–295, Oct. 1980.

[44] K. K. Khama, "On prediction of the fetch-limited wave spectrum in a steady wind," *Finnish Inst. Marine Res., Helsinki, Finland*, vol. 253, pp. 53–78, 1986.

[45] A. Western, W. R. Grayson, and G. Blöschl, "Scaling of soil moisture: A hydrologic perspective," *Annu. Rev. Earth Planet. Sci.*, vol. 30, pp. 149–180, May 2002, doi: 10.1146/annurev.earth.30.091201.140434.

[46] J. Boike *et al.*, "Permafrost—Physical aspects, carbon cycling, databases and uncertainties," in *Recarbonization of the Biosphere — Ecosystems and the Global Carbon Cycle*, R. Lal, K. Lorenz, R. F. J. Hüttl, B. U. Schneider, and J. von Braun, Eds. New York, NY, USA: Springer-Verlag, 2012, p. 545, doi: 10.1007/978-94-007-4159-1.

[47] I. Fedorova *et al.*, "Lena Delta hydrology and geochemistry: Long-term hydrological data and recent field observations," *Biogeosciences*, vol. 12, no. 2, pp. 345–363, Jan. 2015, doi: 10.5194/bg-12-345-2015.

[48] A. M. Plagge, D. C. Vandemark, and D. G. Long, "Coastal validation of ultra-high resolution wind vector retrieval from QuikSCAT in the Gulf of Maine," *IEEE Geosci. Remote Sens. Lett.*, vol. 6, no. 3, pp. 413–417, Jul. 2009.

[49] F. T. Ulaby, R. K. Moore, and A. K. Fung, *Microwave Remote Sensing, Active and Passive, II, Radar Remote Sensing and Surface Scattering and Emission Theory*. London, U.K.: Artech House, 1982.

[50] J. Way, R. Zimmermann, E. Rignot, K. McDonald, and R. Oren, "Winter and spring thaw as observed with imaging radar at BOREAS," *J. Geophys. Res. Atmos.*, vol. 102, no. D24, pp. 29 673–29 684, Dec. 1997.

[51] B. Widhalm, A. Bartsch, and B. Heim, "A novel approach for the characterization of tundra wetland regions with Cb and SAR satellite data," *Int. J. Remote Sens.*, vol. 36, no. 22, pp. 5537–5556, Nov. 2015, doi: 10.1080/01431161.2015.1101505.
[52] J. J. Wilson, P. L. Phillips, J. Figa Saldana, K. Dumper, and T. Fiksel, "Radiometric calibration of the Advanced Wind Scatterometer Radar ASCAT carried on-board the METOP-A satellites," in *Proc. IEEE IGARSS*, Jul. 2005, pp. 3236–3255, doi: 10.1109/IGARSS.2005.1526581.
[53] Y. Yang, X. Li, G. Pichel, and Z. Li, "Comparison of ocean surface winds from ENVISAT ASAR, Metop ASCAT scatterometer, buoy measurements, and NOGAPS model," *IEEE Trans. Geosci. Remote Sens.*, vol. 49, no. 12, pp. 4743–4750, Dec. 2011.
[54] E. D. Yershov, Ed., *Geocryological Map of Russia and Neighboring Republics*, English language edition 1999: Collaborate Map Project. Ottawa, Canada: Carleton Univ., 1991.
[55] W. A. Dorigo *et al.*, "The international soil moisture network: A data hosting facility for global in situ soil moisture measurements," *Hydrol. Earth Syst. Sci.*, vol. 15, pp. 1675–1698, May 2011, doi: 10.5194/hess1516752011.
[56] D. Sabel *et al.*, "Using ENVISAT ScanSAR data for characterizing scaling properties of scatterometer derived soil moisture information over Southern Africa," in *Proc. Envisat Symp.*, H. Lacoste and L. Owehand, Eds., Montreux, Switzerland, Paper ESA SP 636, Apr. 2007.
[57] V. Naemi, Z. Bartalis, and W. Wagner, "ASCAT soil moisture: An assessment of the data quality and consistency with the ERS scatterometer heritage," *J. Hydrometeorol.*, vol. 10, pp. 555–563, Apr. 2009.
[58] V. Naemi, K. Scipal, Z. Bartalis, S. Hasenauer, and W. Wagner, "An improved soil moisture retrieval algorithm for ERS and METOP scatterometer observations," *IEEE Trans. Geosci. Remote Sens.*, vol. 47, no. 7, pp. 1999–2013, Jul. 2009.
[59] I. Gouttevin, G. Krinner, P. Ciais, J. Polcher, and C. Legout, "Multi-scale validation of a new soil freezing scheme for a land-surface model with physically-based hydrology," *Cryosphere*, vol. 6, pp. 407–460, Apr. 2012, doi: 10.5194/tc-6-407-2012.

Elin Högström received the M.S. degree in physical geography from Uppsala University, Uppsala, Sweden, in 2012. She is currently working toward the Ph.D. degree in active microwave remote sensing, for the purpose of application in studies of permafrost in the Arctic, in the Department of Geodesy and Geoinformation, Vienna University of Technology, Vienna, Austria.

Her Ph.D. studies is done within the framework of the FP7 project Changing Permafrost in the Arctic and its Global Effects in the 21st Century (PAGE21). She is also part of the working group Land Surface Remote Sensing in the Austrian Polar Research Institute, Vienna. In 2012, during an employment at Uppsala University, she worked on detecting and quantifying supraglacial and subglacial lakes on the Greenland ice sheet through the use of elevation data from the Ice Cloud and Land Elevation satellite (ICESat) mission.

Annett Bartsch received the M.Sc. degree from Friedrich-Schiller-University Jena, Jena, Germany, in 2000 and the Ph.D. degree in geography from the University of Reading, Reading, U.K., in 2004.

Since 2003, she has been with the Institute of Photogrammetry and Remote Sensing, Vienna University of Technology, Vienna, Austria. She focuses on the application of satellite data at high latitudes related to land surface hydrology and for interdisciplinary studies. She is also currently the Head of the Climate Change Impacts Section at the Central Institute for Meteorology and Geodynamics (ZAMG), Vienna. She is also currently with the Austrian Polar Research Institute, Vienna. Her research interests include active microwave remote sensing techniques for analyses of wetlands, frozen ground, and snow.

Appendix C

Publication 3

Högström, E.; Heim, B.; Bartsch, A.; Bergstedt, H.; Pointner, G.: Evaluation of a MetOp ASCAT-Derived Surface Soil Moisture Product in Tundra Environments. Journal of Geophysical Research: Earth Surface. 2018, 123.

Journal of Geophysical Research: Earth Surface

RESEARCH ARTICLE
10.1029/2018JF004658

Special Section:
The Arctic: An AGU Joint Special Collection

Evaluation of a MetOp ASCAT-Derived Surface Soil Moisture Product in Tundra Environments

Elin Högström[1,2], Birgit Heim[3], Annett Bartsch[1,2,4], Helena Bergstedt[5], and Georg Pointner[4]

[1]Austrian Polar Research Institute, Vienna, Austria, [2]Vienna University of Technology, Vienna, Austria, [3]Alfred Wegener Institute for Polar and Marine Research, Potsdam, Germany, [4]b.geos, Korneuburg, Austria, [5]Department of Geoinformatics-Z_GIS, University of Salzburg, Salzburg, Austria

Abstract Satellite-derived surface soil moisture data are available for the Arctic, but detailed validation is still lacking. Previous studies have shown low correlations between in situ and modeled data. It is hypothesized that soil temperature variations after soil thaw impact MetOp ASCAT satellite-derived surface soil moisture (SSM) measurements in wet tundra environments, as C band backscatter is sensitive to changes in dielectric properties. We compare in situ measurements of water content within the active layer at four sites across the Arctic in Alaska (Barrow, Sagwon, Toolik) and Siberia (Tiksi), taken in the spring after thawing and in autumn prior to freezing. In addition to the long-term measurement fields, where sensors are installed deeper in the ground, we designed a monitoring setup for measuring moisture very close to the surface in the Lena River Delta, Siberia. The volumetric water content (VWC) and soil temperature sensors were placed in the moss organic layer in order to account for the limited penetration depth of the radar signal. ASCAT SSM variations are generally very small, in line with the low variability of in situ VWC. Short-term changes after complete thawing of the upper organic layer, however, seem to be mostly influenced by soil temperature. Correlations between SSM and in situ VWC are generally very low, or even negative. Mean standard deviation matching results in a comparably high root-mean-square error (on average 11%) for predictions of VWC. Further investigations and measurement networks are needed to clarify factors causing temporal variation of C band backscatter in tundra regions.

Key Points:
- Organic layer temperature variations explain temporal behavior of soil moisture derived from C band radar in unfrozen wet tundra
- Temporal variability of volumetric water content from in situ point measurements is representative over distances of several kilometers in tundra
- Near-surface volumetric water content predicted from matched ASCAT data has an average RMSE of 11% across five sites in Alaska and Siberia

Correspondence to:
A. Bartsch,
annett.bartsch@bgeos.com

Citation:
Högström, E., Heim, B., Bartsch, A., Bergstedt, H., & Pointner, G. (2018). Evaluation of a MetOp ASCAT-derived surface soil moisture product in tundra environments. *Journal of Geophysical Research: Earth Surface*, *123*, 3190–3205. https://doi.org/10.1029/2018JF004658

Received 26 FEB 2018
Accepted 8 NOV 2018
Accepted article online 12 NOV 2018
Published online 6 DEC 2018
Corrected 20 DEC 2018

This article was corrected on 20 DEC 2018. See the end of the full text for details.

1. Introduction

The Arctic landscape is characterized by its heterogeneity (e.g., Bartsch et al., 2016; Fletcher et al., 2010), its many surface water bodies (Smith et al., 2007), the presence of permafrost in the ground and frozen surface conditions for the majority of the year (Zhang et al., 2003). The soil layer close to the surface, just above the permafrost table, which experiences seasonal freezing and thawing is referred to as the active layer. In summer, the thaw front penetrates from the surface downward and the active layer deepens as positive soil temperatures prevail. In autumn, the freeze front penetrates downward from the surface, as well as upward from the permafrost table. Knowledge about the amount of water that freezes in the active layer in autumn is of interest, as this water will be available as potentially liquid water for the following spring. This information has been shown to be valuable, for example, for wildfire prediction and is of interest for purposes related to heat transfer from and isolation of the frozen ground (Beer et al., 2007). Ice has a lower thermal conductivity than water. Therefore, the active layer is expected to isolate the underlying permafrost better if the water fraction in the soil is high at the time of freezing in autumn. Soil moisture data are generally in high demand in this region; for example, for permafrost-related applications, specifically modeling and flux upscaling studies (Jung et al., 2010; Marchenko et al., 2008; Zhang et al., 2011).

A wide range of global satellite-derived soil moisture products are available today from microwave sensors, such as the Advanced Microwave Scanning Radiometer for EOS (AMSR-E) (Njoku et al., 2003; Owe et al., 2008), Tropical Rainfall Measuring Mission (TRMM) Microwave Imager (TMI; Owe et al., 2008), Special Sensor Microwave/Imager (SSM/I; Owe et al., 2008), WindSat Polarimetric Radiometer (Li et al., 2010), European Remote Sensing Satellites ERS 1 and 2 (Scipal et al., 2002; Wagner, Lemoine, et al., 1999), and the Advanced Scatterometer (ASCAT) onboard the Meteorological Operational satellite (MetOp; Bartalis et al., 2007; Wagner et al., 2010). More recent data collection programs include the Soil Moisture and Ocean Salinity Mission (SMOS) of the European Space Agency (Kerr et al., 2001) and the Soil Moisture Active and Passive of the United States National Aeronautics and Space Administration (NASA; Entekhabi et al., 2010), which were

specifically designed for the purpose of soil moisture retrieval. Global maps of near surface soil moisture are produced using coarse resolution (~25–50 km) sensors operating in the microwave frequencies, employing passive as well as active systems.

C band scatterometer information is of specific interest in heterogeneous environments due to the availability of higher spatial resolution Synthetic Aperture Radar (SAR) data at this wavelength. SAR can be used to assess the spatial variability and representativity of the scatterometer information (Wagner et al., 2008). The C band scatterometer ASCAT provides operational data in near real time since 2008 (Bartalis et al., 2007; Wagner et al., 2010). The microwave backscatter variations are expected to correspond to soil moisture variations. Surface roughness and volume scattering, which also contribute to the backscatter signal, are parameterized or assumed to be constant under certain conditions (Bartalis et al., 2007; Naeimi, Bartalis, et al., 2009; Naeimi, Scipal, et al., 2009). The measurements available during frozen and snow cover conditions are masked out because soil moisture data, as absolute values or saturation, can only be obtained during the unfrozen period. In addition, the existence of surface water within the scatterometer footprint poses a challenge (Wagner et al., 2013). The water surface roughness can quickly increase at high wind speeds and thus introduce a bias in lake-rich areas (Högström & Bartsch, 2017).

A multitude of studies have validated soil moisture detection approaches through comparison with in situ measurements (Rudiger et al., 2007). The challenge is to compare the point observations of measurement stations to large scatterometer footprints of 25- to 50-km size (Wagner et al., 2013).

In situ measurements are essential for evaluating satellite-based soil moisture estimates and to understand what is represented in the backscatter signal (Ceballos et al., 2005; Wagner et al., 2007). Soil moisture measurements have been used for satellite validation purposes since the 1980s (Wang et al., 1980), and the availability of remotely sensed soil moisture from, for example, SMOS, AMSR-E, and WindSat have led to further validation activities such as the installation of new in situ soil moisture networks (Delwart et al., 2008; Wagner et al., 2007). There is increasing availability of in situ soil moisture data (Krauss et al., 2010), and there have been attempts to collect and disseminate soil moisture data from several networks (Robock et al., 2000). In 2011, the International Soil Moisture Network (ISMN) was established, which is a centralized hosting facility of in situ soil moisture data (Dorigo et al., 2013). Soil moisture observation networks have been installed and used for calibration/validation activities for the Soil Moisture Active Passive Mission (Colliander et al., 2017), the SMOS (Bircher et al., 2012) missions, as well as the European Space Agency Climate Change Initiative soil moisture product (Ikonen et al., 2016). The above mentioned efforts are highly valuable for quantitative assessments of global remote sensing products, but the networks themselves were not always installed for that purpose, which can mean that multiple measurements within a satellite footprint are not provided (Crow et al., 2012). The large spatial variability in soil moisture (Western et al., 2002) is still challenging, and there is a need to understand the variable satellite-derived soil moisture product quality across different environments (De Jeu et al., 2008; Dirmeyer et al., 2004; Sinclair & Pegram, 2010). Small-scale networks also exist with relatively high spatial density (e.g., 3–5 km^2; Jackson et al., 2010). In situ measurements overall are still concentrated in the middle and low latitudes, and there are clearly gaps to be filled across the Arctic.

Scaling between local in situ measurements and 25- to 50-km footprints for scatterometer and microwave radiometer measurements remains problematic for validating results, in particular, due to the spatial and temporal variability of soil moisture (Western et al., 2002). It has been shown that the spatial variability increases with the size of the area up to 10 km^2 but remains relatively constant thereafter and that a small number of measurements are sufficient to obtain accurate areal measurements (Brocca et al., 2012). The difference in depth between the in situ sensor, commonly installed at 10 cm or deeper, and the top layer through which the microwave signal can penetrate is crucial. The microwave signal penetration depth also depends on the moisture level itself (deeper penetration for low percentages of water). In fact, correlations between satellite and in situ measurements are usually not very high. Bartsch, Trofaier, et al. (2012) demonstrated that Pearson correlations for sensors deeper than 10 cm are below 0.4 in tundra environments. But even a lack of correlation does not necessarily mean that the satellite data are wrong. It may, for example, be explained by the fact that the point measured in situ data are not representative for a larger area, such as that of the satellite footprint of the remote sensing data product. The results need to be interpreted in their relative context. Direct comparisons between in situ data and remote sensing products remain an important aspect of validating spatial scaling of predictions and understanding small-scale moisture variations in specific land types. When

interpreting the results of a direct comparison, it is also important to consider the accuracy and quality of the in situ data set (Wagner et al., 2013).

Previous studies that compared in situ water content with satellite data indicate that the shallow installation of sensors is an appropriate choice (Bartsch et al., 2011, 2012). The uppermost sensors are more directly affected by the atmospheric conditions than those in deeper soil layers, where changes in moisture and temperature are slower and damped. Prior estimations of in situ unfrozen water content in tundra over time have been conducted using bulk electrical conductivity and in situ soil temperature data in Alaska, demonstrating the potential to remotely *visualize* permafrost via autonomous monitoring over field-relevant scales (Dafflon et al., 2017).

In this study, in situ data records from four existing monitoring sites in northern Alaska and in Siberia, Russia, were used to investigate how in situ soil moisture data compare with the ASCAT SSM during the period of freezing in autumn and thawing in spring. Additionally, a setup of in situ temperature and soil moisture sensors has been developed specifically for the purpose of ASCAT assessment. Sensors have been installed in a high-latitude Arctic location in order to investigate the validity of near-surface soil moisture retrieved with the ASCAT instrument. It is hypothesized that although absolute values may differ between the in situ measurement sites within the ASCAT footprint, the variation in measured values will be similar. The integrated measurement from a certain ASCAT footprint area is expected to reflect the general moisture level in these landscapes. It is further hypothesized that soil temperature variations during the transition period are reflected in MetOp ASCAT measurements as the dielectric constant of the water within the soil changes with the changing soil temperature (Hallikainen et al., 1985) and in turn influences the microwave backscatter (Naeimi et al., 2012; Ulaby & Long, 2014). Lastly, we investigate whether the ASCAT SSM measurements before freeze-up are valid and to what extent the ASCAT SSM is related to the soil temperature development.

2. Materials and Methods

2.1. MetOp ASCAT Soil Moisture Product

ASCAT is a fan-beam scatterometer with six side-looking antennas that illuminate two 550-km-wide swaths on each side of the satellite track, separated by a gap of 360 km. The instrument is onboard the series of polar orbiting Meteorological Operational (MetOp) satellites: MetOp-A, launched in 2006, MetOp-B in 2012, and MetOp-C is planned to be launched in 2018. The MetOp constellation flies in a near-polar Sun-synchronous orbit with a repeat cycle of 29 days and completing 14 orbits per day. The daily global coverage with one MetOp is about 82%, with full coverage over the poles (>65°), where three to four acquisitions are available per day by combining the ascending and descending orbits, for example, at approximately 2, 5, 9, and 12 p.m. UTC in the Lena Delta, Siberia.

When ASCAT was designed its main purpose was to measure wind speed and direction over the oceans (Figa-Saldaña et al., 2002), but quite soon it turned out that unforeseen land applications were possible as well. EUMETSAT (European Organisation for the Exploitation of Meteorological Satellites) in cooperation with the Vienna University of Technology (TU Wien) have developed a soil moisture retrieval algorithm which is implemented in a software package called the Water Retrieval Package (WARP). Since 2008 near-real-time (within ~135 min after actual acquisition) measurements of SSM are available globally from ASCAT (Bartalis et al., 2007; Wagner et al., 2010). The instrument operates at a frequency of 5.3 GHz (C band), both transmitting and receiving electromagnetic waves in vertical polarization (VV). The ASCAT incidence angle ranges from 25° to 65°, and the backscatter is normalized to a standard incidence angle of 40° (Bartalis et al., 2007). A contrast in dielectric properties between dry and wet soils leads to a strong dependency of C band backscatter intensity on the moisture content in the uppermost soil layer. This contrast forms the basis of the retrieval method. The penetration depth for ASCAT measurements is approximately 5 cm but is known to be higher for dry compared to wet soils. The reason is that water is not only a strong scatterer but also a strong absorber of low-frequency microwaves (Schanda, 1986). The penetration depth increases almost exponentially in water depleted soil (Williams & Greeley, 2001). Besides moisture, the radar signal is also affected by surface roughness, vegetation as well as ice, and snow (Bartsch, 2010; Bartsch et al., 2011; Naeimi et al., 2012). For the ASCAT surface soil moisture retrieval a change detection approach has been developed which assumes roughness and land cover to be stable in time at a given spatial scale (Wagner, Noll, et al., 1999; EUMETSAT repository). Since scattering from vegetation is enhanced at large incidence angles and during the vegetation season, it is corrected for by using the multiincidence angle-viewing capacities of ASCAT. The backscatter values are scaled between a dry (0%) and wet (100%) reference, corresponding to the locally obtained historical minimum and

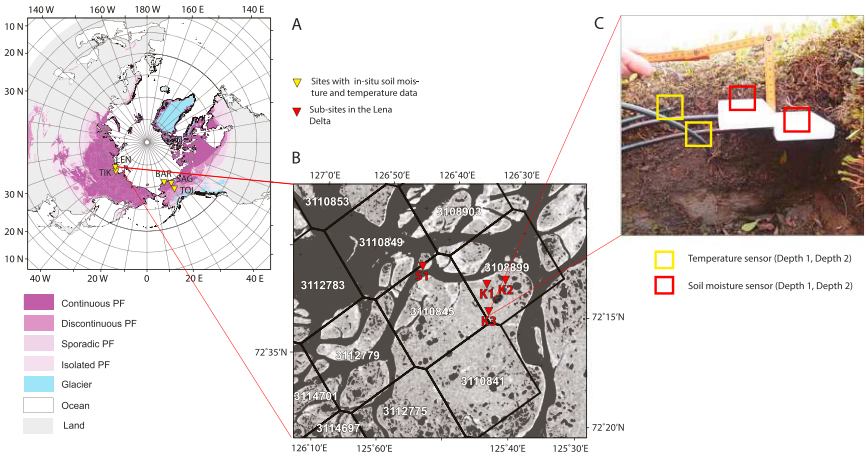

Figure 1. (a) In situ site locations in the Arctic overlain with a simplification (not including subclasses for ground ice content) of the Circum Arctic map of permafrost and ground ice conditions as background (Brown et al., 2002). Projection: Lambert Azimuthal. Classes contained are continuous, discontinuous, sporadic, and isolated permafrost as well as glacier, ocean, and land. (b) ENVISAT ASAR Wide Swath image for the central Lena River Delta, Siberia. The location of the installed stations on the Kurungnakh island in the Lena Delta is indicated in red. Black hexagons represent the approximate ASCAT footprint and are labeled with the ASCAT product ID. Projection: UPS North Stereographic. (c) Setup of the VWC and soil temperature sensor installation at the sites on Kurungnakh: VWC and soil temperature sensors at Depth 1 (SSM D1, T D1) (a depth of 3 cm) and at Depth 2 (SSM D2, T D2) (a depth of 6–7 cm). ENVISAT = Environmental Satellite; ASAR = Advanced Synthetic Aperture Radar; WS = Wide Swath; ASCAT = Advanced Scatterometer; UPS = universal polar stereographic; VWC = volumetric water content; SSM = surface soil moisture.

maximum values, resulting in a relative measurement of the water content (saturation) in the uppermost soil layer (Wagner, Noll, et al., 1999). Validation results for ASCAT have been overall positive, but there are regions that are problematic, such as mountains, deserts, or those with a high water fraction (Högström & Bartsch, 2017; Wagner et al., 2013).

The ASCAT time series data are available for a predefined discrete global grid which is based on the assumption that the Earth can be modeled as a rotated ellipsoid. The grid cells are spatially resampled with an equal spacing of 12.5 km in latitude and longitude and identified by a unique grid cell index (GPI). Each grid cell over land is attributed a time series of backscatter values as well as SSM data (Naeimi, Scipal, et al., 2009). Time series have been extracted from the EUMETSAT Data Center for each location for which in situ data have been available.

Frozen conditions are indicated through a so-called Advisory Flag that ranges from 0 to 100 (unfrozen to frozen), which is available for the SSM data user. An Advisory Flag also exists for snow probability, ranging from 0 to 3 (snow-free to snowy conditions). The flags are both based on analyses of historical data (SSM/I snow cover data and ERA-40 climate data, respectively) and give the probability for snow and/or frozen ground for each day of the year (Nolin et al., 1998; Uppala et al., 2005). This probability does not vary from year to year. However, timing of freezing and thawing can be highly variable (Naeimi et al., 2012). For the present study all frozen and snow-covered conditions are therefore masked out based on the in situ records.

In order to detect thaw and freeze onset dates, a 7-day median-filter is applied on the in situ time series of volumetric soil moisture. The thaw and freeze onsets are defined by the first and last days of the year, respectively, where the filtered time series exceed 20%. All ASCAT measurements before thaw and after freeze onsets were masked out.

2.2. In Situ Soil Temperature and Volumetric Water Content Records

Four sites where in situ soil moisture was already available were selected in Alaska and in Siberia, Russia, for comparison between ASCAT derived SSM and in situ moisture data. All four sites, Barrow, Sagwon and Toolik in Alaska, as well as Tiksi in Siberia are long-term permafrost monitoring sites. The data for Alaska were available through the Natural Resources Conservation Service and for Tiksi through the Finnish Meteorological Institute in Helsinki, Finland. Given that the C band sensors' penetration depth is less than 5 cm the records from in situ sensors at shallow depths correspond well to the ASCAT data records compared to those from deeper

Table 1
Table Overview of the Five Arctic Sites: Their Location, the Sensor Depth, and Brief Description of the Site

Sites	Location	Sensor depth (cm)	Data availability	Description
Toolik	68°37′22.9″N 149°36′35.4″W	9	2007–2011 daily	Tussock tundra, inland, south of Toolik lake.
Sagwon	69°24′08.9″N 148°47′52.9″W	10	2007–2011 daily	Moist acidic tundra, upland, inland.
Barrow	71°18′27.7″N 156°35′19.7″W	10	2007–2011 daily	Tussock tundra, Coastal lowland, polygon landscape.
Tiksi	71°35′39.48″N 128°53′17.4″E	5	2011–2014 hourly	Mid-wet tundra, Coast, hilly with exposed bedrock.
Lena Delta	(see below)		2013–2014 daily	Tundra, high water fraction
Lena Delta Sub sites[a]	Location	Sensor depth (cm)[b]	Profile	Average VWC before freeze-up 2013
K1	72°19′43.88″N	D1:3	moss layer	0.04
	126°14′59.10″E	D2: 6	fibric layer	0.45
K2	72°18′25.11″N	D1:3	moss layer	0.07
	126°12′53.50″E	D2: 8	fibric layer	0.32
K3	72°21′14.23″N	D1:3	moss layer	0.31
	126°08′26.52″E	D2: 6	fibric layer	0.54
S1	72°22′59.71″N	D1:4	moss layer	0.04
	126°28′10.39″E	D2:10	fibric layer	no data

Note. VWC = volumetric water content.
[a]K1-3 and S1 stand for Kurungnakh one to three and Samoylov 1. [b]D1 and D2 stand for depth one and two.

installed sensors (Bartsch, Melzer, et al., 2012). Therefore, although data for more than one depth were available from the Alaskan sites and Tiksi, only records from sensors at shallow depths were included. Figure 1 and Table 1 give an overview of the sites location, the included sensor depth, and the in situ time period covered at the specific sites which also correspond to that of ASCAT measurements (from 2007). For the selected sites, sufficiently continuous soil temperature measurements are only publicly available for Barrow on the Global Terrestrial Network for Permafrost Database (GTN-P). The record ends in 2008, providing two years of overlap with ASCAT measurements.

To get additional data on soil temperature and VWC automatic stations measuring soil temperature and VWC were deployed in the central Lena River Delta, Siberia. They were installed at a very shallow depth and intended for comparison with ASCAT measurements on the islands Kurungnakh and Samoylov (Figure 1). The Lena Delta is underlain by continuous permafrost between about 400 and 600 m below the surface (Yershov et al., 1991). It offers a large suite of different permafrost landscape types. At 72°N the landscape north of the treeline is characterized by a shrubby tundra on top of the Yedoma Islands and by polygonal wet tundra on the Holocene river terraces of the Lena Delta. Samoylov is a small island located within one of the main Lena River channels, where long-term monitoring, including climate and soil measurement stations, has been in progress since 1996 (Boike et al., 2013). The Samoylov research station with its facilities, as well as the long study records, makes this a key site for polar research in the Siberian Arctic. Samoylov Island is dominated by a polygonal wet tundra landscape. The Yedoma landscape unit Kurungnakh is located only a few kilometers south of Samoylov Island. The measurement stations were installed in August 2013 on Kurungnakh and Samoylov and data were collected in August 2014. Three stations were placed on Kurungnakh (K1, K2, and K3) and one on Samoylov (S1). Each station on Kurungnakh consisted of (a) one VWC Campbell Recording Sensor CR625 and one Temperature T109 sensor at a shallow depth, referred to as depth one (W1 and T1), (b) one VWC CR625 sensor and one T109 sensor at a deeper depth, referred to as depth two (W2 and T2; Figure 1c). The station on Samoylov had the same setup as that on Kurungnakh, with the exception that only one depth

Table 2
Pearson Correlation Matrix for Intercomparisons of (top) in Situ Soil Temperatures From the Different Stations, (middle) in Situ Volumetric Water Content (VWC) From the Different Stations, and (bottom) ASCAT-Derived Surface Soil Moisture (SSM) From Four Neighboring GPI

In situ sensor VWC						
	K2 W1	K3 W1	S1 W1	K1 W2	K2 W2	K3 W2
K1 W1	0.980	0.902	0.944	0.937	0.890	0.811
K2 W1		0.902	0.935	0.914	0.838	0.759
K3 W1			0.842	0.890	0.785	0.786
S1 W1				0.819	0.740	0.686
K1 W2					0.935	0.913
K2 W2						0.932
In situ sensor soil temperature						
	K2 T1	K3 T1	S1 T1	K1 T2	K2 T2	K3 T2
K1 T1	0.995	0.990	0.993	0.998	0.988	0.978
K2 T1		0.989	0.997	0.997	0.997	0.987
K3 T1			0.989	0.988	0.981	0.985
S1 T1				0.995	0.995	0.988
K1 T2					0.994	0.987
K2 T2						0.991
ASCAT SSM						
	3110841	3110845	3110849			
3108899	0.95	0.96	0.95			
3110841		0.95	0.91			
3110845			0.95			

could be instrumented (W1 and T1). The sensors at depth one were placed in the lower end of the uppermost porous moss layer (at an average of 5- to 7-cm thickness). The sensors at depth two were placed in the moss fibric layer, a thin layer of ~2 to 3 cm, which is the water storage layer of the moss and always water saturated (Yoshikawa et al., 2004). Below the fibric layer very decomposed old moss and roots from the vascular plant cover frequently form a fibric peat layer of approximately 8 to 10 cm transitioning into mineral-dominated soil. The fibric layer may also directly overlie mineral soil of the active layer. The precise locations of each sensor are given in Table 1. Soil temperature and VWC were recorded at daily intervals. Figure 1 shows the site overview of field work in 2013 in the Lena Delta (a) and a photo of the installation (c).

2.3. Comparison of in Situ and Satellite Records

The temporal sampling of in situ data across the Arctic varied between measurement sites, with daily sampling in Toolik, Sagwon, Barrow, and the Lena Delta. Hourly sampling was available only for the Tiksi data. For the comparison between ASCAT SSM and in situ VWC data, daily means were used for each site and grid point.

In order to compare the ASCAT SSM (percent saturation) and in situ VWC data, two different scaling methods were employed. In the first method, the in situ data are adjusted to match ASCAT SSM values. ASCAT SSM values are determined by scaling each backscatter value to the historical maximum and minimum at that point. The in situ VWC data were therefore likewise scaled to the measured minimum and maximum in situ data. It should be noted that in the Lena Delta, the historical minimum and maximum could only be calculated from 1 year, which were then compared with a 7-year record of ASCAT data combined with historical ERS data (Naeimi, Scipal, et al., 2009). The still mostly frozen soil and permafrost beneath impede percolation of water into the ground. Therefore, it is generally expected that soils are fully saturated after the spring snow melt in tundra environments. The fact that only the near surface is observed here needs to be considered, since this may consist of a green moss layer and thus dry up quickly. In the second comparison method, the ASCAT data are rescaled to the in situ observations using mean standard deviation matching (Brocca et al., 2011), implemented in the Python Toolbox for the Evaluation of Soil Moisture Observations (pytesmo, Paulik et al., 2014). Matching allows determination of the root-mean-square error (RMSE) for predicting VWC from ASCAT SSM. The Pearson correlation has additionally been derived for all sites. All statistical analyses are carried out

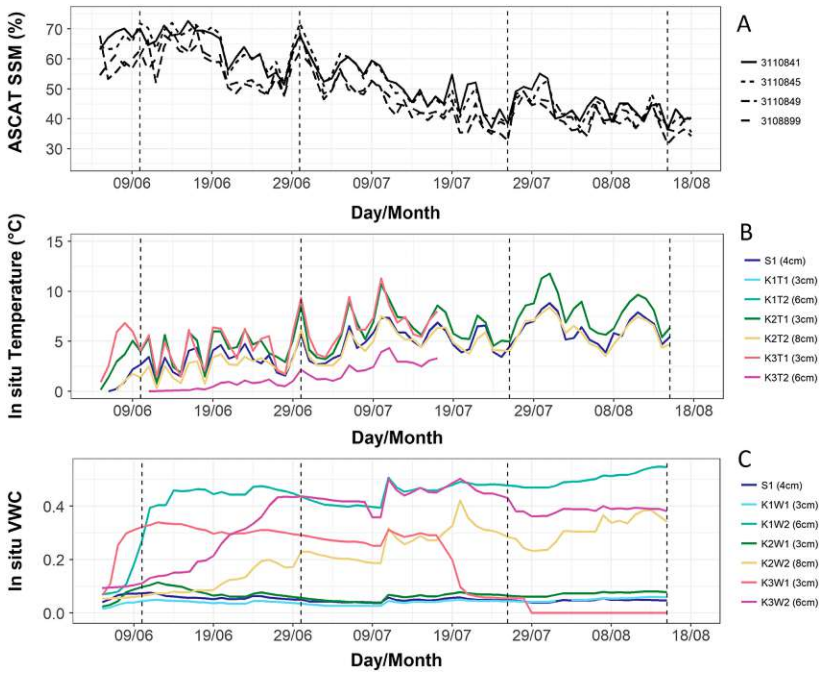

Figure 2. Time series of (a) Advanced Scatterometer (ASCAT) surface soil moisture (SSM), (b) in situ soil temperature, and (c) in situ volumetric water content (VWC) measured in the organic layer (moss and fibric layers) at the Lena River Delta during summer 2014. The curves in panel (a) are for different ASCAT grid points. The soil temperature shown in panel (b) is recorded at each station (K1–K3, S1) at the depth 3 to 4 cm (T1, moss layer) and 6–8 cm (T2, fibric layer). The VWC shown in panel (c) is recorded at each station (K1–K3, S1) at the depth 3 to 4 cm (T1, moss layer), and 6–8 cm (T2, fibric layer). In situ depths and ASCAT GPI are shown according to the legend. Vertical dashed lines indicate the beginning and end of time periods used for analyses in Figures 5 and 6 and Table 3.

separately for the beginning and the end of the unfrozen season, which has been defined by a 20-day period after the thaw onset and prior to the freeze onset detected from the in situ data. The distribution of the in situ and ASCAT records (for both scaling methods, in situ scaled on own minimum-maximum and ASCAT rescaled to in situ using mean standard deviation matching) are further assessed with boxplots for the Lena Delta and Barrow over these time periods.

The representativeness of the in situ data for the four stations in the Lena Delta was investigated by comparing the records from each station with each other. The Pearson correlation coefficient was calculated between the records from each sensor (Table 2). In situ data from the Lena Delta were collected from 2 September 2013 to 15 August 2014. The ASCAT SSM from this time period is applicable only during unfrozen and snow-free conditions. The thaw onset was here defined using data from K1W2, as it showed the steepest increase of VWC of all the sensors. The same median-filter and threshold of 20% as described above in section 2.1. was used. The last day used in the analysis is defined by the in situ data availability (15 August 2014). Thus, the last 20-day period for the Lena Delta is termed *late summer*.

Dependencies between soil temperature and the observed ASCAT backscatter over time have been analyzed for the stations on Kurungnakh and Barrow, based on Pearson correlations over a 20-day period. This duration allows for sufficient samples and at the same time can provide information on changes of this relationship over time, considering the short unfrozen period at the Arctic sites. The Pearson correlation has been derived for the original data as well as detrended versions in order to investigate short-term variability. Sensor soil temperature at depth one and two, as well as satellite records, have been temporally averaged over a 3-day window for this purpose. Three-day windows are often applied to satellite-derived soil moisture records to reduce noise (e.g., Massari et al., 2017). This noise may, however, result from soil temperature variations. The resulting time series have been subtracted from the original data in order to exclude the long-term variations. The correlation analyses for the 20-day period has been repeated with the detrended data set. The same procedure has been applied to the records from Barrow.

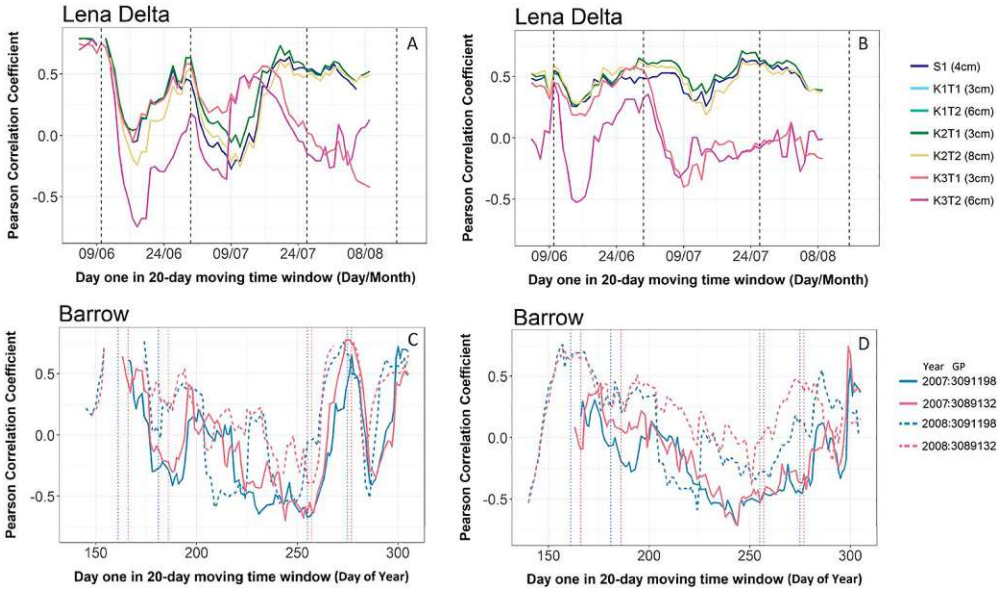

Figure 3. Temporal development of the Pearson correlation between ASCAT SSM and in situ soil temperature time series. (a, b) Lena Delta (GPI 3110845), (c, d) Barrow (3091198 over Barrow with ocean in ASCAT footprint, 3089132 south of Barrow). (left) Results of a 20-day moving time window applied for the full unfrozen summer period. (right) Temporal development of the correlation between detrended ASCAT SSM and in situ soil temperature time series—results of a 20-day moving time window applied for the full unfrozen summer period. Vertical dashed lines indicate the beginning and end of time periods used for analyses in Figures 5 and 6 and Table 3. ASCAT = Advanced Scatterometer; SSM = surface soil moisture.

3. Results

3.1. Soil Moisture and Temperature Dynamics in the Lena Delta

Results from the Pearson correlation analyses showed that for the temporal dynamics of the measured soil temperature in the moss and fibric peat layer the overall agreement between the sensors of the four stations is high (0.978–0.998). Table 2 shows the Pearson correlation matrix between the measured soil temperature at in situ sites. Station K3 with K3T1 and T2 showed the lowest agreement with other sensors (0.978–0.991) and sensors at similar depths showed slightly higher correlations than between different depths. The Pearson correlation for the VWC measurements range from medium to high (0.686–0.980). The lowest values were again from the K3 station (0.686–0.932). For the VWC measurements, the sensors at similar depths clearly showed higher correlations than sensor comparisons between different layers. The VWC record of the uppermost measurement in the moss layer that is in direct exchange with the atmosphere shows the highest temporal dynamics. The moss layer VWC measurements were lower than the VWC in the water-saturated fibric layer, whereas the soil temperature was higher in the moss layer. The VWC record of the fibric layer showed a reduced expression of the same temporal dynamics with much higher wetness. The intercomparisons of SSM from the different ASCAT GPI showed overall high agreement (0.86–0.97). The GPI 3110845 showed the highest agreement with 3108899 and 3110841 (0.97).

The daily recorded in situ soil temperature data showed similar variations as the closest in time daily recorded ASCAT surface moisture (Figure 2). The soil temperature variations for the deeper sensor K3 as well as the soil temperature itself were much lower than for the other sites in the Lena Delta. The Pearson correlation for the 20-day time windows ranged from approximately −0.7 to 0 in early spring, followed by a peak of 0.6 at the end of June (sensor K2 and K3, Figure 3). Correlations were also positive and medium high (values up to 0.6) in summer (mid July) but in some cases (K3) gradually became lower toward the time of freeze-up in autumn. For the detrended data set, correlations with organic layer soil temperature were comparably high during the first 2 weeks, except for K3 at 6-cm depth. They ranged from 0.4 to 0.5 (Figure 3). Correlations decreased for the 20-day periods starting after approximately 10 July 2014 in the case of K1 and K2. This period is characterized by moisture variations (in situ) as shown in Figure 2. The period of higher correlation ends at the end of June for K3. Figure 2 also shows the ASCAT SSM for additional GPI locations near the sites with in situ observations. The variations of in situ VWC in the case of all the Lena Delta sites were not well represented by ASCAT SSM during

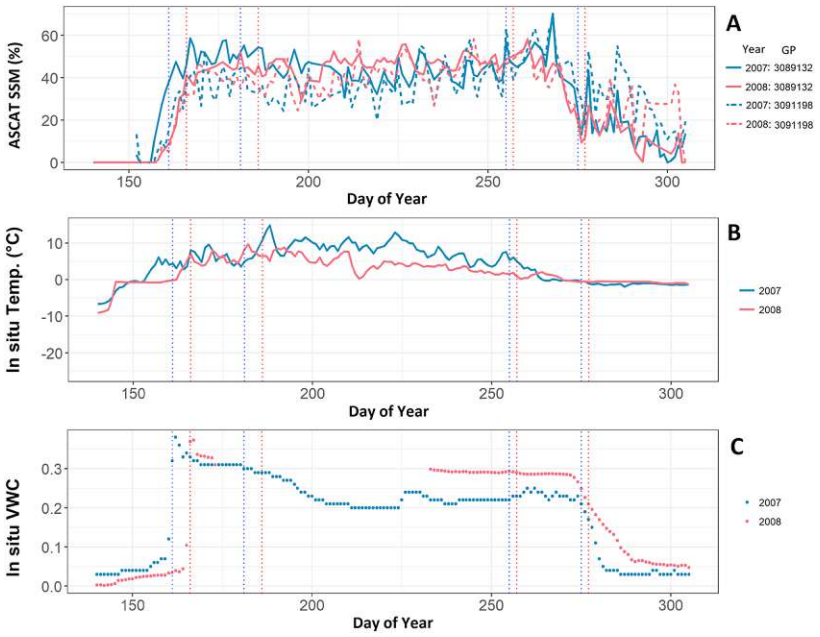

Figure 4. Time series of (a) ASCAT surface soil moisture (SSM), (b) in situ soil temperature, and (c) in situ VWC at Barrow during the summer of 2007 and 2008 for different grid points (3091198 over Barrow with ocean in ASCAT footprint, 3089132 south of Barrow). The sensors in panels (b) and (c) are located at 0-cm (b) and 10-cm (c) sensor depth. ASCAT GPI are shown according to legend. Vertical dashed lines indicate the beginning and end of time periods used for analyses in Figures 5 and 6 and Table 3. ASCAT = Advanced Scatterometer; GPI = grid cell index.

the time period of in situ data availability. A period of lower moisture could be observed toward the end of July at most in situ locations, which coincides with higher SSM/backscatter. Station K1 behaved differently than the other sites in August, displaying increasing VWC. However, a late August expedition to this site showed local changes due to water logging. The installation of the sensors in 2013 seems to have triggered the degradation of this site 1 year later. The VWC sensor of station K2 ceased to operate in mid-July 2014 due to disturbance by animals. The soil temperature records for K3 are shorter than for other sites due to damage to the sensors by rodents. Also, the moisture sensor measurements are disturbed afterward.

3.2. Soil Moisture and Temperature Dynamics in Alaska

Soil temperature, which is measured at 10-cm depth varies less at the Barrow site (Figure 4) compared to observations from the Lena Delta sites. The same applies to the soil moisture record from ASCAT measurements as well as in situ VWC. In addition, ASCAT SSM begins to decrease several days before in situ VWC values in the autumn (Figure 4).

The behavior of the soil temperature and SSM relationship over time is similar to the observations in the Lena Delta (Figure 3). There is a change to positive correlations after detrending but is less pronounced. Correlations are higher for 2008 than for 2007 (Figure 3d).

3.3. Quantitative Comparisons of Soil Moisture Records

Correlations between ASCAT SSM and in situ VWC vary strongly from site to site (Table 3). They can be positive or negative at the same site for different years, especially after snowmelt (average −0.15). Autumn correlations are mostly positive and also higher. The average is 0.16. Maximum values are reached at Barrow, with an average of 0.65. However, it should be noted that the VWC measurements in 2007 have gaps for the analyzed spring period. Correlations are negative for all sensors in the Lena Delta. Low (close to zero) and negative correlations coincide with high RMSE values (17–24% VWC, Table 3) derived from matched ASCAT SSM data. Barrow shows the lowest RMSE with 2.6–10.2% (VWC).

Boxplots for Barrow and the Lena Delta comparing the ASCAT and in situ VWC records during the first 20 days after snow clearance and soil thawing in spring, as well as the last 20 days before freezing in autumn at Barrow and last 20 days before the end of the records in the Lena Delta are shown in Figures 5 and 6. The first and last dates are indicated in Figures 2 and 4.

Table 3
Spring (Spr) and Autumn/Late Summer (Aut/LS) Root-Mean-Square Errors (RMSEs) and Pearson Correlation Coefficients of ASCAT SSM and in Situ VWC for All Sites and All Years

Site name[a]	Year	Spr RMSE	Spr Pearson R	Aut/LS RMSE	Aut/LS Pearson R
Barrow	2007	5.9	-0.42	10.2	0.15
Barrow	2008	8.4	-0.62	3.5	0.64
Barrow	2009	9.8	0.19	2.6	0.76
Barrow	2010	4.4	-0.46	3.9	0.86
Barrow	2011	5.9	-0.50	5.0	0.83
Toolik	2007	12.0	0.03	8.4	0.31
Toolik	2008	9.6	0.21	-	-
Toolik	2009	6.9	0.19	-	-
Toolik	2010	7.7	0.12	12.3	0.64
Toolik	2011	9.9	-0.48	5.6	0.29
Sagwon	2007	34.3	0.29	19.0	0.75
Sagwon	2008	23.3	-0.20	15.1	0.04
Sagwon	2009	23.5	-0.02	18.6	0.15
Sagwon	2010	23.2	-0.23	22.7	-0.55
Sagwon	2011	21.4	0.22	8.6	0.05
Tiksi	2011	13.4	0.02	22.5	-0.78
Tiksi	2012	11.4	-0.10	14.0	0.32
Tiksi	2013	16.9	-0.33	13.3	-0.18
Tiksi	2014	5.8	-0.29	15.5	-0.86
LD 3108899 - K2W2	2014	24.2	-0.64	16.9	-0.58
LD 3110845 - K2W2	2014	24.0	-0.56	17.5	-0.44

[a]For Toolik in autumn 2008 and 2009, no ASCAT data were available. For the Lena Delta (LD), correlations and RMSEs were calculated between K2W2 and ASCAT GPIs 3108899, 3110845.

Our approach for scaling in situ VWC values with ASCAT SSM shows poor agreement at the Barrow site during the spring season, with approximately 20–40% difference in values (Figure 5) ASCAT SSM records are mostly below the scaled in situ values in spring but at a similar (slightly higher) level in autumn. The opposite pattern can be observed for the Lena Delta (Figure 5). However, it should be noted that values for the second period represent late summer at the Lena Delta.

The matching of ASCAT SSM to in situ VWC results in similar levels in the case of Barrow. In contrast to the VWC scaling (Figure 5), matching ASCAT SSM with in situ VWC values produces good agreement at Barrow (Figure 6). Deviations remain for Lena Delta, but reasonable agreement is obtained for the autumn period at station K3.

4. Discussion

4.1. In Situ Measurement Setup and Scales, Lena River Delta

For the ASCAT-specific investigation in the Lena River Delta we installed VWC sensors very close to the surface within the organic layer. Tundra permafrost landscapes are fully covered by moss that overlays the mineral soil of the active layer. The organic layer in the Lena River Delta generally contains a thick moss layer (up to 30 cm) with a persistently wet 2- to 3-cm-thick fibric layer at its base. Under the moss and fibric layer a thick more decomposed organic peat layer is often present. Therefore, the installed VWC sensors do not measure *soil moisture* of a mineral soil body. Installation of VWC sensors in the mineral soil below the 20- to 30-cm organic layer where the fibric layer is persistently wet would not reflect what the ASCAT senses. However, we did not find strong agreement between the time series of the in situ VWC and satellite-derived soil moisture variations in the time period that was studied for the comparison with direct values (Table 3) nor for the median comparisons (Figure 6 and 5). The discrepancy of the temporal behavior between ASCAT SSM and in situ VWC in autumn demonstrates the limitation of the satellite information to the upper few centimeters. The soil temperature records in the soil indicate that freezing started at the surface before the decrease in VWC at 10-cm depth. The soil temperatures remain at 0 °Celsius for several days in this case.

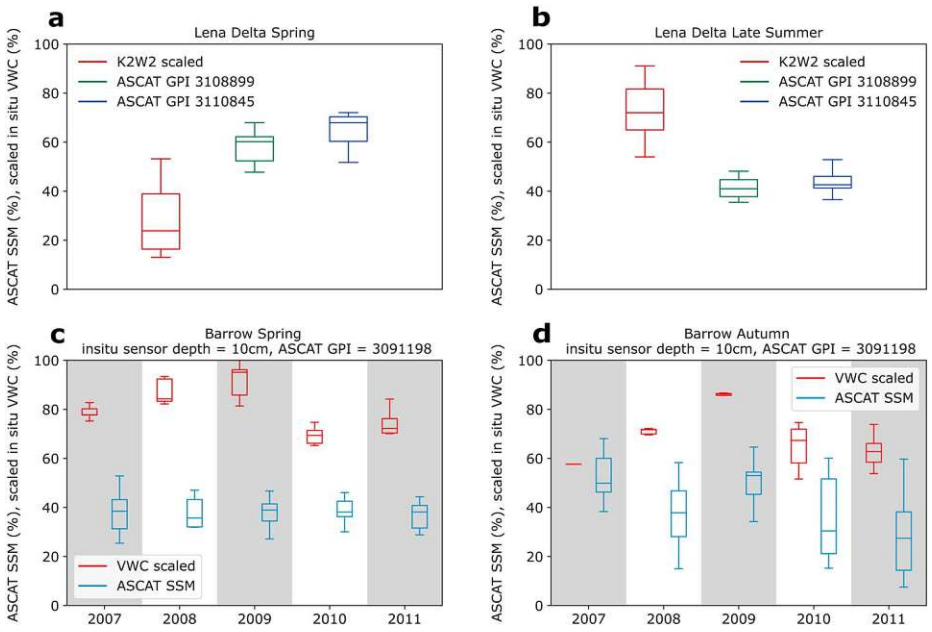

Figure 5. Box plots of Advanced Scatterometer (ASCAT) surface soil moisture (SSM) and in situ volumetric water content (VWC) scaled to their minimum and maximum values during the spring and autumn/late summer of 2007–2011 at the (a, b) Lena Delta and (c, d) Barrow sites. For spring, the first 20 days after thawing (determined from the in situ data) are used. For the autumn values at Barrow, the data during the last 20 days before freeze-up (determined from the in situ data) are used. For the late summer values at Lena Delta, the data during the last 20 days of in situ data availability are used. GPI = grid cell index.

The Lena Delta tundra landscape is characterized by a relatively high surface water fraction which can cause a bias to the ASCAT SSM (Wagner et al., 2013). This results from variations in water surface roughness which also contribute to the backscatter signal. Such water surface roughness can be caused by wind and rain but also by variations in river discharge in the Lena Delta site (Högström et al., 2014). Figure 1b shows the amount of water bodies in each ASCAT GPI. The GPI 3110849 has a high percentage of water bodies (77%) compared to 3108899 (39%), 3110845 (24%), and 3110841 (14%) (Högström & Bartsch, 2017). GPI 3110841 would be the better choice for comparison with ASCAT SSM, but logistic limitations during fieldwork lead to the choice of the more accessible GPI 31118899.

The comparisons of the ASCAT temporal SSM dynamics to the temporal dynamics of the in situ organic layer soil temperature in the Lena Delta suggest that the increase in soil temperature and at the same time increase in backscatter and SSM, respectively, may reflect subtle changes in liquid water content through thawing and refreezing of the active layer during the first 2 weeks after the end of snowmelt. However, this is not supported by the in situ VWC data. The drying up toward autumn suggested by the ASCAT measurements could not be observed in the in situ VWC records. There is more variability for the sensors in the moss layer in direct exchange with the atmosphere than in the persistently water-saturated fibric layer.

The correlations between the sites are relatively high, suggesting a certain level of representativeness. It has been shown that wind influences the backscatter when open water is present in the ASCAT footprint as demonstrated by Högström and Bartsch (2017) for the Lena Delta site. But this has only short-term impacts. Comparisons of satellite-derived soil moisture data with climate model results at high latitudes have also shown that models do not produce this *drying up* suggested by the ASCAT SSM product (Guimberteau et al., 2018). It should be noted that water logging due to local impacts of the sensor installations may also increase the saturation of the site. Water logging has been observed for sensor K1 toward the end of the summer season. Conclusions can therefore not be drawn from the data in the Lena Delta for autumn variations.

The overlying moss layer itself may also play a role with regard to the response to soil temperature in spring and changes toward autumn. The C band signal is expected to penetrate through tundra vegetation and the moss layer when it is dry. The high in situ moisture values at the deeper sensor installed in the fibric layer generally indicate very wet conditions, which is expected, as the fibric layer acts as the water storage layer of

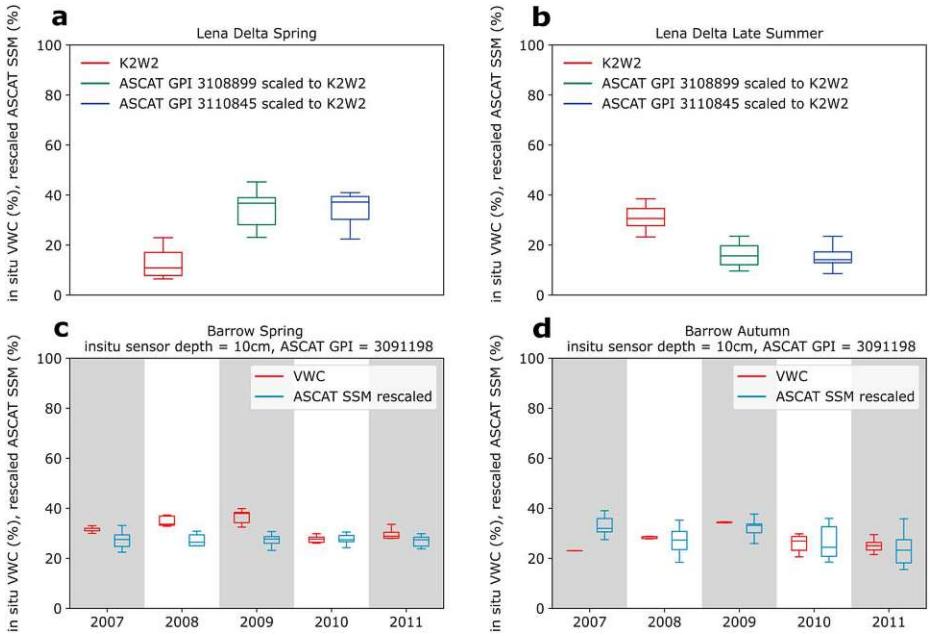

Figure 6. Box plots of in situ volumetric water content (VWC) and Advanced Scatterometer (ASCAT) surface soil moisture (SSM) rescaled to in situ VWC observations using mean standard deviation matching. Values are for the spring and autumn/late summer of 2007–2011 at the (a, b) Lena Delta and (c, d) Barrow sites. For spring, the first 20 days after thaw (determined from the in situ data) are used. For the autumn values at Barrow, the data during the last 20 days before freeze-up (determined from the in situ data) are used. For the late summer values at Lena Delta, the data during the last 20 days of in situ data availability are used. GPI = grid cell index.

the moss. The backscatter range which underlies the variations in SSM in the Lena Delta is only on the order of 1–2 dB across the entire snow-free season (Högström & Bartsch, 2017). In addition, there is low variation in in situ VWC (see Figure 2). The contribution of moisture change may, therefore, play only a minor role. The impact of soil temperature on the dielectric constant (above 0 °C) may have an effect in the case of these highly water-saturated soils and surfaces (Mironov & Savin, 2016).

The impact of soil temperature on ASCAT SSM variations in spring is partially confirmed at the Barrow site. Barrow VWC values are similar to the Lena Delta, but ASCAT SSM levels differ. This may result from the proximity of the site to the ocean and its contribution to the backscatter. The overall low variability of soil moisture observed in the in situ records is, however, captured with ASCAT which leads to the high correlations and good results for the matching with subsequent low RMSE (3–10% for predicted VWC, Table 3). The average of the RMSE for all sites (11% in case of spring as well as autumn) does, however, not meet the general accuracy requirement for satellite-derived soil moisture data sets, which is usually 4% (e.g., Chen et al., 2018; Sanchez et al., 2012).

4.2. Comparison Across Sites

The deviations which can be observed across the sites and seasons (Table 3) need to be discussed in the context of variations within the ASCAT footprint and the assumption that the chosen time period represents unfrozen conditions.

Tiksi is located close to the sea and the measurement site is in a valley surrounded by hills up to 200-m high with bare rock surfaces. The soils at the measurement site (wetland) differ from the surrounding mountain landscape, which may lead to the low correlation and high RMSE (6–22% for predicted VWC, Table 3). Sagwon is also located in a hilly area. Bergstedt and Bartsch (2017) demonstrated a high variability of freeze/thaw transition within the ASCAT footprint at this site. This may have an impact on the accuracy of the determination of the unfrozen period as the in situ location is not representative for the ASCAT footprint.

In general, derived values from satellite measurements are not of the same order as in situ measurement (scaled between minimum and maximum). In situ values range mostly between 45% and 100% compared to ASCAT values, which range between ~20% and 100% for the same time periods. This may result from the

definition of the minimum and maximum for the scaling. This difference is similar at several sites. Only a few years have been available to define the scaling parameters for the in situ data. ASCAT dry and wet references are derived from long-term records which also include its predecessor ERS (Naeimi, Scipal, et al., 2009), which may impact the comparability. Furthermore, the fraction of open water can impact the scaling parameters as exemplified by Högström and Bartsch (2017) for the central Lena Delta. A previous study which compared land surface model derived near SSM with ASCAT SSM also obtained a wide range of correlations, from negative to positive values, across Siberia (Gouttevin et al., 2013). The areas with negative correlations included the Lena Delta. The low correspondence in this region has been attributed to the low density of measurement sites that, in turn, drive model results. Högström et al. (2014) investigated the occurrence of these negative correlations with respect to the water fraction within the ASCAT footprint. High negative correlations coincided with areas with a high water fraction. The subsequent study over the Lena Delta (same ASCAT footprints as this study) by Högström and Bartsch (2017) showed that the high water fraction indeed causes a bias which results from wind action (causing waves which increase the backscatter). However, this bias cannot explain the negative correlations. Our results suggest that it may at least partially result from variations in the ASCAT records which are related to soil temperature variations.

Matching the ASCAT SSM to in situ data allows one to derive error measures. However, the comparably good results for Barrow need to be interpreted with care, since this site has low variability over the summer season. The high RMSE of the near-surface VWC predicted from ASCAT soil moisture data at the Sagwon, Tiksi, and Toolik sites suggest that the error is generally much larger in tundra environments (Table 3). The higher correlations for the autumn period compared to spring indicate better applicability of ASCAT SSM information toward the end of the unfrozen period. The soil temperature influence seems to be lower. A good agreement between scaled in situ data and ASCAT SSM can also be obtained for autumn at Barrow. The record of in situ data is longer at this site which may give more reliable scaling results. However, general conclusions could not be drawn due to the low number of sites studied. More monitoring sites which provide information on multiple parameters, multiple years, and with freely accessible data are required.

K2 has the lowest SSM values of the Kurungnakh Island sites in the Lena Delta in spring. In situ soil temperatures are still close to 0 °C (for 8-cm depth as selected for comparability to other sites, K2T2 in Figure 2) at this site which is lower than at other neighboring sites. It can be expected that the near surface was not yet fully unfrozen. This supports the findings on temporal variability, and the soil temperature dependence of the C band observations, in spring (Figure 2).

The low variation of in situ values observed at several sites and the differences between regions underline the need to use several different sites for assessments in the Arctic. The use of our own sensor setup in the Lena Delta alone would have limited the analyses to a small range of relative moisture as observed by the satellite records.

ASCAT data are only available in VV polarization which does not allow further analysis of scattering mechanisms. This needs to be further investigated with SAR. SAR also allows for better accounting of landscape heterogeneity due to the higher spatial resolution of such data (Högström et al., 2014; Wagner et al., 2008).

Results underline what has been pointed out previously by Wagner et al. (2013) regarding the necessity to build up expert knowledge in order to select those soil moisture values which are fit for application because the quality of the ASCAT SSM product varies in space and time. Disturbance of the ground through sensor installation has been identified as a critical issue for validation of near-surface VWC values in permafrost areas.

5. Conclusions

Satellite SSM measurements from MetOp ASCAT, which represent relative values, can represent general differences in the degree of soil saturation between sites. We compared five sites across the Arctic in Alaska (Barrow, Sagwon, and Toolik) and Siberia (Tiksi, Lena Delta) for soil moisture and two of the sites for the relationship between ASCAT SSM and in situ temperature (Lena Delta and Barrow).

We observe low variability in ASCAT-derived SSM and also low variability in in situ VWC of the uppermost organic layer in this type of landscape over the snow-free season. Scaling for ASCAT SSM uses longer time series, whereas the low variability of the shorter in situ VWC time records limits the comparability of the scaling to minimum/maximum. Matching allows determination of the RMSE for the ASCAT-derived near-surface soil moisture in units of VWC instead of saturation. High error values suggest that ASCAT SSM values need to be

treated with care across tundra environments. However, the investigated sites are all located in heterogeneous environments with a high water fraction or altitude variation in the ASCAT footprint. Continuous measurements, with multiple parameters and comparably homogeneous sites, are required for better understanding the influence of environmental factors on remotely sensed values. Soil temperature sensors distributed over a larger area could be advantageous for determining the complete thaw within the scatterometer footprint. The sensor setup in the Lena Delta, however, demonstrated the represetativeness of single-point measurements for characterizing the temporal variability of VWC in lowland environments. The RMSE of the volumetric water content predicted by ASCAT is on average 11% across the five sites in Alaska and Siberia.

In addition to previous findings regarding the influence of near-surface wind impacting the roughness of water surfaces, variations of C band backscatter are also impacted by soil temperature. The moss layer temperature variations are reflected in soil moisture variations derived from ASCAT during unfrozen conditions. The low variation in soil moisture over the snow-free season may contribute to the dominance of soil temperature on the remotely sensed values at the Lena Delta as well as the Barrow site. In fact, the retrieval of soil moisture is functionally based on the relationship between soil water content and the dielectric constant. However, it also changes with soil temperature under unfrozen conditions.

Acknowledgments

The authors acknowledge financial support by the European Union FP7-ENV project PAGE21 (Changing Permafrost in the Arctic and its global effects in the 21st century) under contract GA282700. The field work in the Lena Delta has been supported by two scholarships for transnational access (2013 and 2014) of the International Network for Terrestrial Research and Monitoring in the Arctic (FP7 INTERACT). This work was further supported by the Austrian Science Fund (Fonds zur Förderung der wissenschaftlichen Forschung, FWF) through the Doctoral College GIScience (DK W1237–N23) and the HORIZON2020 (BG-2017-1) project Nunataryuk. In situ data sharing for Tiksi was made possible through the PAGE21 project (data provided by FMI). We would like to thank Günther Stoof and Niko Bornemann, Moritz Langer and Julia Boike (AWI, Periglacical Research group, Energy- and Waterbalance Research Group of J. Boike) for large support in sensor preparation in the field 2013 as well as allowance of reuse of sensors. We thank Simon Zwieback for supporting data collection in 2014 within the framework of INTERACT Transnational Access. We are grateful for the support of the Russian research station *Samoylov Island*. The data used are listed in the references and tables. In situ soil temperature and VWC data are available for download on PANGAEA as part of the FP7 PAGE21 project data collection (Högström et al., 2018). We especially would like to thank the three anonymous reviewers for their valuable comments.

References

Bartalis, Z., Wagner, W., Naeimi, V., Hasenauer, S., Scipal, K., Bonekamp, H., et al. (2007). Initial soil moisture retrieval from the METOP-A advanced scatterometer. *Geophysical Research Letters*, *34*, L20401. https://doi.org/10.1029/2007GL031088

Bartsch, A. (2010). Ten years of SeaWinds on QuikSCAT for snow applications. *Remote Sensing*, *2*(4), 1142–1156. https://doi.org/10.3390/rs2041142

Bartsch, A., Höfler, A., Kroisleitner, C., & Trofaier, A. M. (2016). Land cover mapping in northern high latitude permafrost regions with satellite data: Achievements and remaining challenges. *Remote Sensing*, *8*(12), 979. https://doi.org/10.3390/rs8120979

Bartsch, A., Melzer, T., Elger, K., & Heim, B. (2012). Soil moisture from Metop ASCAT data at high latitudes. In *Tenth International Conference on Permafrost (TICOP)* (pp. 33–38). Salekhard, Russia.

Bartsch, A., Sabel, D., Wagner, W., & Park, S.-E. (2011). Considerations for derivation and use of soil moisture data from active microwave satellites at high latitudes, *2011 IEEE International Geoscience and Remote Sensing Symposium (IGARSS)* (pp. 3132–3135). Vancouver, British Columbia, Canada: IEEE. https://doi.org/10.1109/IGARSS.2011.6049882

Bartsch, A., Trofaier, A., Hayman, G., Sabel, D., Schlaffer, S., Clark, D., & Blyth, E. (2012). Detection of open water dynamics with ENVISAT ASAR in support of land surface modelling at high latitudes. *Biogeosciences*, *9*(2), 703–714. https://doi.org/10.5194/bg-9-703-2012

Beer, C., Lucht, W., Gerten, D., Thonicke, K., & Schmullius, C. (2007). Effects of soil freezing and thawing on vegetation carbon density in Siberia: A modeling analysis with the Lund-Potsdam-Jena Dynamic Global Vegetation Model (LPJ-DGVM). *Global Biogeochemical Cycles*, *21*, GB1012. https://doi.org/10.1029/2006GB002760

Bergstedt, H., & Bartsch, A. (2017). Surface state across scales; temporal and spatial patterns in land surface freeze/thaw dynamics. *Geosciences*, *7*(3), 65. https://doi.org/10.3390/geosciences7030065

Bircher, S., Skou, N., Jensen, K. H., Walker, J. P., & Rasmussen, L. (2012). A soil moisture and temperature network for SMOS validation in western denmark. *Hydrology and Earth System Sciences*, *16*(5), 1445–1463. https://doi.org/10.5194/hess-16-1445-2012

Boike, J., Kattenstroth, B., Abramova, E., Bornemann, N., Chetverova, A., Fedorova, I., et al. (2013). Baseline characteristics of climate, permafrost and land cover from a new permafrost observatory in the Lena River Delta, Siberia (1998–2011). *Biogeosciences (BG)*, *10*(3), 2105–2128. https://doi.org/10.5194/bg-10-2105-2013

Brocca, L., Hasenauer, S., Lacava, T., Melone, F., Moramarco, T., Wagner, W., et al. (2011). Soil moisture estimation through ASCAT and AMSR-E sensors: An intercomparison and validation study across europe. *Remote Sensing of Environment*, *115*(12), 3390–3408. https://doi.org/10.1016/j.rse.2011.08.003

Brocca, L., Moramarco, T., Melone, F., Wagner, W., Hasenauer, S., & Hahn, S. (2012). Assimilation of surface- and root-zone ASCAT soil moisture products into rainfall-runoff modeling. *IEEE Transactions on Geoscience and Remote Sensing*, *50*(7), 2542–2555. https://doi.org/10.1109/TGRS.2011.2177468

Brown, J., Ferrians, O. J., Heginbottom, J., & Melnikov, E. (2002). Circum-Arctic map of permafrost and ground-ice conditions, Version 2, *Circum-Pacific map series, CP-45*. Boulder, Colorado USA: NSIDC: National Snow and Ice Data Center. https://nsidc.org/data/ggd318

Ceballos, A., Scipal, K., Wagner, W., & Martínez-Fernández, J. (2005). Validation of ERS scatterometer-derived soil moisture data in the central part of the Duero Basin, Spain. *Hydrological processes*, *19*(8), 1549–1566. https://doi.org/10.1002/hyp.5585

Chen, Q., Zeng, J., Cui, C., Li, Z., Chen, K., Bai, X., & Xu, J. (2018). Soil moisture retrieval from SMAP: A validation and error analysis study using ground-based observations over the little Washita watershed. *IEEE Transactions on Geoscience and Remote Sensing*, *56*(3), 1394–1408. https://doi.org/10.1109/TGRS.2017.2762462

Colliander, A., Jackson, T., Bindlish, R., Chan, S., Das, N., Kim, S., et al. (2017). Validation of SMAP surface soil moisture products with core validation sites. *Remote Sensing of Environment*, *191*, 215–231. https://doi.org/https://doi.org/10.1016/j.rse.2017.01.021

Crow, W. T., Berg, A. A., Cosh, M. H., Loew, A., Mohanty, B. P., Panciera, R., et al. (2012). Upscaling sparse ground-based soil moisture observations for the validation of coarse-resolution satellite soil moisture products. *Reviews of Geophysics*, *50*, RG2002. https://doi.org/10.1029/2011RG000372

Dafflon, B., Oktem, R., Peterson, J., Ulrich, C., Tran, A. P., Romanovsky, V., & Hubbard, S. S. (2017). Coincident aboveground and belowground autonomous monitoring to quantify covariability in permafrost, soil, and vegetation properties in Arctic tundra. *Journal of Geophysical Research: Biogeosciences*, *122*, 1321–1342. https://doi.org/10.1002/2016JG003724

De Jeu, R., Wagner, W., Holmes, T., Dolman, A., Van De Giesen, N., & Friesen, J. (2008). Global soil moisture patterns observed by space borne microwave radiometers and scatterometers. *Surveys in Geophysics*, *29*(4-5), 399–420. https://doi.org/10.1007/s10712-008-9044-0

Delwart, S., Bouzinac, C., Wursteisen, P., Berger, M., Drinkwater, M., Martín-Neira, M., & Kerr, Y. H. (2008). SMOS validation and the COSMOS campaigns. *IEEE Transactions on Geoscience and Remote Sensing*, *46*(3), 695–704. https://doi.org/10.1109/TGRS.2007.914811

Dirmeyer, P. A., Guo, Z., & Gao, X. (2004). Comparison, validation, and transferability of eight multiyear global soil wetness products. *Journal of Hydrometeorology*, *5*(6), 1011–1033. https://doi.org/10.1175/JHM-388.1

Dorigo, W., Xaver, A., Vreugdenhil, M., Gruber, A., Hegyiová, A., Sanchis-Dufau, A., et al. (2013). Global automated quality control of in situ soil moisture data from the international soil moisture network. *Vadose Zone Journal*, *12*(3). https://doi.org/10.2136/vzj2012.0097

Entekhabi, D., Njoku, E. G., O'Neill, P. E., Kellogg, K. H., Crow, W. T., Edelstein, W. N., et al. (2010). The soil moisture active passive (SMAP) mission. *Proceedings of the IEEE*, *98*(5), 704–716. https://doi.org/10.1109/JPROC.2010.2043918

Figa-Saldaña, J., Wilson, J. J., Attema, E., Gelsthorpe, R., Drinkwater, M., & Stoffelen, A. (2002). The advanced scatterometer (ASCAT) on the meteorological operational (MetOp) platform: A follow on for European wind scatterometers. *Canadian Journal of Remote Sensing*, *28*(3), 404–412. https://doi.org/10.5589/m02-035

Fletcher, B. J., Press, M. C., Baxter, R., & Phoenix, G. K. (2010). Transition zones between vegetation patches in a heterogeneous Arctic landscape: How plant growth and photosynthesis change with abundance at small scales. *Oecologia*, *163*(1), 47–56. https://doi.org/10.1007/s00442-009-1532-5

Gouttevin, I., Bartsch, A., Krinner, G., & Naeimi, V. (2013). A comparison between remotely-sensed and modelled surface soil moisture (and frozen status) at high latitudes. *Hydrology & Earth System Sciences Discussions*, *10*(8), 11241–11291. https://doi.org/10.5194/hessd-10-11241-2013, 2013

Guimberteau, M., Zhu, D., Maignan, F., Huang, Y., Chao, Y., Dantec-Nédélec, S., et al. (2018). ORCHIDEE-MICT (v8. 4.1), a land surface model for the high latitudes: Model description and validation. *Geoscientific Model Development*, *11*(1), 121. https://doi.org/10.5194/gmd-11-121-2018

Hallikainen, M. T., Ulaby, F. T., Dobson, M. C., El-rayes, M. A., & Wu, L. k. (1985). Microwave dielectric behavior of wet soil-part 1: Empirical models and experimental observations. *IEEE Transactions on Geoscience and Remote Sensing*, *GE-23*(1), 25–34. https://doi.org/10.1109/TGRS.1985.289497

Högström, E., & Bartsch, A. (2017). Impact of backscatter variations over water bodies on coarse-scale radar retrieved soil moisture and the potential of correcting with meteorological data. *IEEE Transactions on Geoscience and Remote Sensing*, *55*(1), 3–13. https://doi.org/10.1109/TGRS.2016.2530845

Högström, E., Heim, B., & Bartsch, A. (2018). Near surface volumetric soil moisture and temperature measurements in the Lena Delta for 2013/2014., PANGAEA. https://doi.org/10.1594/PANGAEA.894706

Högström, E., Trofaier, A. M., Gouttevin, I., & Bartsch, A. (2014). Assessing seasonal backscatter variations with respect to uncertainties in soil moisture retrieval in Siberian tundra regions. *Remote Sensing*, *6*(9), 8718–8738. https://doi.org/10.3390/rs6098718

Ikonen, J., Vehviläinen, J., Rautiainen, K., Smolander, T., Lemmetyinen, J., Bircher, S., & Pulliainen, J. (2016). The Sodankylä in situ soil moisture observation network: An example application of ESA CCI soil moisture product evaluation. *Geoscientific Instrumentation, Methods and Data Systems*, *5*, 95–108. https://doi.org/10.5194/gi-5-95-2016

Jackson, T. J., Cosh, M. H., Bindlish, R., Starks, P. J., Bosch, D. D., Seyfried, M., et al. (2010). Validation of advanced microwave scanning radiometer soil moisture products. *IEEE Transactions on Geoscience and Remote Sensing*, *48*(12), 4256–4272. https://doi.org/10.1109/TGRS.2010.2051035

Jung, M., Reichstein, M., Ciais, P., Seneviratne, S. I., Sheffield, J., Goulden, M. L., et al. (2010). Recent decline in the global land evapotranspiration trend due to limited moisture supply. *Nature*, *467*(7318), 951. https://doi.org/10.1038/nature09396

Kerr, Y. H., Waldteufel, P., Wigneron, J.-P., Martinuzzi, J., Font, J., & Berger, M. (2001). Soil moisture retrieval from space: The soil moisture and ocean salinity (SMOS) mission. *IEEE transactions on Geoscience and remote sensing*, *39*(8), 1729–1735. https://doi.org/10.1109/36.942551

Krauss, L., Hauck, C., & Kottmeier, C. (2010). Spatio-temporal soil moisture variability in Southwest Germany observed with a new monitoring network within the COPS domain. *Meteorologische Zeitschrift*, *19*(6), 523–537. https://doi.org/10.1127/0941-2948/2010/0486

Li, L., Gaiser, P. W., Gao, B.-C., Bevilacqua, R. M., Jackson, T. J., Njoku, E. G., et al. (2010). WindSat global soil moisture retrieval and validation. *IEEE Transactions on Geoscience and Remote Sensing*, *48*(5), 2224–2241. https://doi.org/10.1109/TGRS.2009.2037749

Marchenko, S., Romanovsky, V., & Tipenko, G. (2008). Numerical modeling of spatial permafrost dynamics in Alaska, *Proceedings of the ninth international conference on permafrost* (Vol. 29, pp. 1125–1130). University of Alaska Fairbanks: Institute of Northern Engineering. https://doi.org/10.5194/tc-6-613-2012

Massari, C., Crow, W., & Brocca, L. (2017). An assessment of the performance of global rainfall estimates without ground-based observations. *Hydrology and Earth System Sciences*, *21*(9), 4347–4361. https://doi.org/10.5194/hess-21-4347-2017

Mironov, V., & Savin, I. (2016). Temperature-dependent spectroscopic dielectric model at 0.05–16 ghz for a thawed and frozen Alaskan organic soil, *Satellite Soil Moisture Retrieval* (pp. 169–186): Elsevier. https://doi.org/10.1016/B978-0-12-803388-3.00009-7

Naeimi, V., Bartalis, Z., & Wagner, W. (2009). ASCAT soil moisture: An assessment of the data quality and consistency with the ERS scatterometer heritage. *Journal Of Hydrometeorology*, *10*(2), 555–563. https://doi.org/10.1175/2008JHM1051.1

Naeimi, V., Paulik, C., Bartsch, A., Wagner, W., Kidd, R., Park, S.-E., et al. (2012). ASCAT surface state flag (SSF): Extracting information on surface freeze/thaw conditions from backscatter data using an empirical threshold-analysis algorithm. *IEEE Transactions on Geoscience and Remote Sensing*, *50*(7), 2566–2582. https://doi.org/10.1109/TGRS.2011.2177667

Naeimi, V., Scipal, K., Bartalis, Z., Hasenauer, S., & Wagner, W. (2009). An improved soil moisture retrieval algorithm for ERS and METOP scatterometer observations. *IEEE Transactions on Geoscience and Remote Sensing*, *47*(7), 1999–2013. https://doi.org/10.1109/TGRS.2008.2011617

Njoku, E. G., Jackson, T. J., Lakshmi, V., Chan, T. K., & Nghiem, S. V. (2003). Soil moisture retrieval from AMSR-E. *IEEE Transactions on Geoscience and Remote Sensing*, *41*(2), 215–229. https://doi.org/10.1109/TGRS.2002.808243

Nolin, A., Armstrong, R., & Maslanik, J. (1998). *Near real-time SSM/I EASE-grid daily global ice concentration and snow extent*. Boulder, Colorado: National Snow and Ice Data Center. https://doi.org/10.5067/3KB2JPLFPK3R

Owe, M., de Jeu, R., & Holmes, T. (2008). Multisensor historical climatology of satellite-derived global land surface moisture. *Journal of Geophysical Research*, *113*, F01002. https://doi.org/10.1029/2007JF000769

Paulik, C., Steiner, C., Hahn, S., Melzer, T., Gruber, A., & Wagner, W. (2014). Open source toolbox and web application for soil moisture validation. In *2014 IEEE Geoscience and Remote Sensing Symposium* (pp. 3331–3333). Quebec City, QC, Canada. https://doi.org/10.1109/IGARSS.2014.6947193

Robock, A., Vinnikov, K. Y., Srinivasan, G., Entin, J. K., Hollinger, S. E., Speranskaya, N. A., et al. (2000). The global soil moisture data bank. *Bulletin of the American Meteorological Society*, *81*(6), 1281–1299. https://doi.org/10.1175/1520-0477(2000)081<1281:TGSMDB>2.3.CO;2

Rudiger, C., Calvet, J.-C., Brut, A., Wigneron, J.-P., Berthelot, B., Chanzy, A., et al. (2007). Aggregation and disaggregation of synthetic l-band soil moisture data over south-western France in preparation of SMOS, *Geoscience and Remote Sensing Symposium, 2007. IGARSS 2007. IEEE International* (pp. 1853–1856). Barcelona, Spain: IEEE. https://doi.org/10.1109/IGARSS.2007.4423184

Sanchez, N., Martinez-Fernandez, J., Scaini, A., & Perez-Gutierrez, C. (2012). Validation of the SMOS L2 soil moisture data in the REMEDHUS network (Spain). *IEEE Transactions on Geoscience and Remote Sensing*, *50*(5), 1602–1611. https://doi.org/10.1109/TGRS.2012.2186971

Schanda, E. (1986). *Physical fundamentals of remote sensing*. Berlin Heidelberg: Springer-Verlag.

Scipal, K., Wagner, W., Trommler, M., & Naumann, K. (2002). The global soil moisture archive 1992–2000 from ERS scatterometer data: First results, *IEEE International Geoscience and Remote Sensing Symposium* (Vol. 3, pp. 1399–1401). Toronto, Ontario, Canada, Canada: IEEE. https://doi.org/10.1109/IGARSS.2002.1026129

Sinclair, S., & Pegram, G. (2010). A comparison of ASCAT and modelled soil moisture over South Africa, using TOPKAPI in land surface mode. *Hydrology and Earth System Sciences*, *14*(4), 613. https://doi.org/10.5194/hess-14-613-2010

Smith, L. C., Sheng, Y., & MacDonald, G. M. (2007). A first Pan-Arctic assessment of the influence of glaciation, permafrost, topography and peatlands on Northern Hemisphere lake distribution. *Permafrost and Periglacial Processes*, *18*(2), 201–208. https://doi.org/10.1002/ppp.581

Ulaby, F. T., & Long, D. G. (2014). *Microwave radar and radiometric remote sensing*. Ann Arbor: University of Michigan Press.

Uppala, S. M., Kållberg, P., Simmons, A., Andrae, U., Bechtold, V., Fiorino, M., et al. (2005). The ERA-40 re-analysis. *Quarterly Journal of the Royal Meteorological Society*, *131*(612), 2961–3012. https://doi.org/10.1256/qj.04.176

Wagner, W., Bartalis, Z., Naeimi, V., Park, S.-E., Figa-Saldaña, J., & Bonekamp, H. (2010). Status of the METOP ASCAT soil moisture product, *2010 IEEE International Geoscience and Remote Sensing Symposium* (pp. 276–279). Honolulu, HI, USA: IEEE. https://doi.org/10.1109/IGARSS.2010.5653358

Wagner, W., Hahn, S., Kidd, R., Melzer, T., Bartalis, Z., Hasenauer, S., et al. (2013). The ASCAT soil moisture product: A review of its specifications, validation results, and emerging applications. *Meteorologische Zeitschrift*, *22*(1), 5–33. https://doi.org/10.1127/0941-2948/2013/0399

Wagner, W., Lemoine, G., & Rott, H. (1999). A method for estimating soil moisture from ERS scatterometer and soil data. *Remote Sensing of Environment*, *70*(2), 191–207. https://doi.org/10.1016/S0034-4257(99)00036-X

Wagner, W., Naeimi, V., Scipal, K., de Jeu, R., & Martínez-Fernández, J. (2007). Soil moisture from operational meteorological satellites. *Hydrogeology Journal*, *15*(1), 121–131. https://doi.org/10.1007/s10040-006-0104-6

Wagner, W., Noll, J., Borgeaud, M., & Rott, H. (1999). Monitoring soil moisture over the Canadian prairies with the ERS scatterometer. *IEEE Transactions on Geoscience and Remote Sensing*, *37*(1), 206–216. https://doi.org/10.1109/36.739155

Wagner, W., Pathe, C., Doubkova, M., Sabel, D., Bartsch, A., Hasenauer, S., et al. (2008). Temporal stability of soil moisture and radar backscatter observed by the Advanced Synthetic Aperture Radar (ASAR). *Sensors*, *8*(2), 1174–1197. https://doi.org/10.3390/s80201174

Wang, J. R., Shiue, J. C., & McMurtrey, J. E. (1980). Microwave remote sensing of soil moisture content over bare and vegetated fields. *Geophysical Research Letters*, *7*(10), 801–804. https://doi.org/10.1029/GL007i010p00801

Western, A. W., Grayson, R. B., & Blöschl, G. (2002). Scaling of soil moisture: A hydrologic perspective. *Annual Review of Earth and Planetary Sciences*, *30*(1), 149–180. https://doi.org/10.1146/annurev.earth.30.091201.140434

Williams, K. K., & Greeley, R. (2001). Radar attenuation by sand: Laboratory measurements of radar transmission. *IEEE Transactions on Geoscience and Remote Sensing*, *39*(11), 2521–2526. https://doi.org/10.1109/36.964990

Yershov, E., Kondratieva, K., Loginov, V., & Sychev, I. (1991). Geocryological map of Russia and neighbouring republics. Faculty of Geology, Chair of Geocryology, Lomonosov Moscow State University.

Yoshikawa, K., Overduin, P. P., & Harden, J. W. (2004). Moisture content measurements of moss (Sphagnum spp.) using commercial sensors. *Permafrost and Periglacial Processes*, *15*(4), 309–318. https://doi.org/10.1002/ppp.505

Zhang, T., Barry, R., Knowles, K., Ling, F., & Armstrong, R. (2003). Distribution of seasonally and perennially frozen ground in the Northern Hemisphere, *Proceedings of the 8th International Conference on Permafrost* (Vol. 2, pp. 1289–1294). Zurich, Switzerland: AA Balkema Publishers.

Zhang, N., Yasunari, T., & Ohta, T. (2011). Dynamics of the larch taiga–permafrost coupled system in siberia under climate change. *Environmental Research Letters*, *6*(2), 024–003. https://doi.org/10.1088/1748-9326/6/2/024003

Erratum

The originally published version of this article included several minor typographical errors introduced in typesetting. These have been corrected, and this may be considered the authoritative version of record.